THE UNIVERSITY OF OKLAHOMA

GRADUATE COLLEGE

FAULT DISTRIBUTION IN THE SULPHUR, OKLAHOMA AREA BASED ON GRAVITY, MAGNETIC AND STRUCTURAL DATA

A THESIS

SUBMITTED TO THE GRADUATE FACULTY

in partial fulfillment of the requirements for the

degree of

MASTERS OF SCIENCE

By

STEVEN WILLIAM CATES

Norman, Oklahoma

1989

FAULT DISTRIBUTION IN THE SULPHUR, OKLAHOMA AREA BASED ON GRAVITY, MAGNETIC AND STRUCTURAL DATA

A THESIS

APPROVED FOR THE SCHOOL OF

GEOLOGY AND GEOPHYSICS

[redacted]

CONTENTS

CONTENTS--Continued

LIST OF TABLES

LIST OF ILLUSTRATIONS

ILLUSTRATIONS Page

LIST OF ILLUSTRATIONS-Continued

LIST OF ILLUSTRATIONS-Continued

LIST OF ILLUSTRATIONS-Continued

LIST OF PLATES

PLATE

ACKNOWLEDGEMENTS

I want to dedicate this work to my grandmother Lois Shope, without whose love and financial generosity this work could not have been possible. Many people deserve thanks for help that was given me over the course of my academic career. As I cannot list them all, here is the short list.

I wish to thank my grandparents Harry and Florence Sharpe for their unceasing support and the inspirational example they have always been to me. I thank my mother for instilling in me an inner strength in adversity and the will to never, never give up, ever. I thank my father for setting standards of excellence and achievement that will continue to both inspire and motivate.

I will always be grateful to Jud Ahern for his advise, guidance and patience over the last four years. He taught me how a computer can be your friend, that geophysics is great fun, and that this science must be approached with thoroughness and careful attention to detail. Sometimes one meets the rare educator that can both teach and inspire in a way that effects a life. I have changed having known Jud Ahern.

Thanks go to David Stearns for his time and effort throughout this study. Dr. Stearns has imparted a philosophy of geologic science that will always be a guide to me. I expect that I will always remember him upon arriving at some scientific conclusion. I am certain that I will ask myself, "But what would Dr. Stearns say?". I will always be

grateful to him for his influence on my thinking.

Thanks are greatly due to Charles Harper for his review of the manuscript and his joyful teaching of field geology methods. I would also like to thank all those individuals at the U.S. Geological Survey Water Resources Division Office in Oklahoma City for their continual support and forbearance over the coarse of this study. Thanks are especially due to Ron Hanson for his continual support and encouragement.

Most of all, I wish to thank my wife Cathy. This degree will be awarded to me. But we did it. Without the loving tolerance of an outstanding woman, this academic achievement would not have been possible. Thanks to my children Angela, Joshua, Rosanne and Lea for being there and tolerating me during the difficult period of time that was required for this accomplishment.

ABSTRACT

Declining water flow from springs in the Travertine District, Chickasaw National Recreation Area (CNRA) spurred geologic investigation of the area. Because geologic structure may influence hydrology, knowledge of structure was needed to understand the problem of declining spring flow. Pennsylvanian-aged conglomerate covers CNRA, obscuring the geology beneath the park that controls the hydrology. To further understand the geologic structure below and contiguous to CNRA, a geological and geophysical investigation was carried out. Ordovician outcrop is found east of CNRA and at a few isolated locations where it has been exposed by erosion of Pennsylvanian rock. Subsurface data from oil wells is available for the area west of CNRA. In those areas where Pre-Pennsylvanian rocks can be seen, surface geological reconnaissance was done. Maps and cross-sections were constructed from subsurface and outcrop data to define structural trends.

Gravity and magnetic data were acquired for the area surrounding and including CNRA between the outcrop data and the subsurface data. Analysis of gravity and magnetic data, obtained from 180 data stations in a 125 square kilometer area surrounding, and including, CNRA, is presented. These data are analyzed using a Fast Fourier Transform computer program. Second vertical derivatives are computed and incremental downward continuation of the gravity and magnetic fields is carried out.

Utilizing geologic data from various sources, density model inversion of gravity data was done using a least-squares matrix inversion computer program. North-south observed gravity profiles were used to develop geologically feasible models of the structural geometry for areas of limited geologic data.

Interpretation and synthesis of these data sets resulted in the interpolation of fault locations beneath the Pennsylvanian-aged conglomerate.

INTRODUCTION

The Chickasaw National Recreation Area (CNRA) is located in Murray County, south-central Oklahoma (Figure 1). Several springs within this park are significant to the popularity of the park. Flow from these springs has decreased and a few have completely dried up. This has raised concern both in the local community of Sulphur, Oklahoma and within the National Park Service. The National Park Service commissioned the U.S. Geological Survey to study the hydrology affecting these springs. This thesis is part of that effort by the Oklahoma office of the U.S. Geological Survey Water Resources Division to collect, compile, and interpret data pertinent to the problem.

Several distinctly different water types are found within three kilometers of one another in the CNRA area. North of the park several artesian wells have been drilled since 1900 (Figure 2). These well waters have various degrees of mineralization and some have the strong smell of hydrogen sulfide. In the park there are several mineral springs whose water chemistries are different from those of the artesian well waters. In the most eastern section of the park are two springs named Antelope Springs and Buffalo Springs that normally have high volume flow of bicarbonate waters. These spring waters are chemically different from both the mineral springs and the artesian wells.

The possibility that these waters flow through different geologic

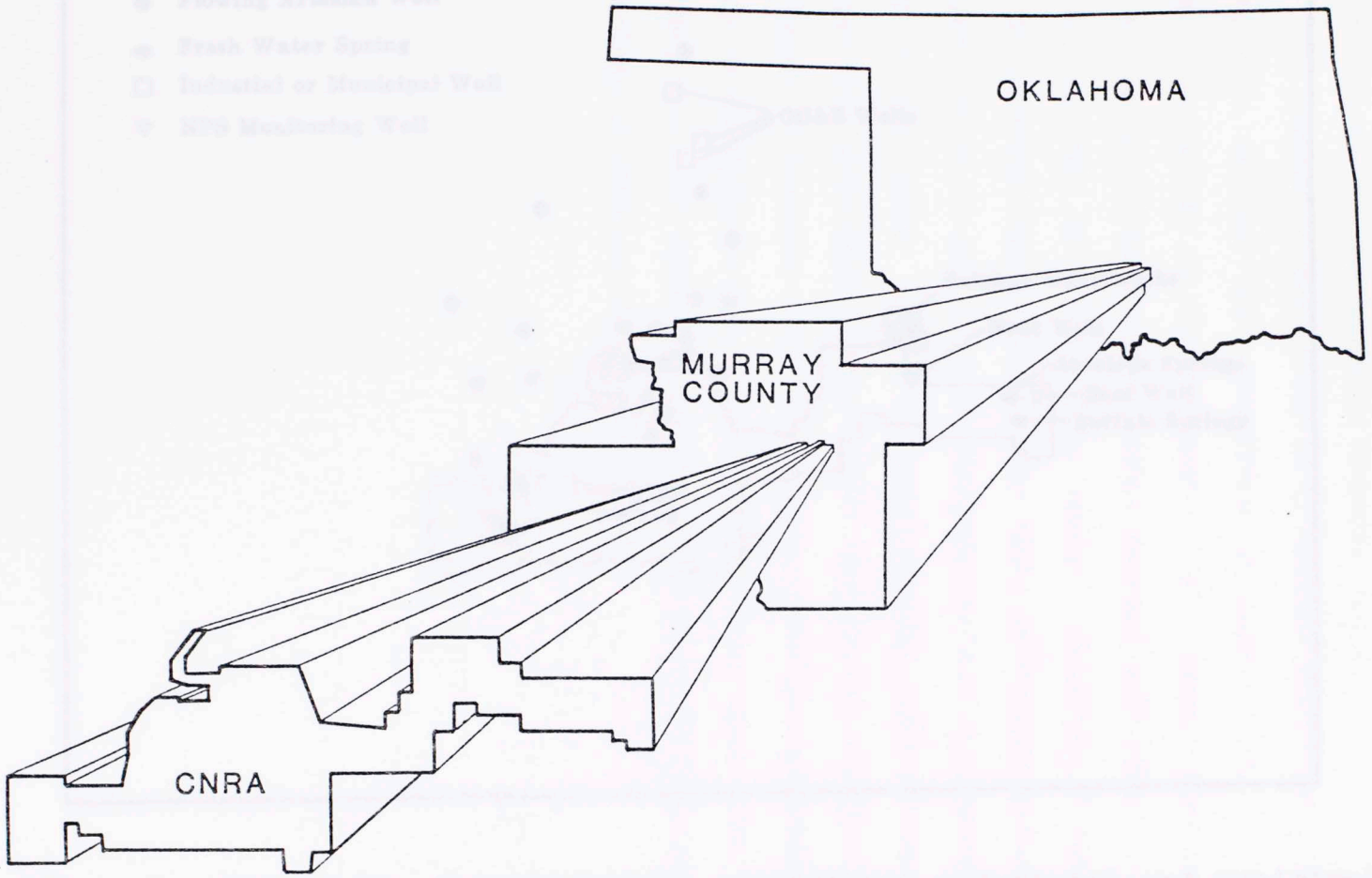

Figure 1. Map of Oklahoma showing location of Chickasaw National Recreation Area.

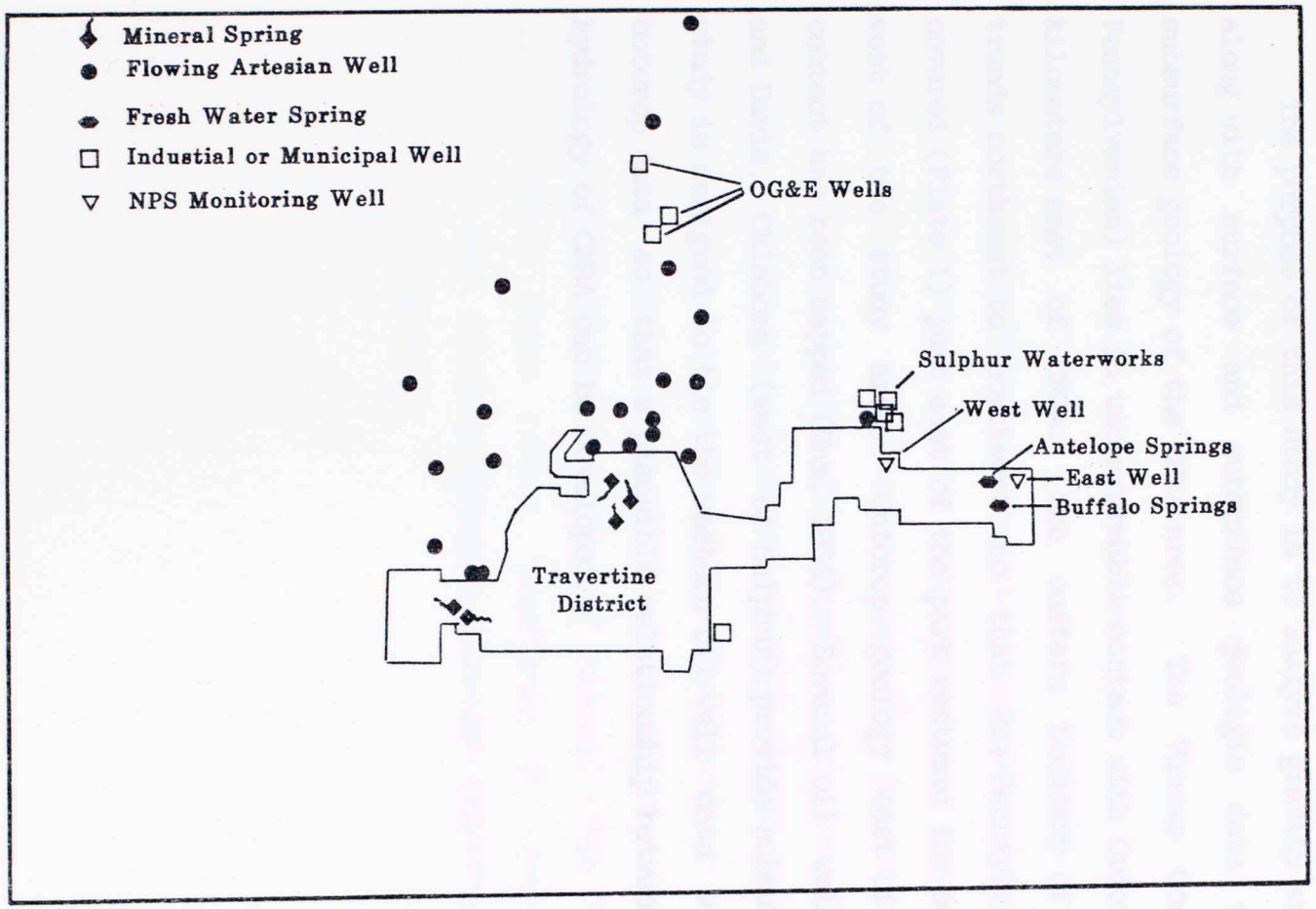

Figure 2. Map of the flowing wells, significant industrial and municipal wells, East and West Observation wells, and springs of the CNRA area.

formations might account for their variation in character. A geological map of this area (Plate 1) shows deformation that is characteristic of the Arbuckle Mountain region.

The purpose of this study is to analyze gravity and magnetic data along with surface and subsurface geologic data to delineate the subsurface geology of the CNRA area. The Vanoss Conglomerate (late Pennsylvanian) lies in unconformable contact with Ordovician rock three kilometers east of CNRA. The eastern boundary of the conglomerate trends northeast to southwest so that Pre-Pennsylvanian rocks are covered (Plate 1) just east of the park westward for several kilometers west of the study area. Outcrop geology east of the conglomerate contact has been mapped (Ham, 1954). Several oil wells between CNRA and Davis, Oklahoma (west of Sulphur) provide subsurface data. This study is designed to tie the western oil well data with the eastern outcrop data so that a plausible relationship between geology and the hydrology of CNRA can be developed.

REGIONAL GEOLOGY

Oklahoma Aulacogen

The Southern Oklahoma Aulacogen (Figure 3), in the southwestern portion of the state, trends NW-SE and is made up of several pairs of basins and uplifts. At its southeastern edge the aulacogen intersects the Ouachita Mountains. The formation of the Southern Oklahoma Aulacogen included lower Paleozoic syndepositional faulting parallel to the trend of this long narrow basin. Fault movement that was related to the rapid subsidence resulted in some especially thick sedimentary packages (Figure 4) found within this sinking trough (Feinstein, 1981). Reactivation of these faults, especially in Pennsylvanian time, resulted in the Southern Oklahoma Aulacogen imprinting a fault fabric on the region (Figure 5).

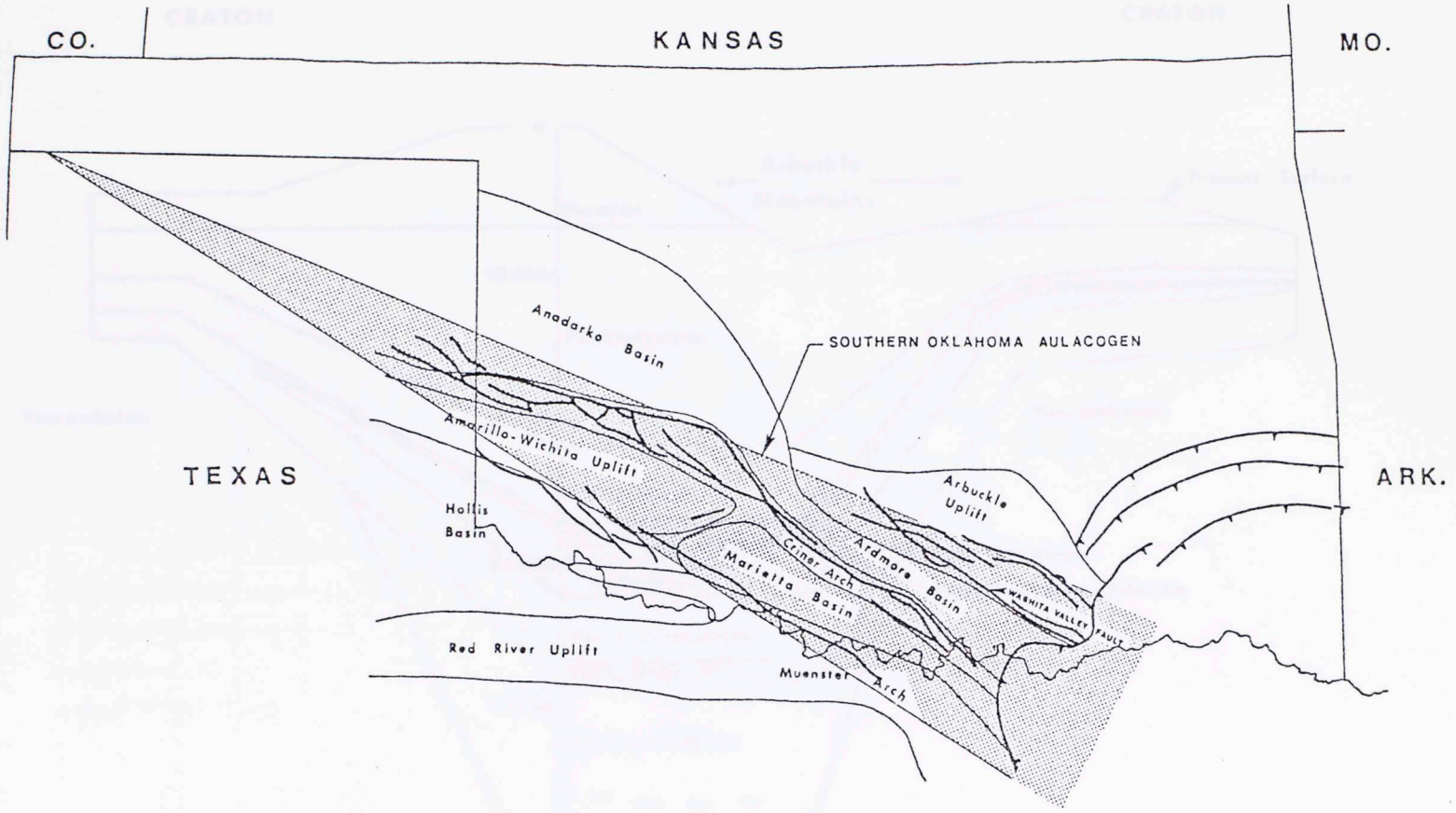

Figure 3. Map of the Southern Oklahoma Aulacogen showing the paired basins and uplifts, major faults and inferred extent of the Aulacogen. Modified from Walper (1976) and Pruatt (1975).

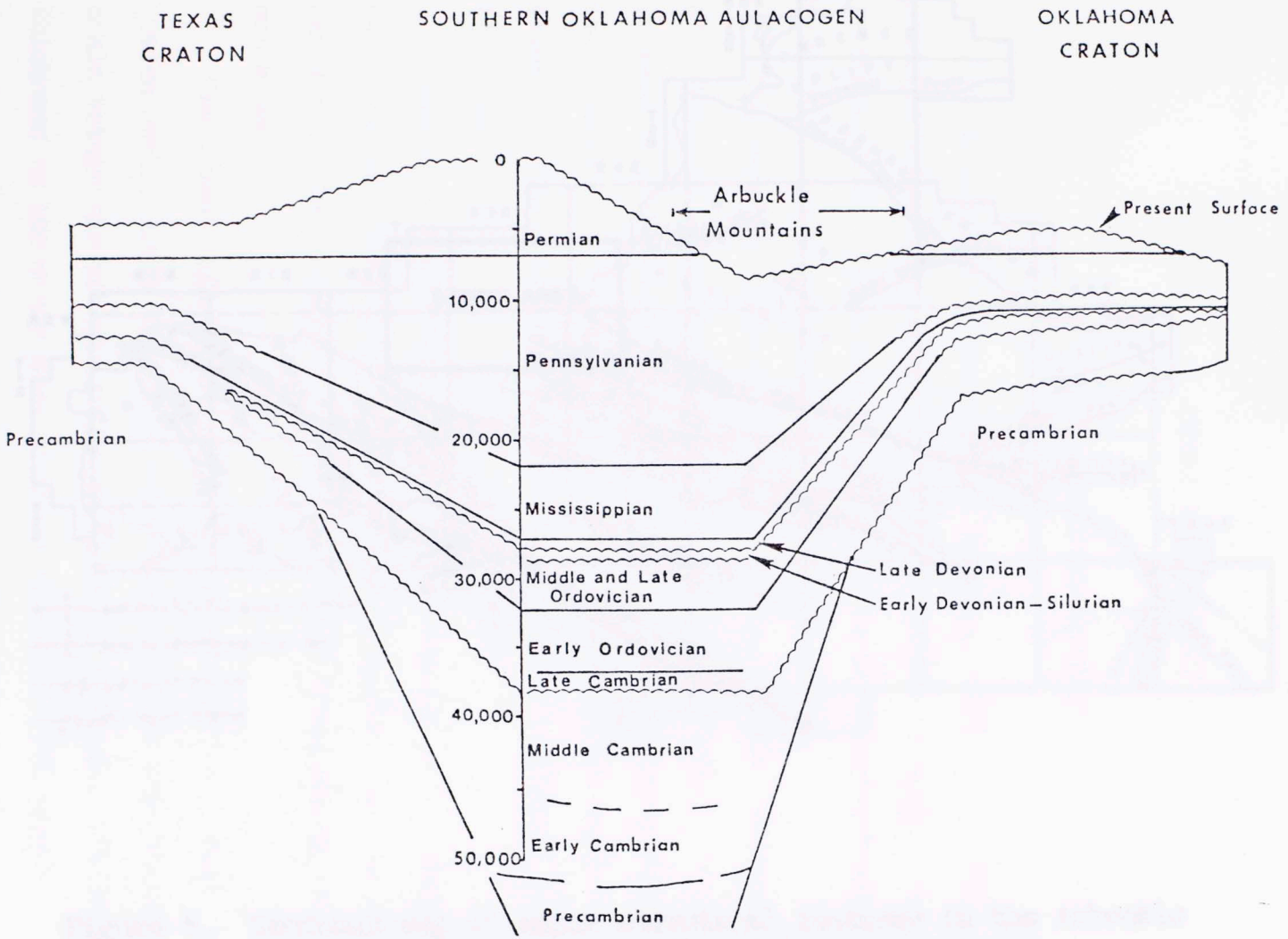

Figure 4. Generalized cross-section of Southern Oklahoma Aulacogen showing stratigraphic thicknesses, relative distribution relationships, and major unconformities. Taken from Ham, 1978.

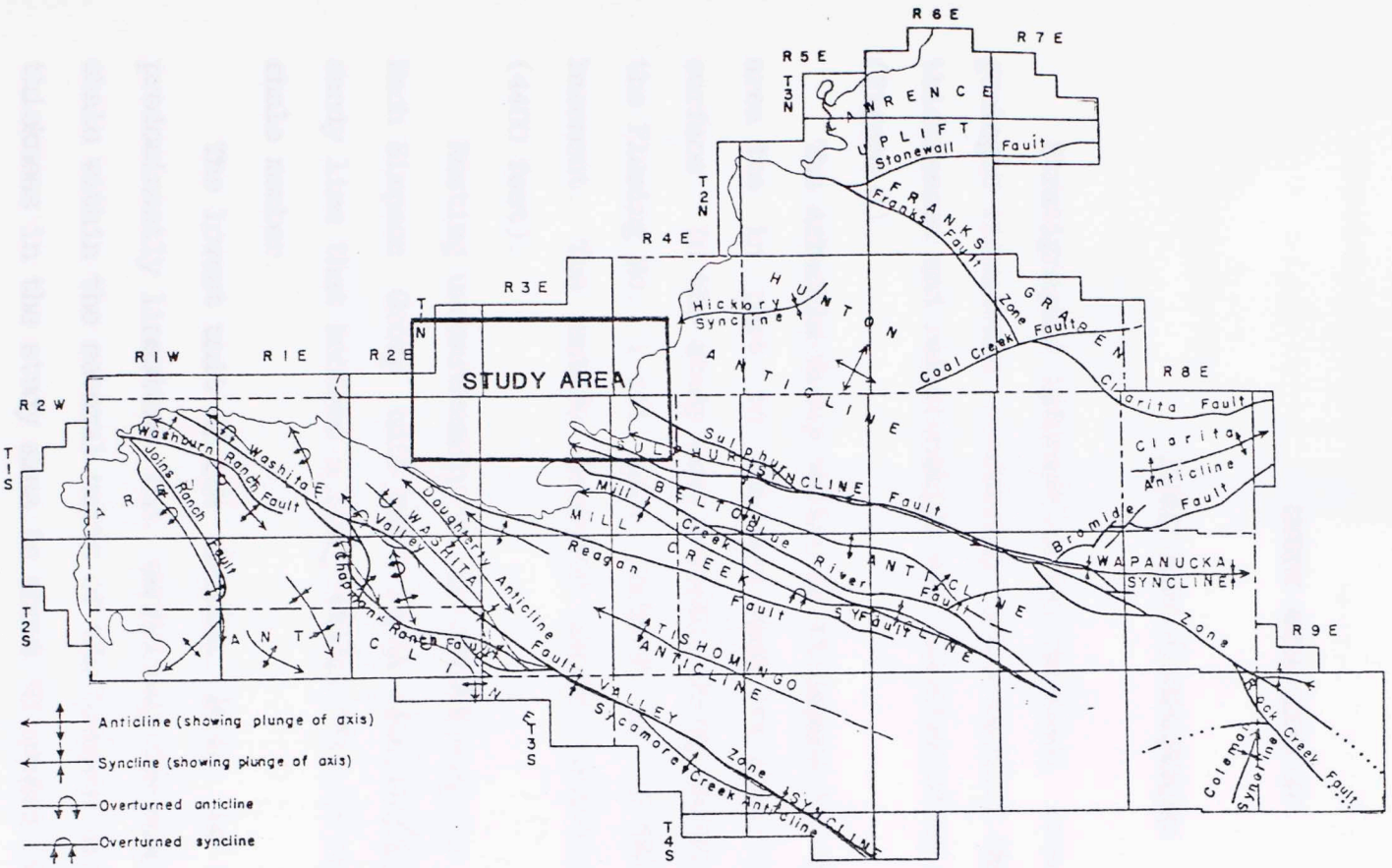

Figure 5. Tectonic map of major structural features in the Arbuckle Mountains. Study area outlined in center of map. Modified after Ham, 1954.

STUDY AREA GEOLOGY

Study Area Stratigraphy

Stratigraphic information was obtained from oil well logs and geologic literature concerning south-central Oklahoma. Stratigraphic thicknesses and relationships are illustrated as a stratigraphic column (Figure 6).

The Arbuckle Group varies in thickness in the Arbuckle Mountain area due in part to the fact that its upper contact is an erosional surface. In the study area Arbuckle Group thickness is determined from the Fleming No. 1 oil well located at 1N-3E-32 which drilled to basement. The entire Arbuckle Group section drilled is 1341 meters (4400 feet).

Resting unconformably on the Arbuckle Group is the Simpson Group. Each Simpson Group unit has a basal well-sorted sand and above that a sandy lime that becomes a limey shale, then is succeeded by a top-most shale member.

The lowest unit of the Simpson Group is the Joins Formation, predominantly limestone but exhibiting the most significant amount of shale within the several units of the Simpson Group. The average Joins thickness in the study area is about 76 meters (250 feet).

Next in upward progression is the Oil Creek Formation which consists of an upper limestone unit and a basal sandstone. The average

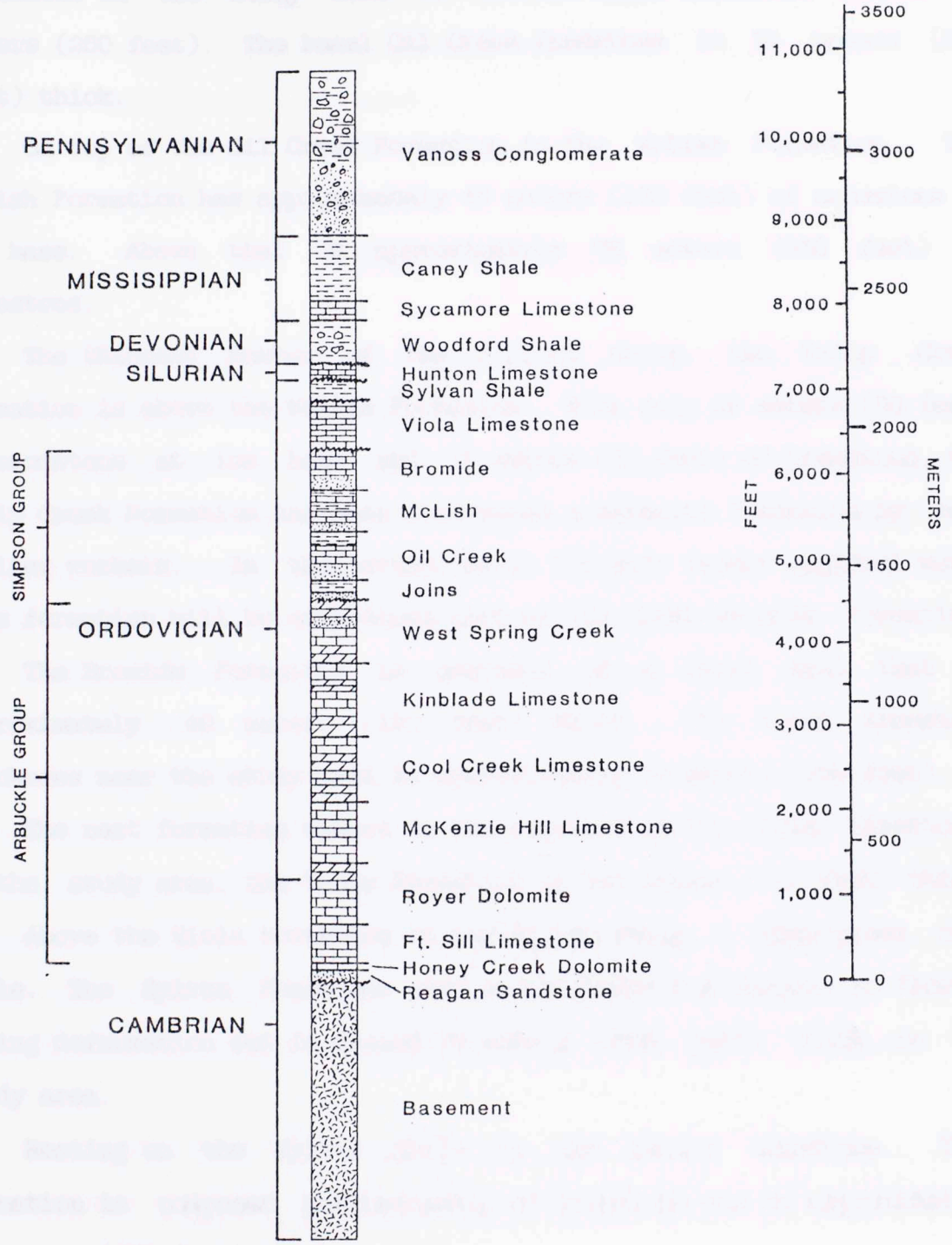

Figure 6. Stratigraphic Section for the area of the Chickasaw National Recreation Area.

thickness in the study area of the Oil Creek Limestone is about 76 meters (250 feet). The basal Oil Creek Sandstone is 91 meters (300 feet) thick.

On top of the Oil Creek Formation is the McLish Formation. The McLish Formation has approximately 45 meters (150 feet) of sandstone at its base. Above that is approximately 76 meters (250 feet) of limestone.

The thinnest member of the Simpson Group, the Tulip Creek Formation is above the McLish Formation. With only 15 meters (50 feet) of sandstone at its base and 15 meters (50 feet) of limestone, the Tulip Creek Formation has been considered a separate formation by some earlier workers. In this study, as in the more recent regional work, this formation will be considered part of the basal Bromide Formation.

The Bromide Formation is composed of a basal sand that is approximately 40 meters (130 feet) thick. The total limestone thickness near the study area is approximately 76 meters (250 feet).

The next formation upward in the sequence is the Viola Limestone. In the study area, the Viola Formation is 183 meters (600 feet) thick.

Above the Viola Formation is the Sylvan Shale, a gray-green clay shale. The Sylvan Shale can vary in thickness due largely to flowage during deformation but is around 76 meters (250 feet) thick in the study area.

Resting on the Sylvan Shale is the Hunton Limestone. This formation is composed predominantly of limestone and is approximately 76 meters (250 feet) thick.

The Woodford Shale lies above the Hunton Limestone. This formation consists almost exclusively of black shale. This thick shale is around 152 meters (500 feet) thick when a full noneroded portion is

found in the study area. Within a 16 kilometer (10 mile) radius of the study area rock younger than the Devonian Woodford Shale and older than the Late Pennsylvanian is absent.

Study Area Structure

Faulting in the Arbuckle Mountain region has geometries consistent with strike-slip, dip-slip, and overthrust faulting. In this study interpretation of the area accepts left-lateral, strike-slip faulting to be the dominant mechanism of deformation with long, north-west trending strike-slip regional faults (Tanner, 1966; Wickham, 1978; Wiltse, 1978; Booth, 1978; Haas, 1978; Tapp, 1988).

The North Sulphur Fault has a nearly linear trace (Plate 1) that begins just over 12.9 km (8 miles) southeast of Sulphur, Oklahoma and is covered by the Vanoss Conglomerate at a point less than 2.4 km (1.5 miles) east of the park. South of Sulphur, a fault, about parallel to the North Sulphur Fault, outcrops to the south into section 13 of township 1N range 3E. There are steeply northern dipping beds on the north side and gently western dipping beds on the south side of the fault (Plate 1); fault orientation in the subsurface is unknown.

SURFACE GEOLOGY

Vanoss Conglomerate is the predominant surface rock in CNRA and most of the immediate surrounding area. In a few places erosion has exposed underlying formations. Field reconnaissance was done in two areas (Figure 7) where these underlying formations are exposed. To signify a location as an outcrop data location, the prefix OC is used with a number to differentiate one location from another. Locations OC1, OC2 and OC3 are found southwest of CNRA and locations OC4 through OC17 are east of CNRA (Figure 7).

Locations OC1, OC2 and OC3 (Figure 8) are in the central part of the southwest quarter of 1S-3E-9 and the eastern part of the northwest corner of 1S-3E-16. There, along Rock Creek, several outcrops of lower Viola Limestone are found. The Viola Formation strikes N45W and dips N53 at location OC1.

Data locations OC2 and OC3 in section 16 are found in an eroded ravine. On the north side of the ravine (OC2), the rock is highly fractured. The strike at this location is N65W and the dip is N33. Twenty meters (60 feet) south of OC2 is OC3. At location OC3 the same rock is found as that at OC2 but is not fractured and strikes N55W and dips N45.

Steeply dipping beds and high rock damage seen in this area, as well as the fact that these outcrops are on trend with the fault zone forming the northern border of the Mill Creek Syncline, suggest

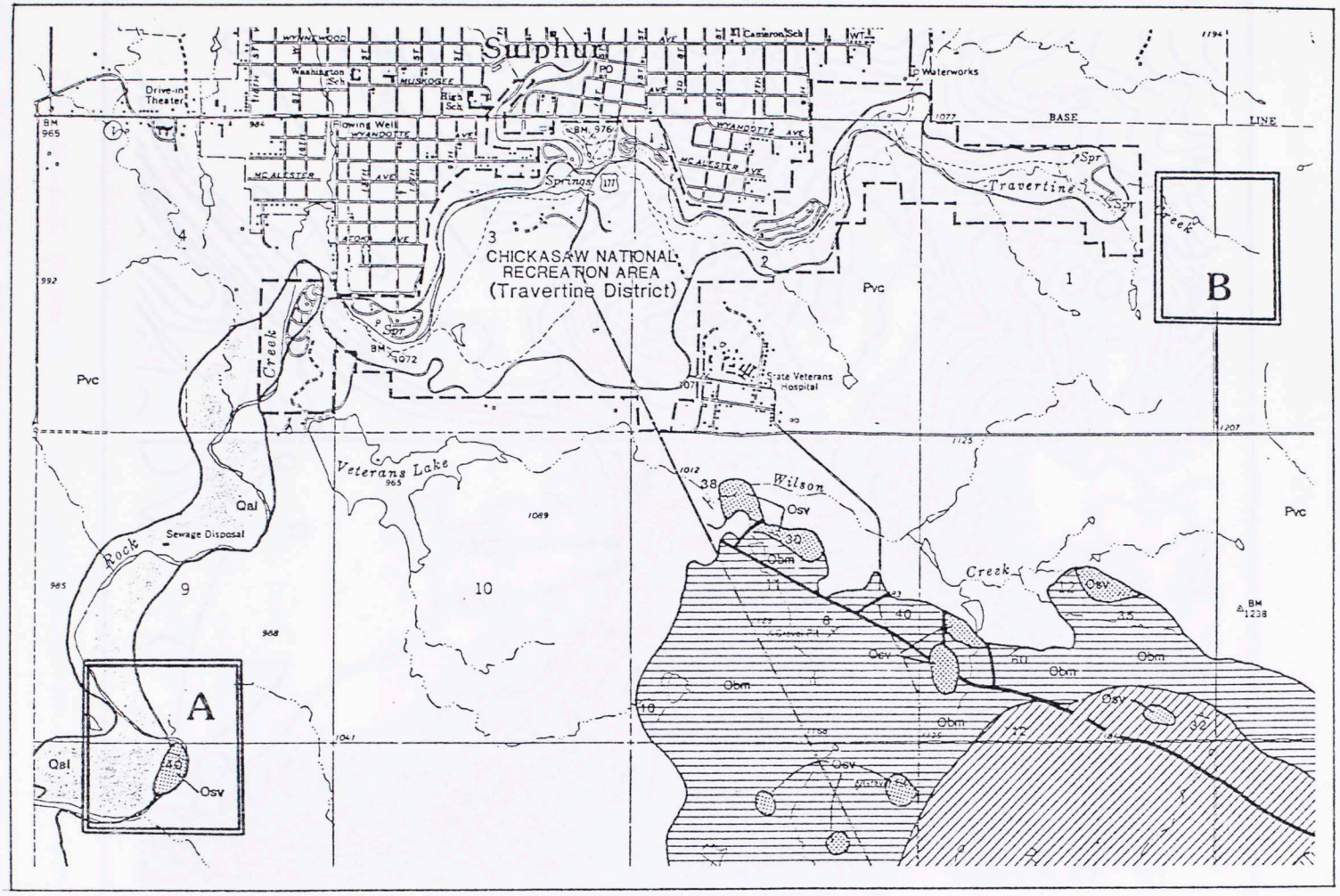

Figure 7. Map showing outcrop geology locations for A) locations OC1, OC2, and OC3 southwest and, B) locations OC4 thru OC17 east of CNRA. Dashed outline is of the Travertine District, Chickasaw National Recreation Area.

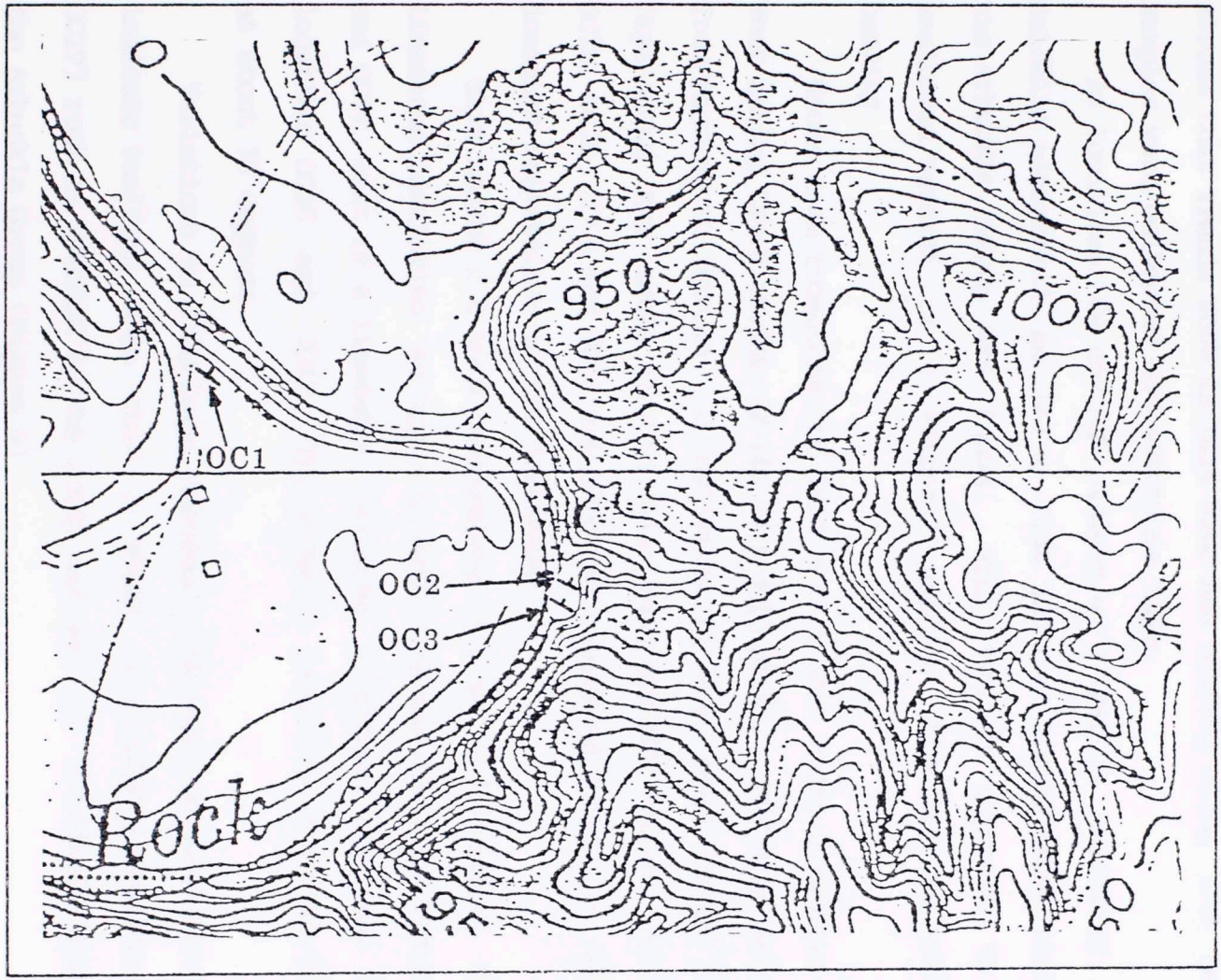

Figure 8. Map showing enlarged view of outcrop locations OC1, OC2, and OC3, southwest of CNRA. Contour interval, 10 feet.

faulting in close proximity to this area.

Locations OC4 through OC17 are just east of the eastern-most boundary of CNRA in 1S-3E-1 and 1S-4E-6 (Figure 9). The ephemeral stream that trends N65W in this area has outcrop along its bed where samples were collected and attitudes taken.

At locations OC4 and OC5 outcrop of a highly weathered sucrosic dolomite identified as being from the West Spring Creek Formation of the Arbuckle Group was found. This outcrop appeared to be the weathered remnant of a formerly massive limestone and exhibited no bedding.

Rocks from locations OC6-OC15 were a tan, muddy limestone from the West Spring Creek member of the Arbuckle Group. Outcrop here varies from massive to thinner, 10 centimeter (4 inch) thick bedded limestone. Dips along the north side of this creek are NNW and NW. At locations OC12, OC13, OC14 and OC15 the rock was shattered without a discernible dominant orientation to the fractures.

Thin bedded 3.8 to 5 centimeters (1.5 to 2.0 inches) white-gray limestone identified as upper Bromide rock was found at locations OC16 and OC17, east of a lineament dividing locations OC4 and OC5 from locations OC16 and OC17. The rocks at locations OC16 and OC17 dip SW at about 15 degrees.

Variations in lithilogy, deformed rock and juxtaposition of rocks indicate faulting such that a wedge of Bromide Formation (OC16 AND OC17) rock is bounded to the north and west by different portions of the Arbuckle Group (Figure 9).

The outcrop geometry and the approximate 26 degree dip of Simpson Group rock within the Sulphur Syncline indicates a northwest plunge of the structure. If this structure continues to plunge beneath the

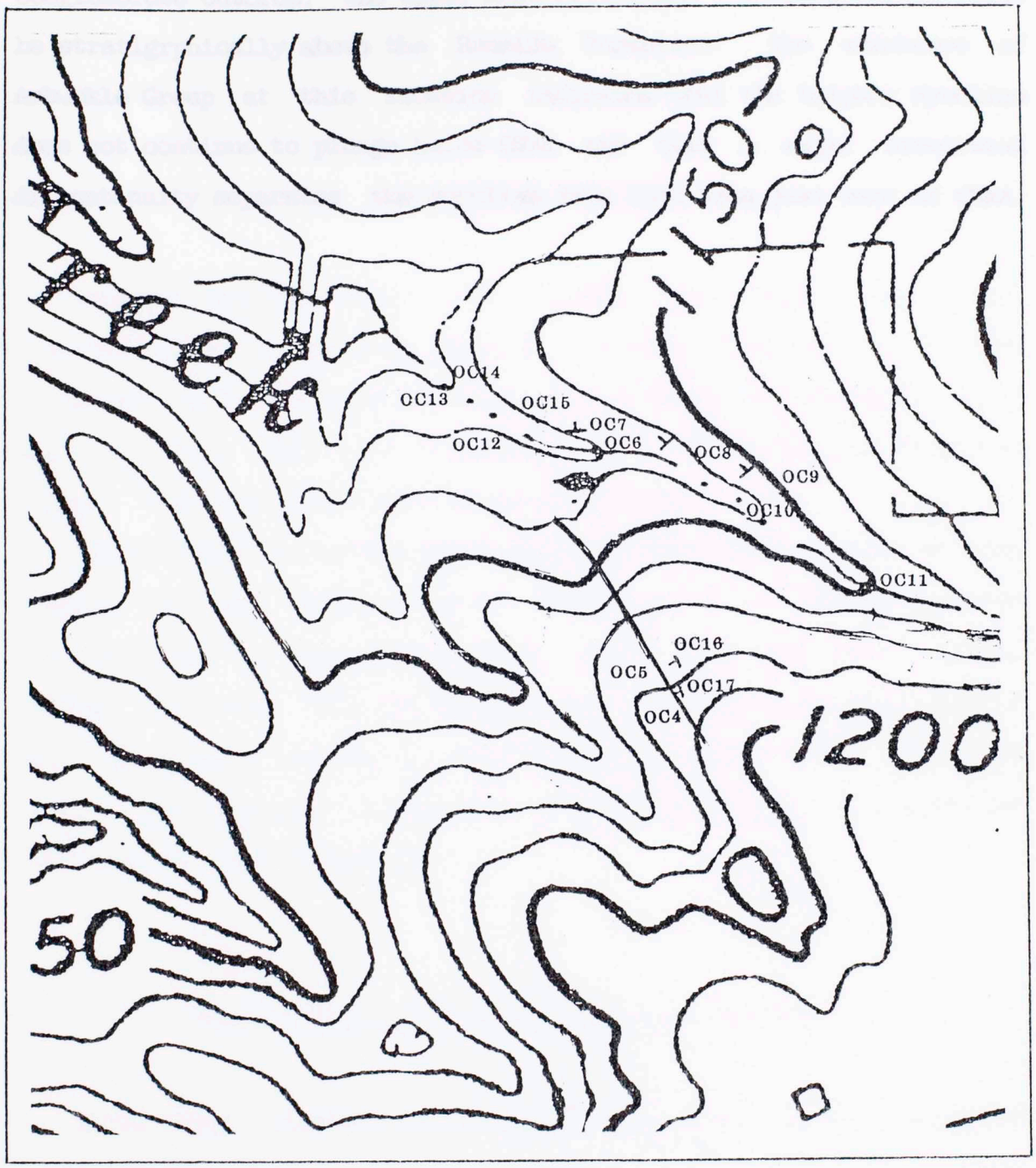

Figure 9. Map showing enlarged view of outcrop locations OC4 thru OC17, east of CNRA. Contour interval, 10 feet.

conglomerate outcrop, the upper-most Ordovician rock encountered would be stratigrphically above the Bromide Formation. The existence of Arbuckle Group at this location indicates that the Sulphur Syncline does not continue to plunge below CNRA and that a major structural discontinuity separates the syncline from this area just east of CNRA.

SUBSURFACE DATA

Geologic data that would give insight into geology below and adjacent to CNRA is extremely limited. Oil well data from west of CNRA is available and useful for inference of structural relationships below CNRA. Oil well logs are available for oil fields between Davis and Sulphur. The subsurface data are given in Table 1.

Records kept during the development of three water wells at the Oklahoma Gas and Electric power plant north of Sulphur provide subsurface data for the area north of CNRA. Two monitoring wells, known as the East Well and the West Well were drilled within CNRA in 1972. These wells provide the only lithologic data within the park itself. The majority of available subsurface data for this study was found west of CNRA (Figure 10).

Oklahoma Gas and Electric Company Water Wells

Three large industrial water supply wells were drilled north of Sulphur between August of 1951 and April of 1952 (Figure 11). Drill cuttings from the wells were examined microscopically by W. Ham and M.E. McKinley of the Oklahoma Geological Survey. The following summary is taken from McKinley's written sample report dated July 23, 1953.

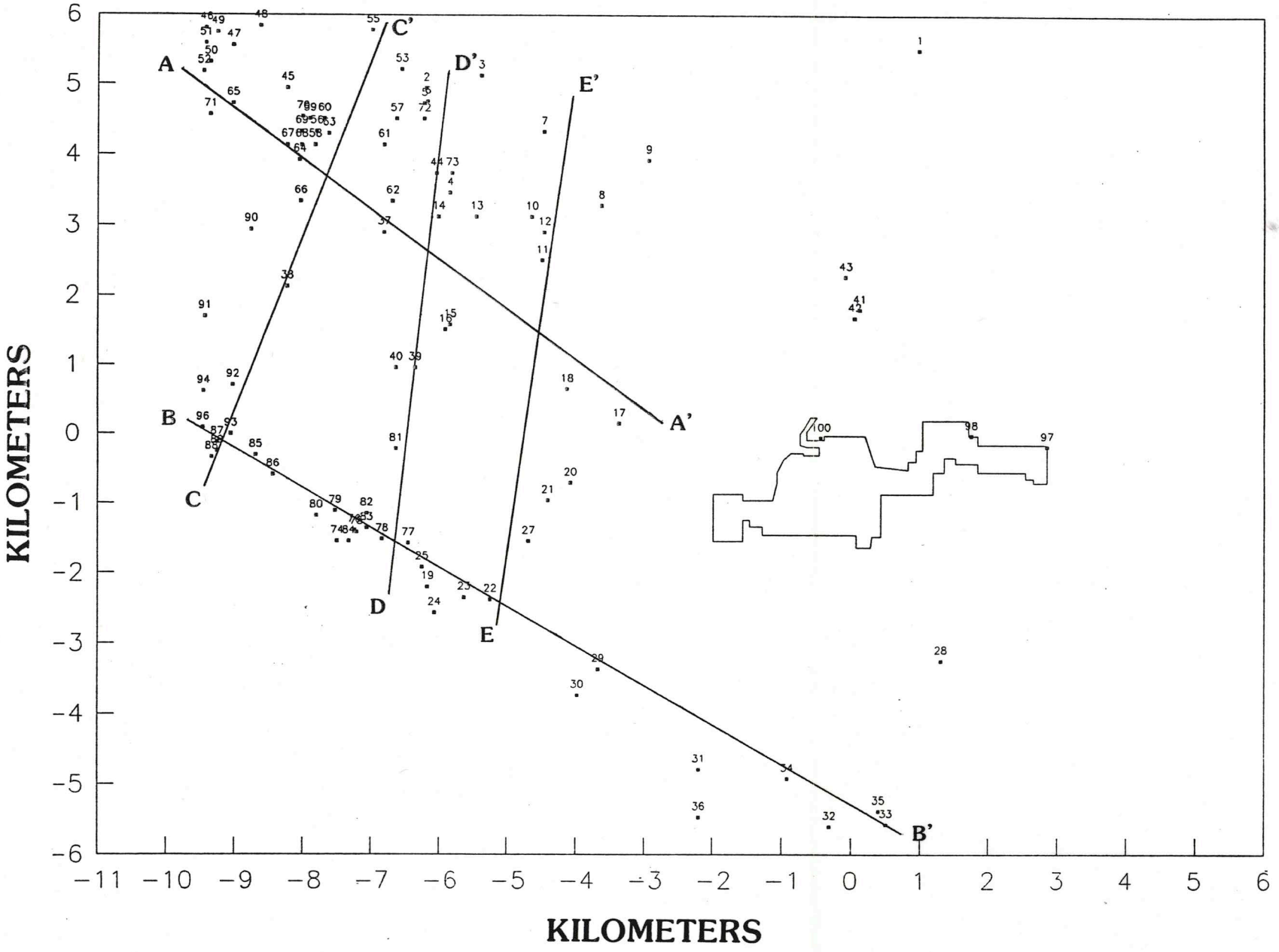

Figure 12. Map showing locations of geologic cross-sections. Outline is of theTravertine District, Chickasaw National Recreation Area. Origin of the coordinate system is the intersection of Oklahoma State Highway 7 and Oklahoma State Highway 177.

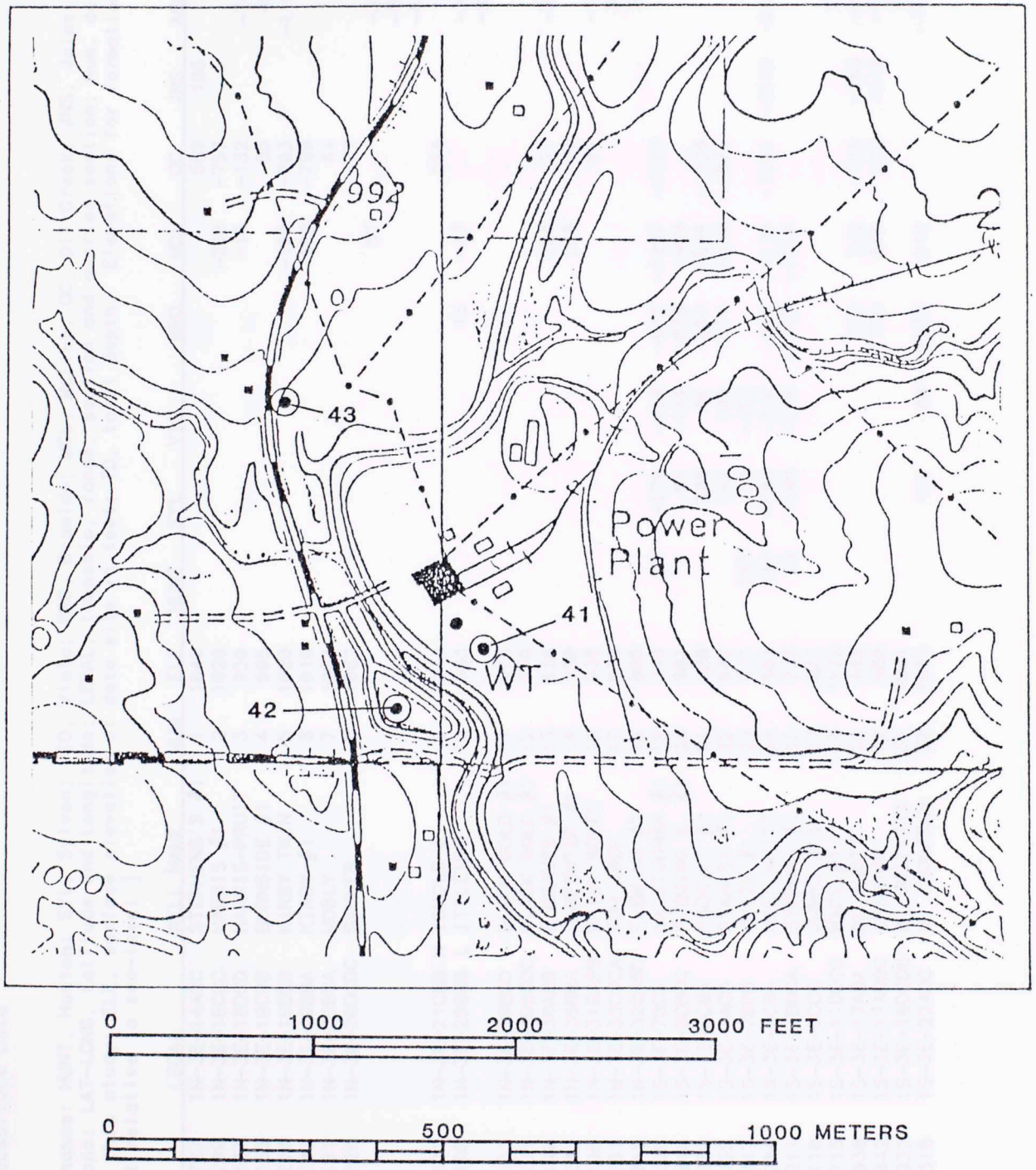

Figure 11. Map showing locations of the three Oklahoma Gas and Electric Company industrial water wells north of Sulphur, Oklahoma. Topographic contour interval, 10 feet.

Table 1.—Subsurface Data

[Formation names: HUNT, Hunton; SYL, Sylvan; VIO, Viola; BRO, Bromide; MCL, McLish; OC, Oil Creek; JNS, Joins. Abbreviations: LAT-LONG, Latitude and Longitude; LEGAL, township, range, section and quarter section; Num, data site number for this study; ELE, surface elevation of data site in feet; TD, total depth. Elevations for formation tops are in feet relative to sea-level.]

LAT-LONG	LEGAL	WELL NAME	NUM	ELE	HUNT	SYL	VIO	BRO	MCL	OC	JNS	ARB	TD
343321 0965727	1N-3E-14ACC	STEPHENS'S #1	1	1040						589	105		1000
343303 0970209	1N-3E-18CCC	HARRIS #1	2	1020					-268	-757			2081
343309 0970137	1N-3E-18DCD	HARRIS-PRUIT	3	950					-15	-132		-746	2068
343215 0970155	1N-3E-19CDB	BURNSIDE #1	4	995						55		407	1553
343256 0970210	1N-3E-19BBB	KIRBY TWIN	5	1020					-105	-703		-1194	1934
343257 0970208	1N-3E-19BBA	KIRBY #1	6	1010					-188	-799			2020
343243 0970101	1N-3E-20BCA	MOBLY	7	1004						64			1239
343209 0970028	1N-3E-20DCDC	BAHNER	8	1062						177			1755
									57			-390	1755
												-550	
												-630	
343230 0970001	1N-3E-21CBB N	ICHOLS #1	9	1074						554		164	1410
343204 0970108	1N-3E-29BBB L	ITTLETON	10	983				15	-47			-395	1988
												-895	
343144 0970102	1N-3E-29BCD	BLACK GOLD #1	11	976									1123
343157 0970101	1N-3E-29BBDC	BLACK GOLD #2	12	970									1190
343204 0970140	1N-3E-30ABB	E.GRAVES #1	13	936					266	71		-360	
343204 0970202	1N-3E-30BBA	CARPENTER #1	14	980					230	50			1118
343114 0970155	1N-3E-31BABB	DAISY WOLFE	15	936						81		-164	1425
343001 0970101	1N-3E-32CCCA	TOM JACK	17	970								370	800
343044 0970048	1N-3E-32CABD	FLEMING #1	18	995								395	5178
342912 0970208	1S-3E-7BCB	SA.STEDMAN #1	19	919	59	-179	-419	-935	-1267	-1793			3260
343000 0970046	1S-3E-5CBCC	FLEMING E. #1	20	981		81	-179	-619	-969				2226
342952 0970059	1S-3E-5CBA	PACKNIT #1	21	920		290	80	-390	-840	-1230			2155
342906 0970132	1S-3E-7ACD	STANLEY #1	22	949		249	109	-371	-810	-1251			2697
342907 0970147	1S-3E-7BDD	WHITE #1	23	977	297	77	-153						1614
342900 0970204	1S-3E-7CBA	NOEL WHITE	24	894	124	-106	-316	-676	-1126	-1581	-2229	-2456	3365
342921 0970211	1S-3E-7BBCA	STEDMAN #1	25	930	20	-380	-610	-1105	-1540				2900
342933 0970110	1S-3E-5CCC	JUMAS #15	27	896									460
342838 0965715	1S-3E-11DDCC	WADE #1	28	1178								278	1878
342834 0970030	1S-3E-17ABA	WL SCOTT	29	945				725	345	-135	-565	-805	2210
342822 0970042	1S-3E-17ADBC	CHEVRON	30	985				760	665	235	-215	-435	1431
342748 0965932	1S-3E-16DCDB	W. GRIFFITS	31	1041								460	2500
342722 0965818	1S-3E-22ADC	M. THOMPSON	32	1064		414	64	-538	-916			-1071	2650

Table 1.—Subsurface Data—Continued

LAT-LONG	LEGAL	WELL NAME	NUM	ELE	HUNT	SYL	VIO	BRO	MCL	OC	JNS	ARB	TD
342723 0965746	1S-3E-23BDC	G. SNETHEN	33	1071		444	194	-307	-776	-1256	-1806		2876
342744 0965842	1S-3E-22BAAA	JG GRIFFITS	34	1054							974	564	2180
342729 0965750	1S-3E-23BCAA	PRUITT #1	35	1071		671	411	-129		-1164		-1559	2735
343157 0970233	1N-2E-25ABD	EB BROOKS	37	975						-563			1892
343132 0970233	1N-2E-26DAC	EMERSON #1	38	1020				-310	-450	-930		-1470	2550
343054 0970215	1N-2E-36ADD	LITTLETON #1	39	919						-26		-441	2500
343054 0970226	1N-2E-36ADC	M. THOMPSON	40	941									1000
343122 0965802	1N-3E-26CCBC	OGEW #1	41	973								608	532
343118 0965804	1N-3E-27DDDD	OGEW #2	42	970						587		419	841
343132 0965810	1N-3E-27DACA	OGEW #3	43	969								639	868
343224 0970203	1N-3E-19CBD	JACK #2	44	1010									1287
343303 0970329	1N-2E-14DDC	1-14 KING	45	936						-454			1800
343331 0970416	1N-2E-14BCC	JAMESON #5	46	921						-914			2200
343323 0970400	1N-2E-14CAB	PARNELL #3	47	942						-938			2226
343332 0970345	1N-2E-14AC	RATLIFF #1	48	1005						-905			2396
343329 0970409	1N-2E-14BCD	JAMESON #2	49	947						-857			2206
343315 0970413	1N-2E-14CBD	JAMESON #3	50	956						-904			2135
343324 0970416	1N-2E-14CBB	JAMESON #1	51	915						-845			2250
343311 0970417	1N-2E-14CCB	PARNELL #1	52	934						-886			2194
343312 0970223	1N-2E-13DDA	MCCLURE #1	53	1024					-456	-796		-1316	2508
343348 0970225	1N-2E-14AAB	CAPE #1	54	1055						-755	-1305		2538
343330 0970240	1N-2E-13ACC	MOSS #1	55	984						-836			2170
343243 0970312	1N-2E-24BCB	WADE #2	56	945						-295			1540
343249 0970226	1N-2E-24AAC	BURNSIDE #1	57	1005					-335	-830			2011
343237 0970313	1N-2E-24BCC	WADE #1	58	918					-442				1512
343249 0970316	1N-2E-24BBC	WOMMACK #3	59	918						-282			1750
343249 0970308	1N-2E-24BBD	WOMMACK #1	60	956						-344			1575
343237 0970233	1N-2E-24ACD	BURNSIDE #1	61	972					-558	-935			2250
343211 0970228	1N-2E-24DDC	BURNSIDE #1.1	62	1001						-516			1944
343242 0970305	1N-2E-24BCA	WOMMACK #2	63	953						-527	-817		1941
343230 0970322	1N-2E-23DAA	MILLER #1	64	931								-1014	2005
343256 0970400	1N-2E-23BAB	LOW #1	65	940						-560	-1163	-1247	2285
343211 0970321	1N-2E-23DDD	EMERSON #1	66	910						-885			2226

Table 1.—Subsurface Data—Continued

LAT-LONG	LEGAL	WELL NAME	NUM	ELE	HUNT	SYL	VIO	BRO	MCL	OC	JNS	ARB	TD
343237 0970329	1N-2E-23ADC	PURTLE #2	67	899						-343			1545
343237 0970321	1N-2E-23ADD	PURTLE #1	68	900						-320			1567
343243 0970321	1N-2E-23ADA	PURTLE #3	69	901						-320			1498
343250 0970320	1N-2E-23AAD	PURTLE #4	70	922						-318			1540
343251 0970413	1N-2E-23BBC	LOW JILL #1	71	948					-512	-902			2442
343249 0970210	1N-2E-19BBC	SOOD	72	1015					-200	-687			1965
343224 0970154	1N-3E-19CAC	DAYTON #1	73	987						-43			1560
342933 0970300	1S-2E-1CDC	WOODRUFF #1	74	991	-867	-1097	-1307	-1817	-2282	-2442			4000
342937 0970249	1S-2E-1CDAD	HALE #3	75	1020	-766	-1031	-1246	-1721	-2176	-2341			3929
342938 0970250	1S-2E-1CDA	HALE #1	76	1005	-785	-1070	-1285	-1780	-2235	-2335			3976
342932 0970219	1S-2E-1DDD	NACE #1	77	910	-618	-892	-992	-1418	-1872	-2252			3724
342934 0970234	1S-2E-1DCD	NACE #3	78	945	-523	-814	-1014	-1495	-1954				3174
342947 0970301	1S-2E-1CAC	HALE #2	79	999	-865	-1095	-1285	-1795	-2099	-2576	-3141		4160
342945 0970312	1S-2E-1CBD	ARMS #1	80	962	-827	-1072	-1287	-1762	-2237	-2707			4260
343016 0970226	1S-2E-1AA	GOSS #1	81	960		-298	-486	-956		-1915			3480
342946 0970243	1S-2E-1DBC	HARR-ARMS	82	955	-750	-1057	-1275		-2138	-2453	-2968		3940
342939 0970243	1S-2E-1DCB	NACE #2	83	980	-671	-930	-1141	-1783	-2086	-2633			3930
342933 0970253	1S-2E-1CDD	WOOD #1	84	1011	-757	-1003	-1220		-2594	-2756			3868
343013 0970347	1S-2E-1ABC	BRASSFIELD	85	954	-1618	-1894	-2110		-2858	-3188			4520
343004 0970337	1S-2E-2AC	COOPER #2	86	958	-1474	-1714	-1870		-2716	-3166			4515
343019 0970409	1S-2E-2BBA	CHAFFIN UNIT	87	921		-1848	-2033						3543
343012 0970412	1S-2E-2BBD	MORRISON	88	934	-1746	-2008	-2215						3526
343015 0970409	1S-2E-2BBD	MORRISON #2	89	923	-1759	-2029	-2223						3373
343158 0970350	1N-2E-26BAD	CRAWFORD #1	90	935						-1024			2380
343118 0970416	1N-2E-26CCC	BROWN #1	91	922				-520	-998				2000
343046 0970400	1N-2E-35CAB	M.C.CHAFFIN	92	946	-877	-1275	-1487		-2679	-3168			4640
343023 0970401	1N-2E-35CDC	2-A CHAFFIN	93	949	-2239	-2479	-2599	-2979					4004
343043 0970417	1N-2E-35CBB	CHAFFIN #1	94	945	-1017	-1379							4000
343026 0970417	1N-2E-35BBB	CHAFFIN EST.	96		-1748	-2046	-2266	-2591		-3379			4703
343017 0965614	1S-3E-1ABA	EAST OBSERV.	97	1140								1020	230
343022 0965657	1S-3E-1BBB	WEST OBSERV.	98	1080								930	420
343021 0965823	1S-3E-3ABA	VENDOME	100	950									365

In the area of these three wells the outcropping rock is the Vanoss Formation. The base of Vanoss Formation in Well 41 (OGE well No. 1), is at a depth of 110 meters (360 feet). There, the Vanoss Formation rests unconformably on the West Spring Creek Formation of the Arbuckle Group. This formation is represented in this well by a sequence of fine-crystalline cream and tan, partly laminated, sandy dolomite. Total depth of the well is 162 meters (532 feet).

Well 42 (OGE well No. 2) is started in the Vanoss Formation. In this well, the Vanoss Formation rests unconformably on the eroded surface of the sandstone portion of the Oil Creek Formation at a depth of 115 meters (377 feet).

In this well, the Oil Creek Formation (Simpson Group) consists of 52 meters (173 feet) of sandstone and dolomitic sandstone with thin 0.75 to 3 meter (2-10 feet) thick units of sandy dolomite. Base of the Oil Creek Sandstone is at a depth of 168 meters (551 feet) where normal stratigraphic sequence is maintained as it rests on the West Spring Creek Formation of the Arbuckle Group. Represented by 87 meters (287 feet) of samples, the West Spring Creek Formation is composed of fine-crystalline cream and tan sandy to very sandy dolomite. The well is completed in a West Spring Creek dolomite at a total depth of 256 meters (841 feet).

Well 43 (OGE well No. 3) is started atop the Vanoss Formation. The Vanoss Formation extends to a depth of 100 meters (330 feet) and there rests unconformably on the West Spring Creek Formation of the Arbuckle Group.

West Spring Creek Formation is represented in this well by fine-crystalline cream and tan, partly laminated dolomite containing sporadic intervals of very sandy dolomite 3 to 5 meters in thickness.

The well is completed at a depth of 265 meters (868 feet) in a dolomitic unit of the West Spring Creek Formation.

Examination of drillers lithological logs, provided by the Oklahoma Gas and Electric Company, indicate little correlation of units in the Vanoss section between the three wells. This lack of similarity in such a small area could be due to the high energy, rapidly changing current directions characteristic of conglomerate deposition. Below the conglomerate, wells 42 and 43 have similar thick sections of white limestone. Well 41 has very different lithology than either well 42 or 43.

Because the Vanoss Conglomerate rests on West Spring Creek Formation (Arbuckle Group) in wells 41 and 43, and erosion of the West Spring Creek Formation previous to Vanoss Conglomerate deposition can be assumed, location in the Arbuckle Group section is uncertain in these two wells. In well 42 the first occurrence of Arbuckle Group is known to be the top of the West Spring Creek Formation. Given this information it is seen that at least 64 meters (211 feet) of Oil Creek Formation section is missing from well 41 relative to well 42. Though location in the section is unknown in well 41, if it is assumed that the Arbuckle-Vanoss interface is at the top of the West Spring Creek Formation here, a minimum southwest dip of 22 degrees for the West Spring Creek Formation would be required to explain this geometry by dip alone. If the Vanoss-Arbuckle contact in well 41 is not the top of the West Spring Creek Formation, dip between wells 41 and 42, could be significantly greater than 22 degrees. This raises the possibility of a fault between these two wells. Such a fault would underlie Rock Creek below the creek segment that trends approximately N35W (Figures 2 and 11). But the fault could vary in trend nearly 90 degrees if wells

41 and 43 are considered to be on one side of the fault and well 42 on the other.

Outcrop southeast of CNRA (Plate 1) suggests that the Sulphur Syncline plunges beneath CNRA and the city of Sulphur. If this syncline were to continue to plunge below these well sites, the Arbuckle Group would be encountered at a much greater depth than it is. The Oklahoma Gas and Electric Company water well data shows that this syncline does not extend to the area beneath wells 41, 42 or 43.

East and West Observation Wells

Two wells were drilled in August of 1972 within CNRA to monitor ground-water levels (Figure 2). These wells were developed to determine if heavy pumpage adjacent to the park might be adversely affecting water levels and spring flows within CNRA. The following information regarding depths and lithology was taken from a letter dated November 6, 1972, from James Irwin, District Chief, U.S. Geological Survey (USGS) to Garland Moore of the National Park Service (NPS). The letter was presented in fulfillment of an agreement between the USGS and the NPS.

The 'East Well' (No. 97) is located in the northeast quarter section of 1S-3E-1 (Figure 2). This well was started in the conglomerate member of the Vanoss Formation. Samples from the upper 37 meters (120 feet) of this hole represented typical rock types occurring in the conglomerate member of the Vanoss Formation. The samples from 37 meters (120 feet) to 70 meters (230 feet) are typical of the rock types occurring in the West Spring Creek Formation of the Arbuckle

Group.

The 'West Well' (No. 98) is located in the northwestern corner of 1S-3E-1 (Figure 2). This well was started in the Conglomerate Member of the Vanoss Formation with samples similar to those in well 97. These samples of the upper 45 meters (150 feet) consisted of Vanoss Conglomerate. Samples between 45 meters (150 feet) to 128 meters (420 feet) are primarily dolomite typical of the West Spring Creek Formation of the Arbuckle Group.

The fact that these two wells both are completed in the West Spring Creek Formation of the Arbuckle Group is significant. If the Sulphur Syncline continues to plunge below CNRA as previously believed, these two wells should be completed stratigraphically above the Viola Limestone. Data indicates that at least 488 meters (1600 feet) of section is missing from the two wells relative to nearby outcrop. This can be accounted for only by inference of a fault between the two wells in CNRA and the Simpson Group outcrop within the Sulphur Syncline to the southeast (Plate 1).

Oil Well Data

Oil well logs are generally available for sites west of the study area (Figure 10). These logs provide depths to formation tops, formation thicknesses and formation characteristics. The majority of these logs provided spontaneous potential and resistivity curves. Though some distance from the specific area of interest, these oil well logs provide control on the major structures in the area. Used with outcrop information from east of CNRA, gravity, magnetic and water well data in the park vicinity, the major structural relationships can be extrapolated to areas of little or no data.

Cross-sections

Using the oil well logs, five cross-sections, a structure contour map of the top of the Oil Creek Formation and a map of the Pennsylvanian subcrop were constructed. Due to well distribution and structural complexity these geologic cross-sections have some inherent limitations and can only illustrate general trends rather than specific relationships. Collapse of the well data to lines of cross-section (Figure 12) resulted in graphic distortion such that the illustrations do not reflect true subsurface relationships along a particular line of cross-section. Since these cross-sections were constructed to illustrate major trends and relationships, correlation of faults from one well to another is not attempted and is considered beyond the scope

of this study.

On Cross-section A-A' (Plate 2), a general northwest gentle dip of rocks can be seen with wells 17 and 18 encountering the Arbuckle Group in contact with the Vanoss Conglomerate. Faults are inferred between well 62 and 4, and wells 15 and 18 by formation offset.

On Cross-section B-B' (Plate 3), similar thickening of the conglomerate is indicated to the northwest as indicated on cross-section A-A'. The Pennsylvanian base rests on rock significantly farther up section than in cross-section A-A'. The general northwest dip illustrated in cross-section B-B' is in the same direction as cross-section A-A' but steeper.

Faults have been inferred on cross-section B-B' between wells 29 and 31 and wells 34 and 32. The fault inferred between wells 29 and 31 is based on outcrop at locations OC1, OC2 and OC3 (Figure 8). Considering the outcrop to be lower Viola, using locally known formation thickness, and placing the bottom of the Viola as the outcrop, results in the extrapolated subsurface relation (between wells 29 and 31) illustrated by cross-section B-B' (Plate 3).

On Cross-section C-C' (Plate 4) faults have been interpreted to be between wells 93 and 92, and wells 92 and 38. An anticlinal feature is indicated by wells 66, 67, 56, 60 and 57. Offset between wells 38 and 92 is 683 meters (2240 feet). Offset between wells 93 and 92 is 229 meters (750 feet).

On Cross-section D-D' (Plate 5) faults have been interpreted to be between wells 81 and 39 and between wells 15 and 37. The offset between well 81 and 39 is 442 meters (1450 feet). The offset between well 15 and well 37 is 244 meters (800 feet). Between these two faults is what appears to be a southward dipping horst block. Two data

locations and two-dimensional aspect of the illustration precludes definite identification of this feature as a horst.

On Cross-section E-E' (Plate 6) faults have been interpreted to be between wells 20 and 18 and between wells 18 and 11. An offset between well 20 and 18 is at least 853 meters (2800 feet). The offset between wells 18 and 11 is approximately 488 meters (1600 feet).

Subsurface Maps

Two maps, constructed using the oil well log data, are valid only for delineation of trends. Not all well logs were used, and only locations where specific horizons were identified with certainty were used. The horizon for the structure contour map of the top of the Oil Creek Formation is the contact between the basal McLish sandstone and the top-most shale portion of the Oil Creek Formation. Although the Oil Creek Formation is found in many wells, only those with a clearly identifiable contact were used in map construction. Likewise, only wells that showed the Pennsylvanian basal unconformity and where the lithology below this contact could positively be identified were used to construct the Pennsylvanian subcrop map.

These data criteria account for the discrepancies between the cross-sections, the structure contour map of the top of the Oil Creek Formation and the Pennsylvanian subcrop map. Some contour geometries are artifacts of data distribution of these computer generated maps. These two maps provide trend information but due to low data density, they cannot be considered definitive.

Structure Contour Map of Top of the Oil Creek Formation

Fifty-six subsurface data locations were used in construction of the structure contour map of top of the Oil Creek Formation (Figure 13). A strong contour gradient northwest of the western edge of CNRA trends N70W and is the most the most prominent feature on this map. Maximum north-south elevation difference across this gradient of about 640 meters (2100 feet) feet is found between data locations A (-9.0,0.75) and B (-8.15,2.25). South of this feature the data indicates a downward slope from just south of CNRA to the northwest. The trend of the contours in the region south of the NW trending feature is approximately N30E.

To the north of the N70W trending feature is a high labeled C (-8.0,4.5). Also north of the main feature is a contour gradient labeled D, trending N28E. The region east of this gradient has significantly higher Oil Creek Formation elevation than the area west of the main, northwest trending gradient.

Pennsylvanian Subcrop Map

The subcrop map was constructed using 87 data sites (Figure 14). Like the structure contour map of the top of the Oil Creek Formation, a high contour gradient trending N65W is seen northwest of the western boundary of CNRA, labeled A (-6.5,1). Northeast of this feature appears a broad and flat area, but due to lack of data control, this is highly interpretive. From southwest of CNRA, B, (-4.0,-4.0) to C, (-8.5,0.25) westward decrease of subcrop elevation is indicated with

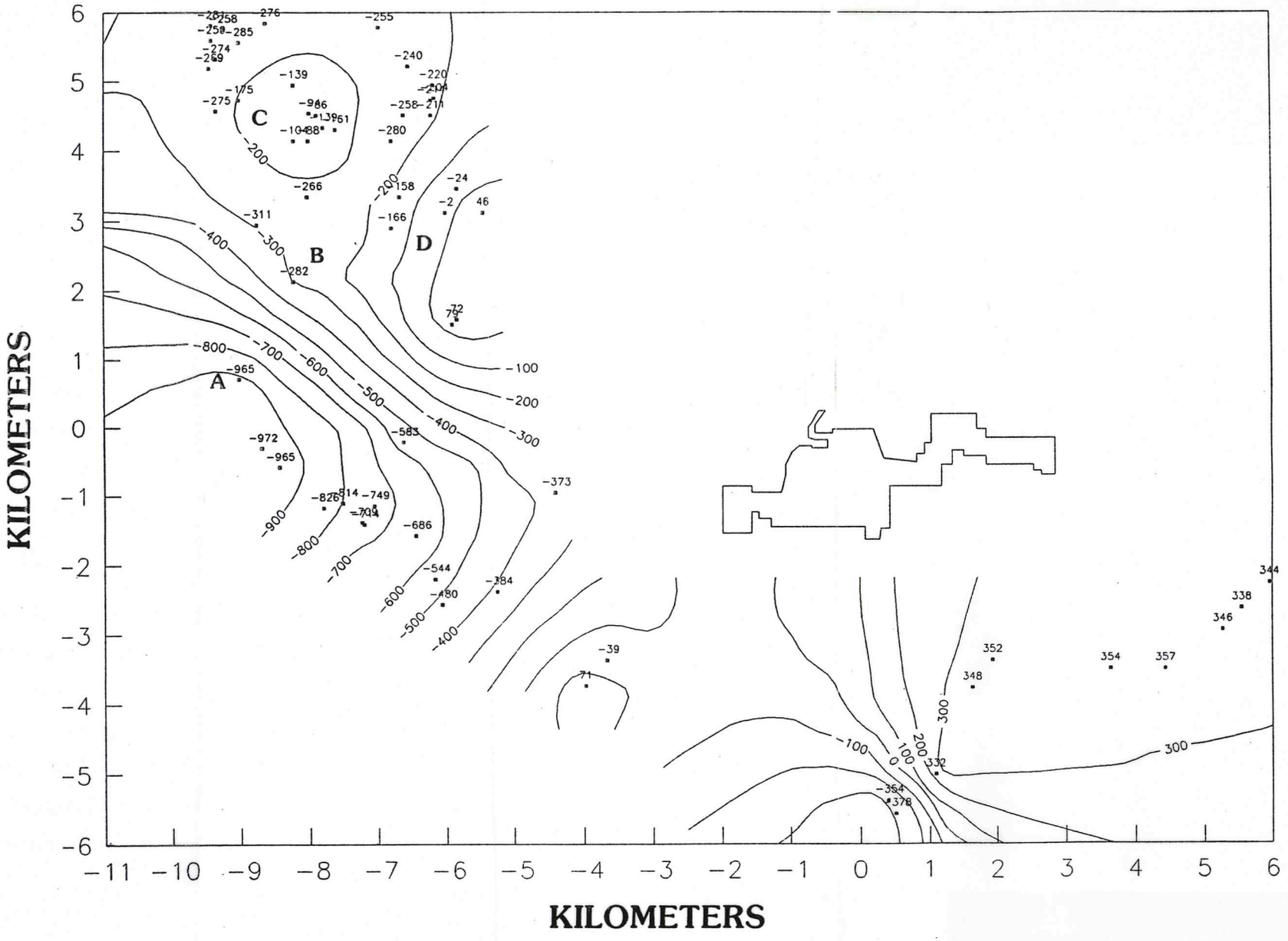

Figure 13. Structure contour map of top of the Oil Creek Formation west of Chickasaw National Recreation Area. Outline is of the Travertine District. Origin of the coordinate system is the intersection of Oklahoma State Highway 7 and Oklahoma State Highway 177. Elevation is in meters referenced to sea-level. Contour interval, 100 meters.

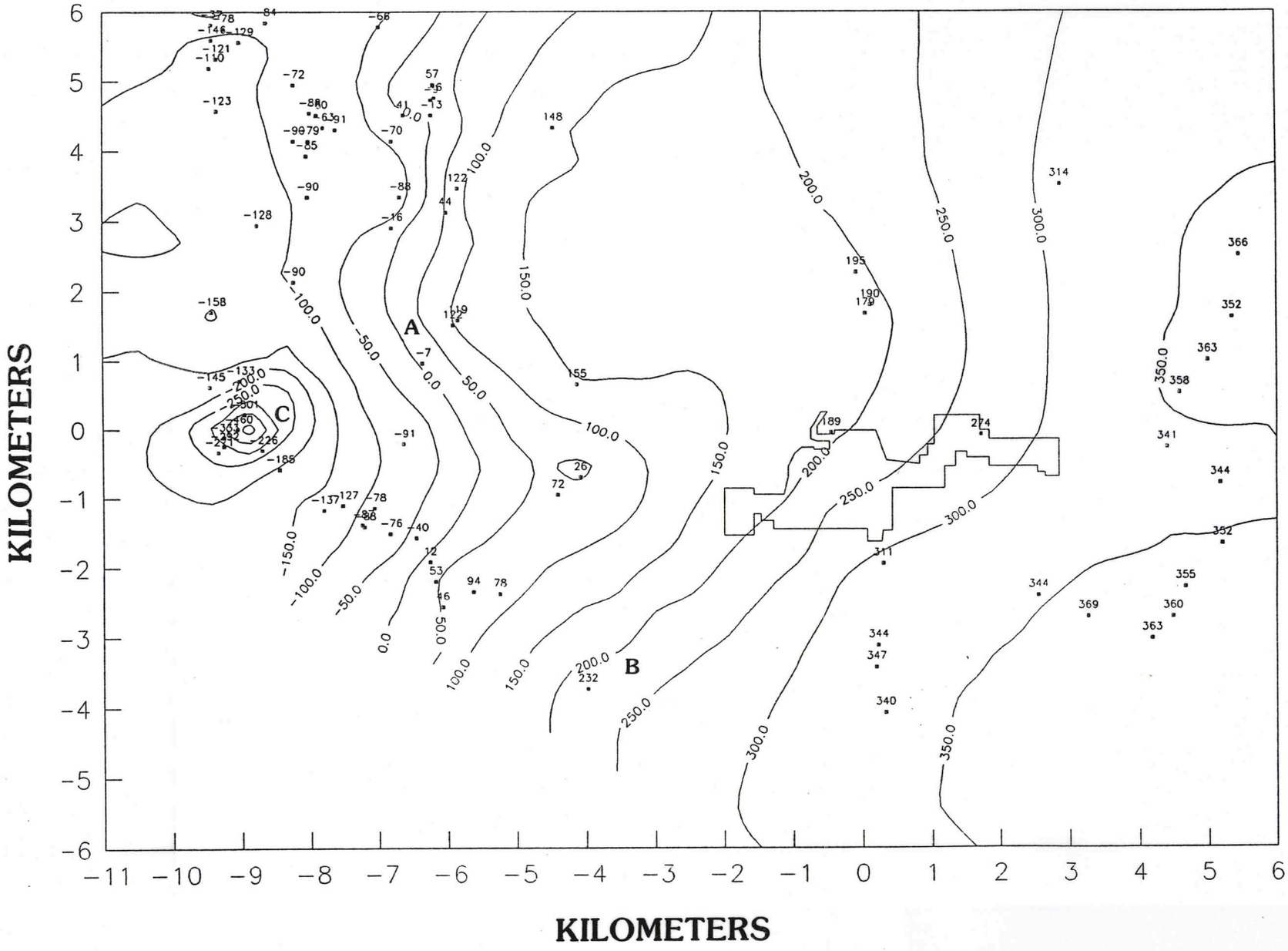

Figure 14. Map showing elevation of Pennsylvanian subcrop in the area of Chickasaw National Recreation Area. Outline is of the Travertine District. Origin of the coordinate system is the intersection of Oklahoma State Highway 7 and Oklahoma State Highway 177. Elevation is in meters referenced to sea-level. Contour interval, 50 meters.

contour gradient trends ranging from N30E just southwest of CNRA to about N10E, west of the western boarder of CNRA at the location labeled C.

Northwest of CNRA is seen a N25E trending contour gradient that separates a region of higher values to the east from those in the northwest corner of the map.

Discussion of Subsurface Maps

Similarity in geometry of both the Pennsylvanian subcrop map and the structure contour map of the top of the Oil Creek Formation indicate correlation between paleotopography and the predeposition structure.

The location and slight variation in trend of the prominent contour gradient west of CNRA on both maps suggests a major fault at this location. The downthrown block to the south of this fault dipping northwest is evident on both maps. A N28E trending gradient is seen at the same location northwest CNRA on both maps. Both maps show a relative high east of this trend with lower elevations to the west. Examination of these two maps indicate 1) faulting previous to Pennsylvanian deposition, and 2) paleotopography correlates with structures indicating fault domination of the depositional surface.

COLLECTION AND REDUCTION OF GRAVITY AND MAGNETIC DATA

To gain understanding of the subsurface in the study area, where no previous data were available, a gravity and magnetic survey was initiated. This survey was designed to provide some indication of the structural geometry in a two-dimensional map view sense. Furthermore, construction of a density model, developed from the gravity data in a location of known geology, allows development of models for areas of no geologic data.

Location of Gravity and Magnetic Survey

The gravity and magnetic survey covers an area of approximately 125 square kilometers. Station locations are numbered in the chronological sequence that each station was occupied. One hundred and fifty-four stations where occupied in August of 1987 (Figure 15). Later more locations were occupied as further data needs became evident. In January of 1988, 20 additional readings were taken (stations 154 through 173). In May of 1989, 10 additional readings were taken (stations 174 through 183).

Most readings were taken along section-line roads. Since the dominant structural trend of the region is N65W, quarter mile spacing for stations along north-south traverses was chosen to best delineate

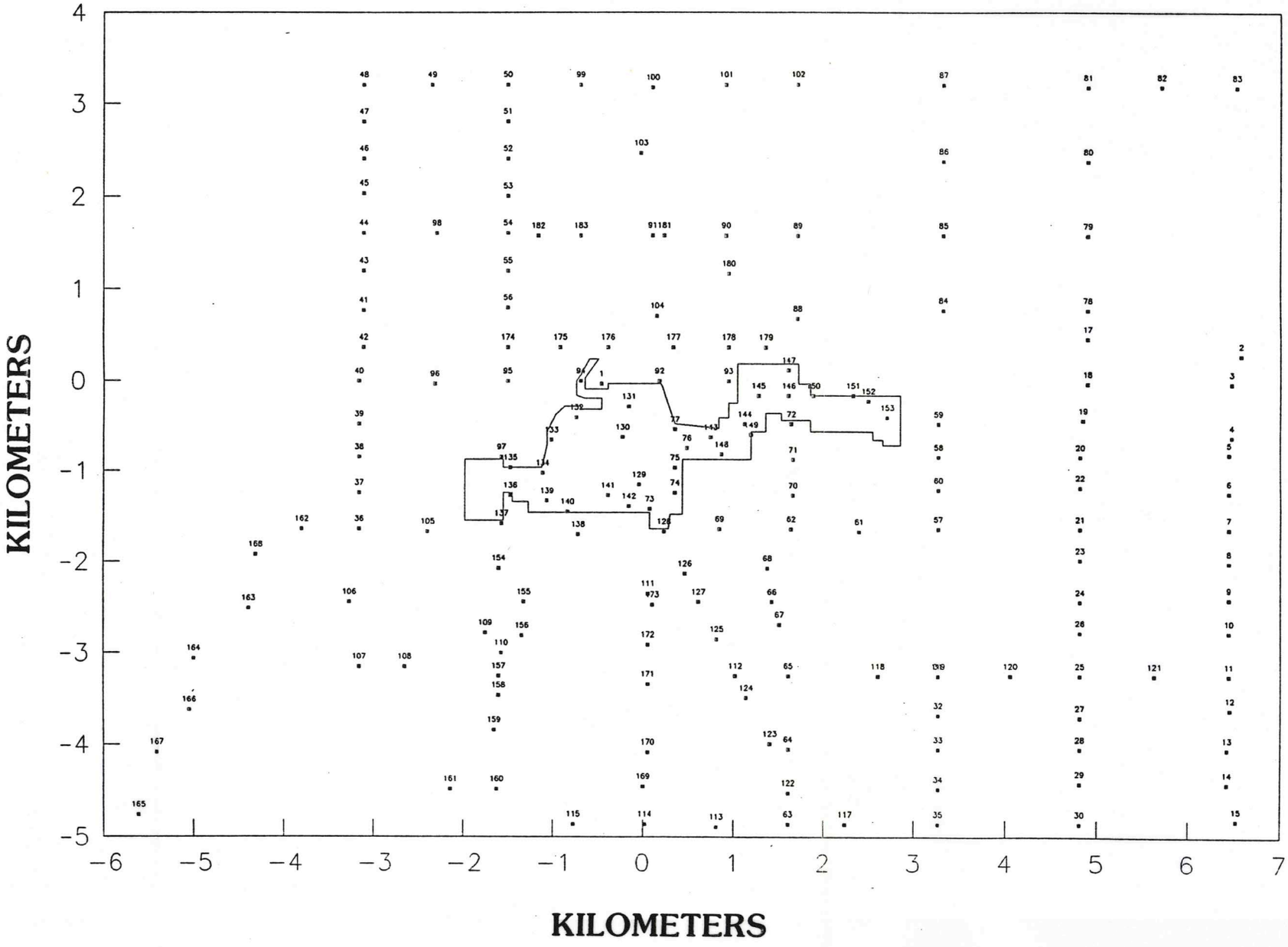

Figure 15. Map showing gravity and magnetic data stations in area of Chickasaw National Recreation Area. Outline is of the Travertine District, Chickasaw National Recreation Area. Origin of the coordinate system is the intersection of Oklahoma State Highway 7 and Oklahoma State Highway 177.

the underlying structures. Along east-west roads data locations were at half-mile spacings. Off road data locations were chosen where the location could be verified from a topographic map. Fence-line intersections, ponds and hilltops were used to verify location at these sites.

Data Acquisition

The Vendome Well (station #1) was used as the base station for this survey. As such, this location was occupied at the beginning and end of data gathering periods (loops). Data gathering loops spanned no more than 3 hours so that a linear drift correction could be made. This drift correction involves using the rate of change between the first and last readings of the loop (at the base station) to correct intermediate data readings. In this way the effects of instrument drift and tidal effects are mitigated. Because this time span is small in contrast to the diurnal variation, linearity of this variation can be assumed. At each station location the site number, time, and elevation were recorded. Then three different gravity and three different magnetic readings were taken and recorded. Readings were averaged for both gravity and magnetic readings at each station.

Elevations and locations were estimated using United States Geological Survey topographic maps. These seven minute quadrangle maps have a scale of 1:24000 and an elevation contour interval of 10 feet. Because of the interpolation required between these 10 foot contours, there was the possibility that error in this estimation could introduce error into the survey. To minimize this error the survey was done by

two people. Both individuals independently located the station and estimated the elevation from the topo map. Subsequent comparison and discussion is considered to have greatly decreased the chance of introducing this type of error.

Equipment and Accuracy

The gravity survey was conducted using a Texas Instruments Worden gravity meter. This instrument was provided by the University of Oklahoma School of Geology and Geophysics. A quartz spring balance that is relatively unaffected by temperature variations during operation is the basis for this instrument's operation. The Worden gravimeter has a dial division constant of 0.0965 mgal/division and can be read to one-tenth of a dial division (approximately 0.01 mgal).

The instrument used to obtain magnetic data was a Geomtrics model G 816 proton precession magnetometer. This instrument utilizes the concept of nuclear magnetic resonance. Certain nuclei have a net magnetic moment that, coupled with their spin, results in their precession about an axial magnetic field. Measurement of the free-precession frequency of protons (hydrogen nuclei), after removing an induced polarization field gives absolute magnetic field values. The magnetometer can be read to one gamma.

Discussion of Error

Several opportunities for error are possible during a gravity survey. Possible sources of error include: error in correct location of station, error in the estimation of elevation, and error in the accuracy of reading the instrument.

Errors in station location can result in both erroneous elevations as well as incorrect horizontal spatial relationships between stations. Errors in elevation determination can result in incorrectly calculated free air and Bouguer anomaly values. Using maps with 10 foot contour intervals could lead to elevation extrapolation error of up to 5 feet. This amounts to an error in computing the Bouguer and free-air corrections of as much as 0.4 mgal (Eg1).

Error in instrument reading leads to a discrepancy of 0.0965 mgal per dial division. Average variation between the three readings at each station, taken to be the instrument reading error, was 0.09 mgal (Eg2).

The variation of dial readings at beginning and end of loops averages 1.647 mgals. Considering the error in making the drift correction to be 1/5 of average error in loop closure, the drift correction error is estimated to be 0.03228 mgal (Eg3).

Use of the two-person survey crew method mentioned above is considered to have minimized errors involving location and elevation. Simplicity of using the Worden gravimeter allows little chance of improper instrument readings. After the field survey, the data points were plotted by computer on topo maps and the locations and elevations

checked against the field records. In light of the care given to ensure data accuracy through employment of several safeguards, the author estimates total error to be about 0.5 mgal. Propagation of error indicates the total error (TEg) to be:

$$TEg = (Eg1^2 + Eg2^2 + Eg3^2).5$$

Thus, the total error in gravity readings for this survey is estimated to be 0.41 mgals.

Error in the magnetic data could be introduced by instrument reading error or drift correction error. Average variation between the three readings at each station, taken to be the instrument reading error, was 37.2 gammas (Em1).

Variation of instrument readings at beginning and end of loops averages 55.8 gammas. Error in making this drift correction is considered to be 1/5 of average error in loop closure, estimated to be 11.2 gammas (Em2). The total magnetic error (TEm) is:

$$TEm = (Em1^2 + Em2^2).5$$

The total magnetic reading error is thereby estimated to be 38.8 gammas.

Gravity Data Reduction

The raw data for both gravity and magnetic surveys requires correction before interpretive use. The magnetic data needs to be drift corrected. The gravity data requires drift, latitude, free-air and Bouguer corrections. The FORTRAN programs GRAVCOR.FOR and MAGCOR.FOR (APPENDIX) were written to make the needed corrections.

The first step for both magnetic and gravity data is to read and average the three data readings at each station. Second, the tidal drift correction is done within each loop. Third, a shift is done to correct for the variation over the day the readings were collected as well as the variation from day to day. This completes the corrections for magnetic data. Since the Worden gravity meter is a relative instrument, a constant is added to relative gravity readings to correct them to absolute gravity. The resulting data value is used to compute the observed gravity (GOB). This computation is done with the equation

(1) GOB = (DRIFT CORRECTED VALUE) + 979657.4 - (70.9) (mgals)

In this equation, the number 979657.4 is the known absolute gravity value in the south-east corner of the basement of Gould Hall, on the campus of the University of Oklahoma, in Norman, Oklahoma. The number 70.9 is the difference of a reading in Gould Hall and a reading at the Vendome Well (survey base station). These were taken 90 minutes apart.

Next, the observed gravity (GOB) is corrected for gravitational variation with latitude. This variation is due to the earth's elliptical shape and rotation. Computation of the theoretical gravity

(IGF) on a rotating reference spheroid is done by using the 1967 International Gravity Formula

$$(2)\quad IGF = 978031.8(1.0 + 0.0053024\sin^2(lat) - 0.0000059\sin^2(2 \times lat)) \quad (mgals)$$

Since the theoretical gravity (IGF) for a certain latitude is calculated for a station at sea-level elevation, a free-air correction is needed to account for the station's elevation above sea level. The free-air correction is given by

$$(3)\quad FAC = (0.3085 \times elevation) \quad (mgals)$$

where the elevation is in meters.

Because the elevations are above sea-level, the FAC is added in equation 4 to obtain the free-air gravity value (GFA).

$$(4)\quad GFA = GOB - IGF + FAC$$

Having applied the preceding corrections to the observed gravity reading, the value of the Bouguer gravity (GBU) is obtained using the equation:

$$(5)\quad GBU = GFA - (2.0 \times 3.14159 \times 2670 \times 6.6732\times10^{-11}) \times elevation \times 100{,}000 \quad (mgals)$$

where 3.14159 is pi to 5 significant digits, 2670 is the standard Bouguer reduction density in kg/m^3, 6.6732×10^{-11} is the Universal Gravitation Constant, elevation is station elevation in meters, and the constant 100,000 converts m/s^2 to milligals.

Due to the very slight relief in the study area, terrain corrections were not necessary.

Reduced gravity data are given in Table 2.

Table 2.—Gravity and Magnetic Data

[SITE #, gravity and magnetic data site number; LAT-LONG, latitude and longitude; ELEV, elevation above sea level in meters; GOBS, absolute observed gravity value in miligals; FA, free-air graviy value in miligals; GBU, corrected Bouguer gravity value in miligals; MAG, corrected magnetic value in nanoteslas.]

SITE #	LAT-LONG		ELEV	GOBS	FA	GBU	MAG
1	343022	965824	298.6	979619.8	18.1	-14.3	53267.0
2	343032	965348	345.9	979605.2	20.7	-18.1	53086.0
3	343022	965352	350.5	979604.8	21.9	-17.4	53084.9
4	343003	965352	362.1	979602.5	23.7	-16.9	53090.1
5	342957	965353	357.2	979602.8	22.6	-17.4	53101.9
6	342943	965353	352.6	979604.3	23.0	-16.5	53137.9
7	342930	965353	351.4	979602.9	21.5	-17.8	53108.6
8	342918	965353	352.3	979602.7	21.9	-17.6	53105.2
9	342905	965353	349.3	979603.2	21.8	-17.4	52882.2
10	342853	965353	342.9	979604.5	21.3	-17.1	53089.1
11	342838	965353	341.7	979604.8	21.7	-16.6	53088.2
12	342826	965353	340.4	979605.4	22.1	-16.0	53060.9
13	342812	965354	332.2	979608.1	22.6	-14.6	53106.5
14	342800	965354	330.7	979608.8	23.2	-13.9	53037.7
15	342747	965350	330.1	979609.5	23.9	-13.1	53047.1
16	342741	965346	328.6	979609.5	23.6	-13.2	53066.8
17	343038	965454	356.6	979604.3	22.9	-17.0	53265.9
18	343022	965454	352.3	979605.0	22.7	-16.8	53235.1
19	343009	965456	354.5	979603.9	22.6	-17.1	53255.6
20	342956	965457	352.9	979602.8	21.3	-18.3	53238.1
21	342930	965457	352.6	979602.0	21.0	-18.5	53125.4
22	342945	965457	350.2	979603.1	21.0	-18.2	53187.1
23	342919	965457	344.1	979603.1	19.7	-18.8	53149.0
24	342904	965457	355.1	979601.8	22.1	-17.6	53118.3
25	342838	965457	353.9	979602.6	23.1	-16.5	53052.6
26	342853	965457	353.5	979602.3	22.4	-17.2	53115.7
27	342823	965457	350.8	979603.3	23.3	-16.0	53044.5
28	342812	965457	341.4	979605.8	23.0	-15.2	53018.9
29	342800	965457	345.9	979606.5	25.5	-13.2	52998.0
30	342746	965457	348.1	979606.8	26.8	-12.2	
31	342838	965558	346.9	979604.4	22.8	-16.0	53119.7
32	342824	965558	343.8	979606.3	24.1	-14.4	53077.2
33	342812	965558	343.5	979607.1	25.1	-13.4	53094.1
34	342758	965558	344.4	979606.4	25.0	-13.6	53080.6
35	342746	965558	344.7	979606.5	25.5	-13.1	53085.8
36	342930	970010	289.5	979615.9	15.4	-17.1	53340.0
37	342943	970010	301.1	979613.3	16.1	-17.7	53332.3
38	342956	970010	302.4	979613.8	16.6	-17.2	53307.3
39	343008	970010	296.3	979615.6	16.4	-16.8	53290.3
40	343023	970010	293.2	979617.4	16.8	-16.1	53347.9
41	343048	970008	300.2	979617.8	18.8	-14.9	53201.9
42	343035	970008	299.6	979617.5	18.6	-14.9	53391.0
43	343102	970008	300.8	979618.2	19.0	-14.7	53205.7
44	343115	970008	304.2	979617.5	19.1	-15.0	53169.0
45	343129	970008	308.1	979616.9	19.4	-15.1	53163.0
46	343141	970008	314.5	979615.4	19.6	-15.6	53181.0
47	343154	970008	314.8	979615.3	19.2	-16.0	53012.9
48	343207	970008	317.6	979614.6	19.1	-16.5	53125.2
49	343207	965938	320.9	979613.9	19.4	-16.6	53081.9

Table 2.—Gravity and Magnetic Data—Continued

SITE #	LAT	LONG	ELEV	GOBS	FA	GBU	MAG
50	343207	965905	314.8	979615.3	18.9	−16.4	53104.4
51	343154	965905	306.6	979616.8	18.2	−16.2	53111.1
52	343141	965905	308.8	979616.1	18.5	−16.1	53166.8
53	343128	965905	311.2	979615.8	19.2	−15.6	53124.3
54	343115	965905	306.9	979616.8	19.2	−15.1	53175.8
55	343102	965905	303.9	979617.3	19.0	−15.0	53193.5
56	343049	965905	299.6	979618.0	18.8	−14.7	53125.2
57	342930	965558	368.5	979599.6	23.5	−17.8	53171.9
58	342956	965558	365.7	979602.9	25.3	−15.7	53186.1
59	343008	965558	343.8	979607.6	23.0	−15.5	53113.8
60	342944	965558	369.7	979600.9	24.8	−16.6	53179.3
61	342929	965632	349.9	979603.9	22.1	−17.1	53155.7
62	342930	965702	336.2	979607.1	21.0	−16.6	53170.9
63	342746	965703	335.3	979606.4	22.5	−15.1	53029.3
64	342812	965703	339.8	979606.1	22.9	−15.1	52975.0
65	342838	965703	346.2	979604.2	22.5	−16.3	53056.9
66	342904	965710	330.4	979607.7	20.4	−16.6	53187.6
67	342856	965707	341.4	979606.2	22.5	−15.8	53230.1
68	342916	965712	322.2	979609.4	19.2	−16.8	53165.5
69	342930	965733	332.2	979608.7	21.4	−15.8	53164.8
70	342942	965701	344.4	979607.2	23.4	−15.2	53212.6
71	342955	965701	338.3	979608.8	22.7	−15.2	53310.9
72	343008	965702	335.6	979609.1	21.9	−15.7	53206.6
73	342937	965803	311.2	979613.9	20.0	−14.8	53330.1
74	342943	965752	320.6	979612.9	21.7	−14.2	53392.3
75	342952	965752	320.0	979613.0	21.4	−14.4	53368.5
76	342959	965747	306.3	979615.9	19.9	−14.4	53178.0
77	343006	965752	293.5	979617.9	17.8	−15.1	53212.5
78	343048	965454	358.7	979604.1	23.1	−17.1	53186.4
79	343114	965454	359.6	979604.2	22.9	−17.4	53213.4
80	343140	965454	367.0	979603.7	24.0	−17.1	53224.8
81	343206	965454	357.2	979605.1	21.9	−18.1	53223.4
82	343206	965422	362.4	979603.8	22.2	−18.4	53229.2
83	343206	965350	362.1	979603.3	21.6	−19.0	53179.3
84	343048	965556	359.0	979605.2	24.3	−15.9	53147.8
85	343114	965556	350.5	979607.1	23.0	−16.2	53129.0
86	343140	965556	353.3	979607.1	23.2	−16.3	53214.1
87	343207	965556	337.4	979610.3	20.9	−16.9	53195.5
88	343045	965659	330.1	979610.9	21.1	−15.8	53143.3
89	343114	965659	332.8	979611.4	21.8	−15.5	53138.2
90	343114	965730	307.8	979616.8	19.5	−14.9	53128.3
91	343114	965802	290.2	979620.3	17.6	−14.9	53072.9
92	343023	965759	301.7	979616.8	18.9	−14.9	52955.4
93	343023	965729	322.2	979612.5	20.8	−15.3	53174.7
94	343023	965833	285.9	979620.2	17.3	−14.7	52567.1
95	343023	965905	290.8	979619.9	18.5	−14.0	52960.0
96	343022	965937	290.5	979619.4	18.0	−14.6	52942.1
97	342956	965908	284.1	979619.9	17.1	−14.7	53340.8

Table 2.—Gravity and Magnetic Data—Continued

SITE #	LAT	LONG	ELEV	GOBS	FA	GBU	MAG
98	343115	965936	307.8	979617.2	19.9	-14.6	53455.3
99	343207	965833	311.5	979616.4	19.0	-15.9	53123.6
100	343206	965802	295.6	979618.9	16.7	-16.4	53215.1
101	343207	965730	308.8	979616.6	18.3	-16.2	53146.2
102	343207	965659	324.6	979612.8	19.5	-16.9	53187.9
103	343143	965807	302.0	979618.1	18.4	-15.4	53168.8
104	343046	965800	302.6	979616.9	18.7	-15.2	
105	342929	965940	281.9	979617.8	15.0	-16.6	53327.4
106	342904	970014	304.8	979614.8	19.6	-14.5	53323.9
107	342841	970010	296.0	979613.7	16.4	-16.8	53237.2
108	342841	965950	272.2	979619.6	14.9	-15.6	53303.2
109	342853	965915	306.0	979614.7	20.2	-14.1	53201.5
110	342846	965908	314.5	979610.9	19.1	-16.1	53251.4
111	342907	965804	329.2	979608.8	21.1	-15.8	53245.2
112	342838	965726	355.1	979602.5	23.5	-16.3	53218.5
113	342745	965734	328.6	979606.3	20.3	-16.5	53096.9
114	342746	965805	343.8	979604.1	22.8	-15.7	52978.1
115	342746	965836	320.0	979610.7	22.0	-13.8	53164.4
116	342740	965908	307.8	979612.5	20.2	-14.3	53205.4
117	342746	965638	333.7	979607.6	23.2	-14.2	53083.8
118	342838	965624	363.9	979601.3	25.0	-15.8	53130.2
119	342838	965558	345.9	979604.6	22.8	-15.9	52908.5
120	342838	965527	356.6	979601.7	23.1	-16.8	53080.2
121	342838	965425	339.2	979605.3	21.4	-16.6	53088.9
122	342757	965703	331.6	979607.6	22.2	-14.9	53102.8
123	342814	965711	339.5	979605.8	22.6	-15.4	53210.6
124	342830	965721	353.3	979602.7	23.3	-16.3	53215.1
125	342851	965734	349.9	979603.8	22.8	-16.4	53266.6
126	342914	965748	326.1	979608.9	20.0	-16.5	53255.6
127	342904	965742	334.6	979606.9	21.0	-16.5	53242.7
128	342929	965757	311.5	979613.6	20.0	-14.9	53294.5
129	342946	965808	320.6	979612.8	21.5	-14.5	53309.3
130	343003	965815	300.5	979617.2	19.3	-14.4	53286.5
131	343014	965812	286.8	979619.3	17.0	-15.1	53304.6
132	343010	965835	284.4	979620.4	17.4	-14.5	53312.3
133	343002	965846	285.0	979620.6	17.9	-14.0	53269.7
134	342950	965850	284.4	979619.6	17.0	-14.8	53312.2
135	342952	965904	284.7	979619.3	16.8	-15.1	53389.1
136	342942	965904	304.8	979613.6	17.5	-16.6	53321.3
137	342932	965908	297.2	979615.4	17.2	-16.0	53368.2
138	342928	965834	299.3	979615.6	18.2	-15.3	53328.0
139	342940	965848	317.6	979611.0	18.9	-16.6	53332.9
140	342936	965839	310.3	979613.6	19.3	-15.4	53296.8
141	342942	965821	308.8	979614.5	19.7	-14.9	53304.3
142	342938	965812	319.4	979612.6	21.1	-14.7	53298.8
143	343003	965737	299.0	979616.6	18.2	-15.3	53602.4
144	343008	965722	301.7	979615.8	18.1	-15.7	53602.2
145	343018	965716	308.1	979615.1	19.3	-15.2	53661.9
146	343018	965703	319.4	979612.8	20.4	-15.4	54037.8

Table 2.—Gravity and Magnetic Data—Continued

SITE #	LAT--LONG		ELEV	GOBS	FA	GBU	MAG
147	343027	965703	313.0	979614.3	19.7	-15.3	53747.4
148	342957	965732	308.1	979614.9	19.5	-15.0	54060.7
149	343004	965719	310.9	979613.7	19.0	-15.9	53832.5
150	343018	965652	324.0	979611.9	20.9	-15.4	53829.0
151	343018	965635	330.7	979610.9	22.0	-15.0	53885.8
152	343016	965628	329.8	979610.8	21.7	-15.3	53749.3
153	343010	965620	330.1	979610.3	21.4	-15.6	53207.7
154	342916	965909	302.4	979614.1	17.9	-16.0	52368.2
155	342904	965858	313.9	979611.2	18.8	-16.4	52531.6
156	342852	965859	317.6	979610.4	19.5	-16.1	52462.4
157	342838	965909	317.3	979610.8	20.1	-15.5	52576.8
158	342831	965909	303.6	979613.6	18.8	-15.2	52689.1
159	342819	965911	315.1	979611.3	20.3	-15.0	52777.5
160	342758	965910	322.8	979609.7	21.6	-14.5	52895.7
161	342758	965930	323.7	979608.7	20.9	-15.4	53017.8
162	342930	970035	312.1	979610.8	17.2	-17.7	53345.0
163	342902	970058	312.4	979609.4	16.7	-18.3	53330.0
164	342844	970122	307.8	979609.4	15.6	-18.8	52830.7
165	342749	970146	312.1	979607.1	15.9	-19.0	53213.1
166	342826	970124	308.4	979608.9	15.8	-18.8	53332.6
167	342811	970138	303.6	979609.7	15.4	-18.6	53252.8
168	342921	970055	316.7	979609.6	17.7	-17.7	53330.3
169	342759	965806	339.8	979606.4	23.6	-14.5	54401.5
170	342811	965804	342.0	979605.3	22.8	-15.5	53222.9
171	342835	965804	341.7	979604.4	21.4	-16.9	53233.3
172	342849	965804	338.9	979606.1	21.8	-16.1	53251.1
173	342903	965802	331.6	979606.7	19.8	-17.3	53267.4
174	343035	965905	296.3	979618.6	18.7	-14.5	53580.7
175	343035	965842	293.2	979618.9	18.0	-14.8	53321.6
176	343035	965821	289.5	979619.0	17.0	-15.4	52764.4
177	343035	965753	317.9	979613.5	20.3	-15.3	53098.4
178	343035	965729	320.0	979613.1	20.5	-15.3	53282.7
179	343035	965713	332.2	979610.4	21.6	-15.6	53109.4
180	343101	965729	319.4	979613.6	20.2	-15.6	53206.0
181	343114	965757	293.2	979619.3	17.5	-15.3	53026.2
182	343114	965852	308.4	979616.3	19.2	-15.4	52870.5
183	343114	965833	308.1	979616.5	19.3	-15.2	53208.4

Magnetic Data Reduction

The magnetic data required correction for diurnal drift only. This was achieved by the drift-correction program MAGCOR.FOR (APPENDIX). The reduced magnetic data are found in Table 2.

DATA FILTERING

Analysis of the Bouguer gravity anomaly map and the magnetic anomaly map were done using a two dimensional fast Fourier transform (FFT) filtering program designed by Hildenbrand (1983). Reduction of the magnetic data to a pole was done using the FFT program. First and second vertical derivatives were computed and the graphic result examined and analyzed for both gravity and magnetic data. Downward continuation for both the gravity and magnetic anomaly data was done to accentuate local rather than regional features of the respective data.

In order to filter the data and contour it, a grid of evenly spaced values was required. Using Golden Software's Surfer package, data was gridded with .5 km spacing (17 rows by 29 columns). The grid spacing of .5 km was decided upon because the majority of data stations in the study area were .5 km apart. Minimum curvature was the algorithm used for grid generation.

Magnetic Reduction to the Pole

Neither the magnetization of a body nor the geomagnetic field is vertical at the earth's middle latitudes. Thus, a direct correlation between a causative magnetic body and the resultant anomaly is skewed either south in the northern hemisphere or north in the southern

hemisphere. Repositioning of anomalies more symmetrically over the magnetic body is done using the FFT program by a reduction-to-the-pole procedure. This procedure involves determination of magnetic anomalies produced by the magnetic bodies if the bodies were vertically magnetized and the anomalies were observed from the geomagnetic pole. The FFT program makes this reduction by way of Fast Fourier transformation in the spectral domain.

Second Vertical Derivative

Field-derivative calculations using the FFT program were done to separate regional and local anomalies in both gravity and magnetic data. Because the second vertical derivative enhances near-surface effects and subdues the effects of deeper anomaly sources, there is a connection between a second-derivative map and a residual map. Curvature is a mathematical expression of how sharply curved or distorted the anomaly surface is at a particular location. The second vertical derivative is a measure of that curvature. Large curvatures are associated with shallow or residual anomalies.

Downward Continuation

G.G. Stokes originated the theorem for upward and downward continuation. The theorem states that if the potential field's values are known on a surface, values at any point higher or lower can be calculated. In this way, potential field data from one datum is

mathematically projected either upward to surfaces above the datum or downward to surfaces below the datum. In upward continuation, the regional anomaly pattern is more clearly revealed essentially smoothing the anomaly effect. Downward continuation causes a sharpening of the anomalies obtained at the ground surface.

For both the Bouguer gravity and the magnetic data downward continuation was employed to help resolve overlapping effects of sources and to estimate the depth at which the continued field shows extreme fluctuations. This depth approximates the depth of anomaly causing bodies. Successive steps of downward continuation were done until the anomaly maps showed extreme discontinuity or bulls-eye type orientation around data stations.

GRAVITY AND MAGNETIC ANOMALY MAPS

Bouguer Gravity Anomaly Maps

The contoured Bouguer Gravity Anomaly map (Figure 16) shows several distinct positive anomalies separated by steep contour gradients from regions of lower gravity values. Cutting across the western edge of CNRA (A on Figure 16) is a gradient trending N45W with a pronounced high to the northeast and a region of lower values to the southwest. Just south of the eastern half of CNRA is a N65E trending gravity gradient (B on Figure 16), that separates an area of high gravity values to the northwest from a triangular shaped area of relatively low Bouguer values to the southeast. This region of low values is bounded on the south by an east-west trending gradient (C on Figure 16). South of this gradient is the region with the highest Bouguer gravity values on the map. Southwest of CNRA, a steep gradient is found in the region of (D on Figure 16) with a region of low values to the north and west with a region of higher values trending about N30W (E on Figure 16) to the southwest.

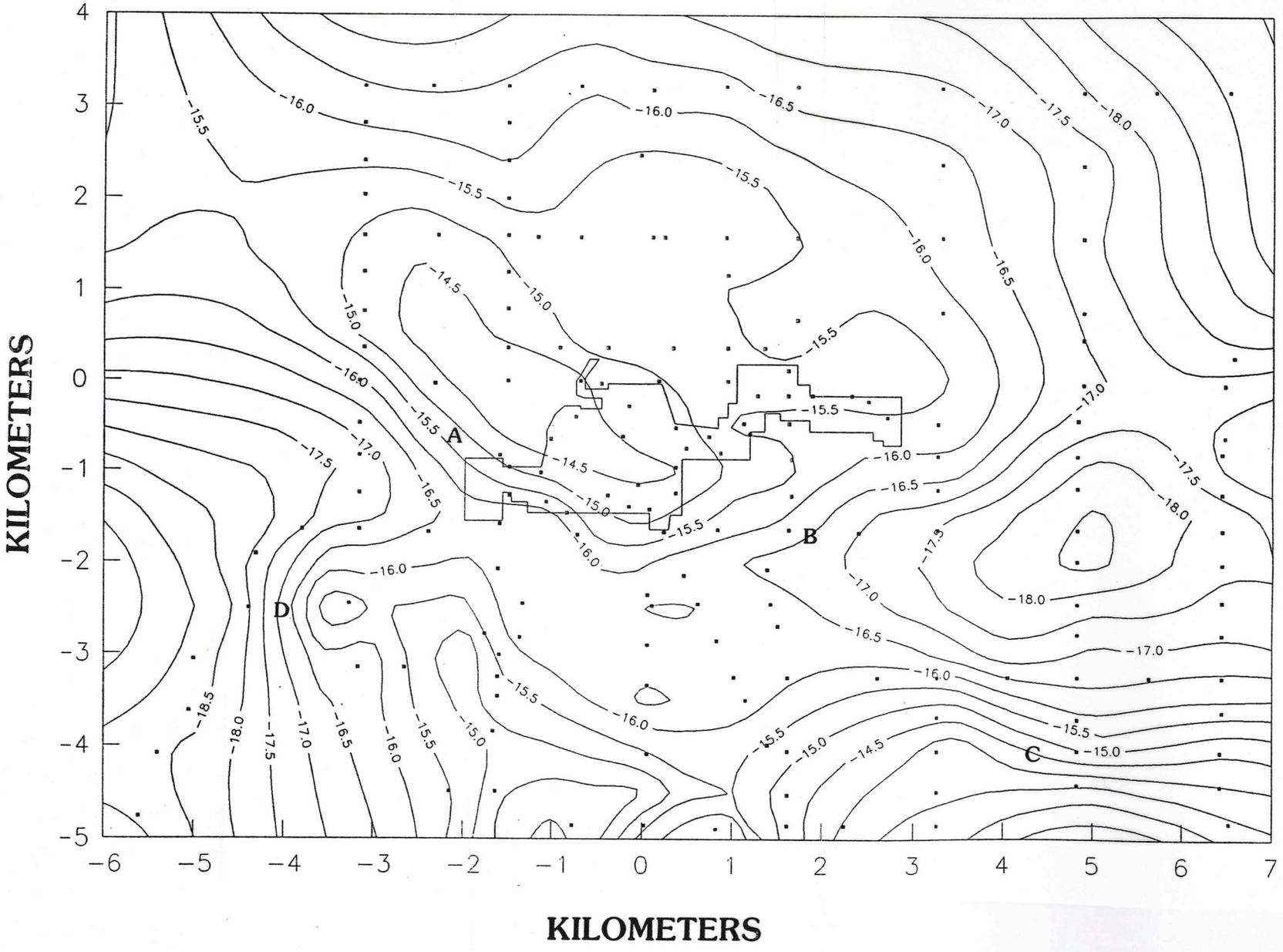

Figure 16. Map showing Bouguer Gravity Anomalies for the area of Chickasaw National Recreation Area. Outline is of the Travertine District, Chickasaw National Recreation Area. Origin of the coordinate system is the intersection of Oklahoma State Highway 7 and Oklahoma State Highway 177. Contour interval, 0.5 mgal

Second Vertical Derivative of Bouguer Gravity

The second vertical derivative map of the Bouguer gravity (Figure 17) was constructed to accentuate near surface gravity variations. The shaded area of this figure is an east-west trending region of low second vertical derivative values. The eastern-most location of this region coincides with that of the Sulphur syncline where Simpson Group outcrop is found southeast of CNRA. Superposed on this map are the fault locations from Ham (1954). The second vertical derivative enhances the trend of the low gravity values and indicates the continuation of a "gravity trough" westward from the location of the downthrown Simpson Group rocks.

Downward Continuation of Bouguer Gravity

Downward continuation was done in 0.10 km increments beginning at 0.25 km below sea-level (Figures 18, 19, and 20). The progression from 0.25 to 0.45 km below sea level shows distinct loss of coherency at an altitude of approximately 457.3 meters below sea level (2600 feet below the land surface). This indicates a domination of the Bouguer Gravity by near surface density contrasts. Effect of basement rock on local gravity anomalies can therefore be considered negligible for this study.

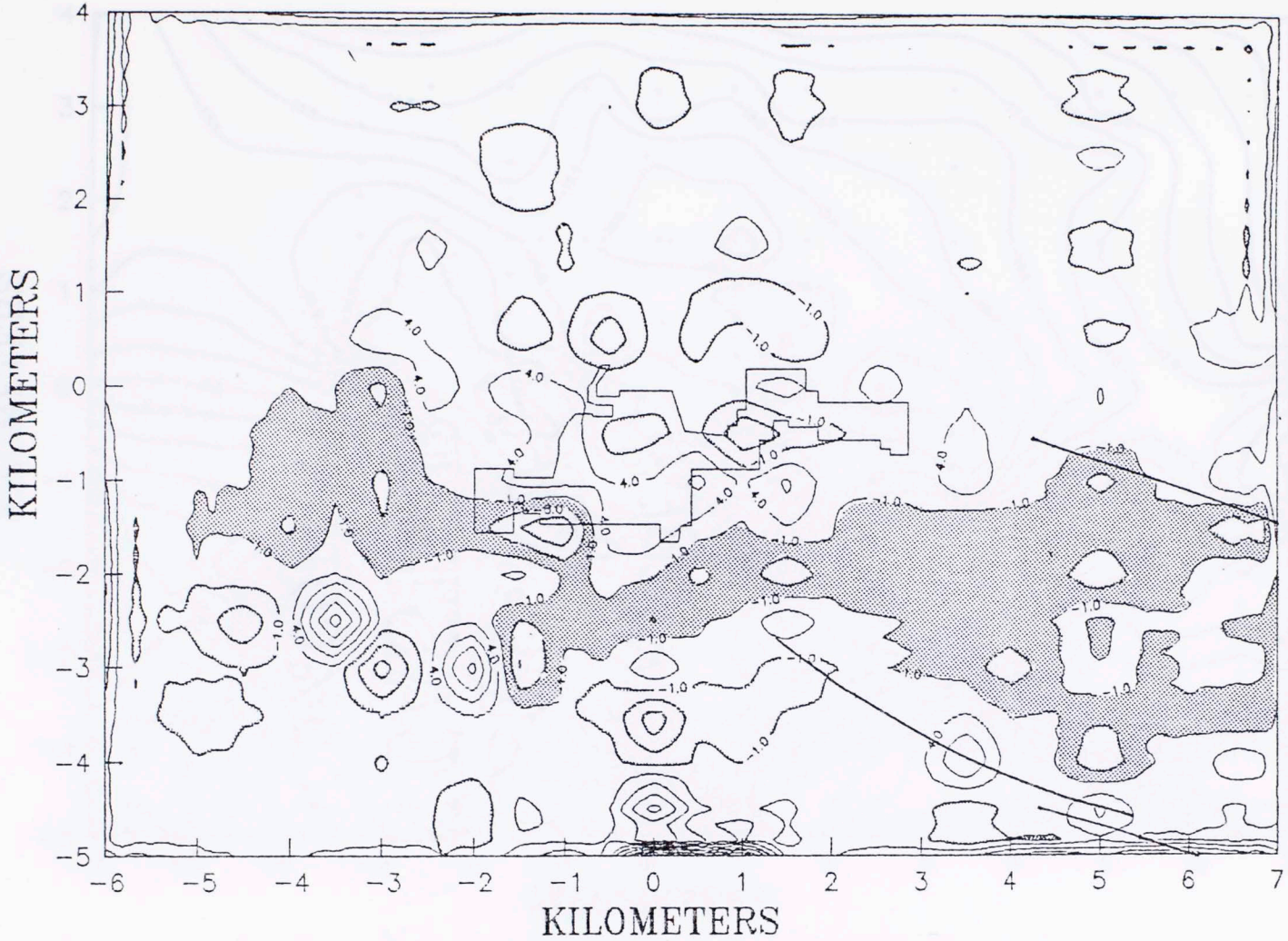

Figure 17. Map showing Second Vertical Derivative of Bouguer Gravity with superposition of known faults for the area of Chickasaw National Recreation Area. Outline is of the Travertine District, Chickasaw National Recreation Area. Origin of the coordinate system is intersection of Oklahoma State Highway 7 and Oklahoma State Highway 177 Contour interval, 5.0 miligal/kilometer squared.

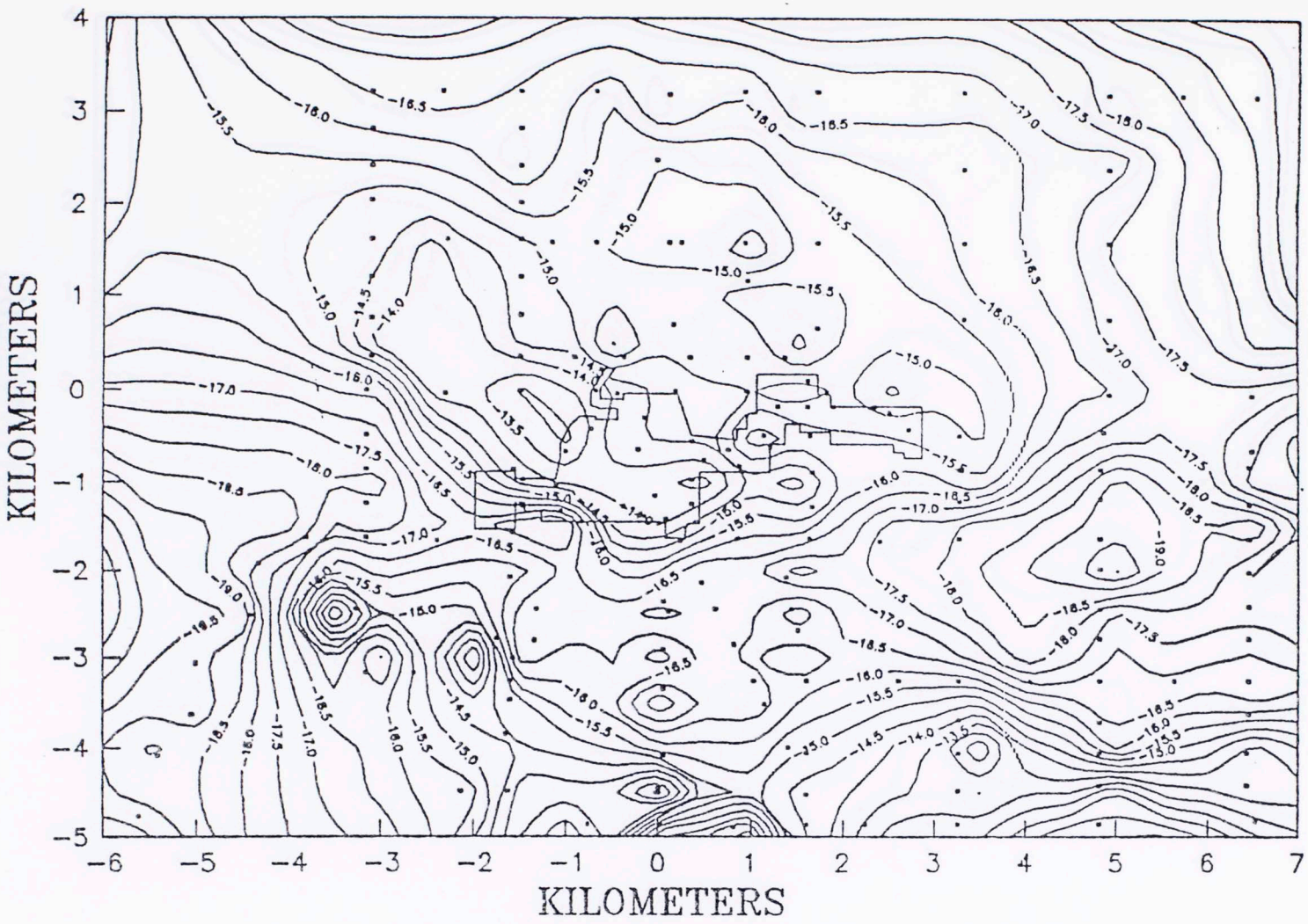

Figure 18. Map showing 0.25 KM downward continuation of Bouguer gravity for area of Chickasaw National Recreation Area. Outline is of the Travertine District, Chickasaw National Recreation Area. Origin of the coordinate system is the intersection of Oklahoma State Highway 7 and Oklahoma State Highway 177. Contour interval, 0.5 mgal.

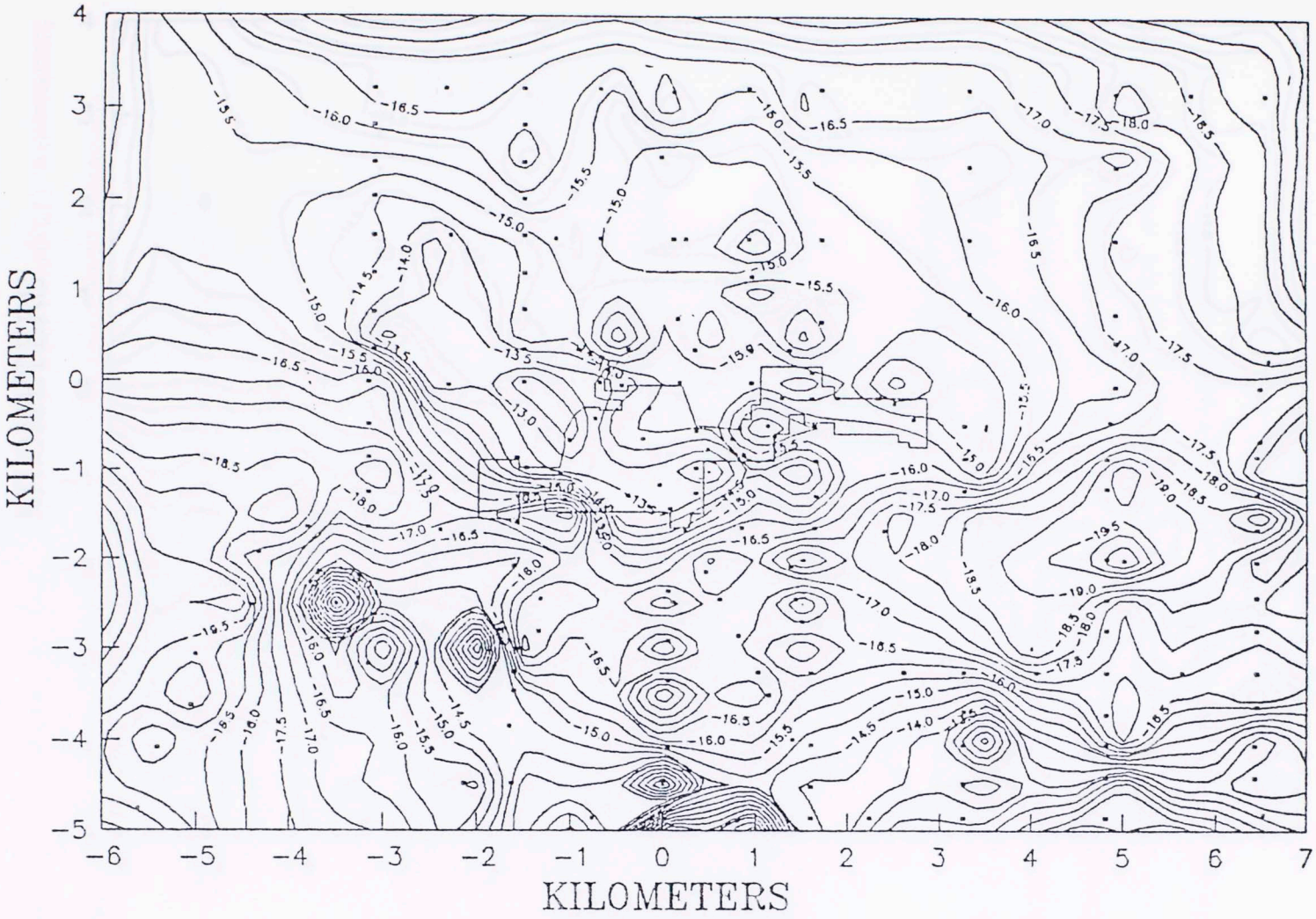

Figure 19. Map showing 0.35 KM downward continuation of Bouguer gravity for area of Chickasaw National Recreation Area. Outline is of the Travertine District, Chickasaw National Recreation Area. Origin of the coordinate system is the intersection of Oklahoma State Highway 7 and Oklahoma State Highway 177. Contour interval, 0.5 mgal.

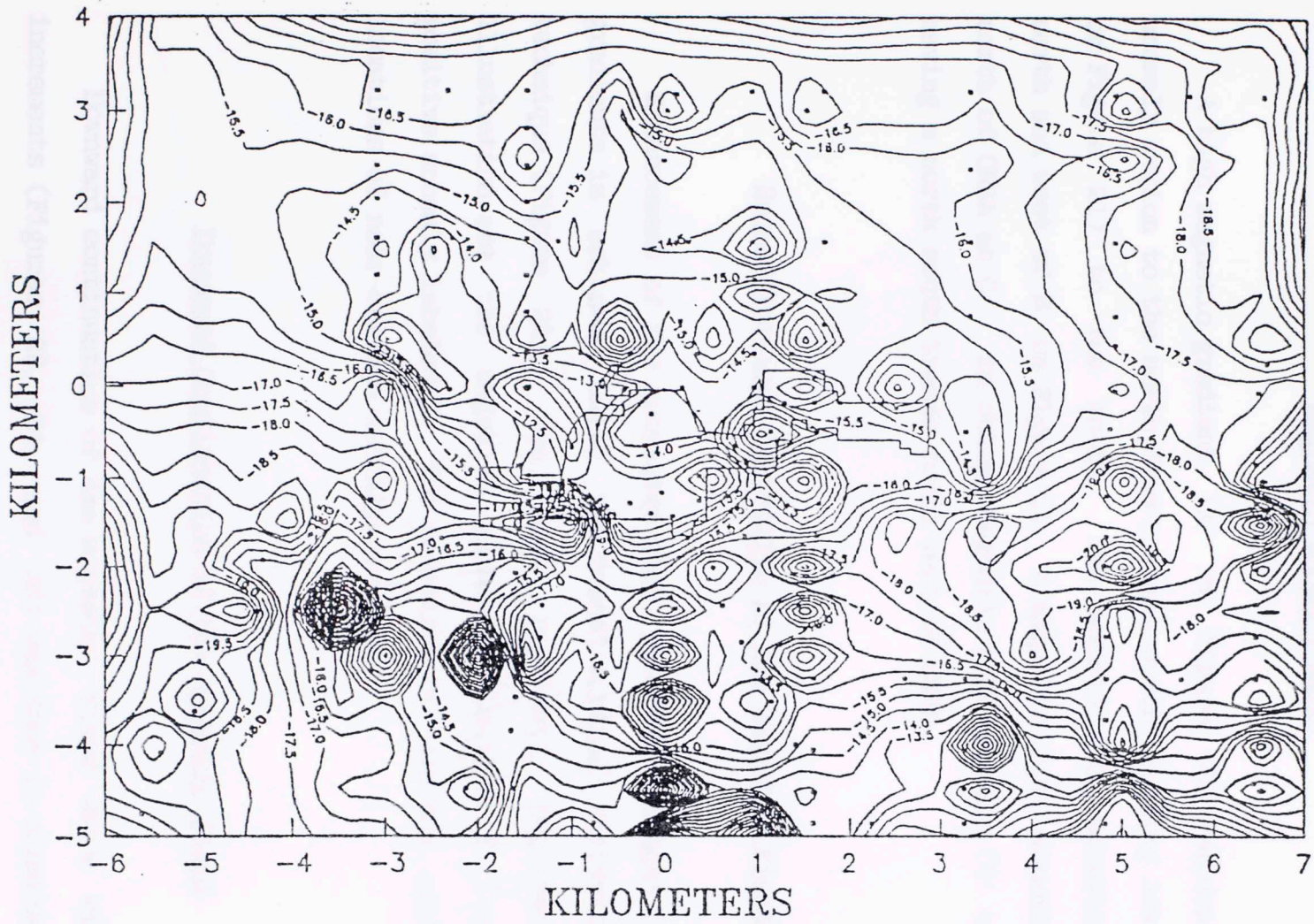

Figure 20. Map showing 0.45 KM downward continuation of Bouguer gravity for area of Chickasaw National Recreation Area. Outline is of the Travertine District, Chickasaw National Recreation Area. Origin of the coordinate system is the intersection of Oklahoma State Highway 7 and Oklahoma State Highway 177. Contour interval, 0.5 mgal.

Magnetic Anomaly Maps

A high magnetic gradient (A′ on Figure 21) separates a high anomaly region to the north from a north-south trending low anomaly (E′ on Figure 21) to the south. Two magnetic high anomalies are found north and west of B′ on Figure 21. A magnetic high anomaly is found north of CNRA at C′. An oblong magnetic high anomaly (D′ on Figure 21) having a north-south trends found west of CNRA.

Second Vertical Derivative of the Magnetic Field

Enhancement of the anomalies with greatest changes in magnetic gradients is achieved using the second vertical derivative filtering technique (Figure 22). The most prominent features of this illustration are the negative anomalies labeled W, Y and Z and the positive anomaly labeled X. The anomalies on this map accentuate the locations of near-surface anomaly sources.

Downward Continuation of the Magnetic Field

Downward continuation of the magnetic field data with 0.10 km increments (Figures 23, 24, and 25) was done to constrain depths of anomaly sources. The loss of continuity between 0.35 and 0.45 km below sea level indicate source of magnetic anomalies as near surface.

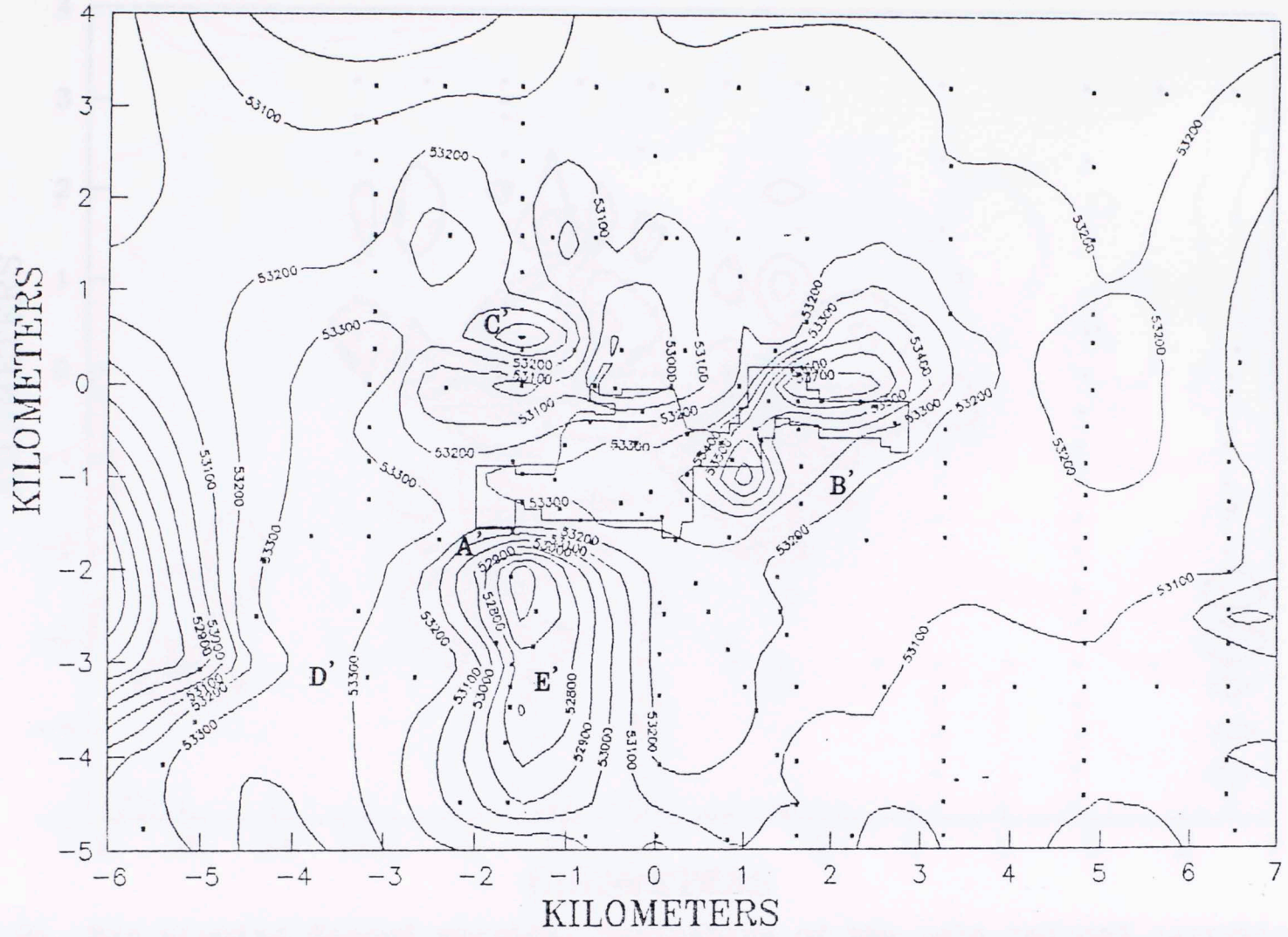

Figure 21. Map showing magnetic anomalies for the area of Chickasaw National Recreation Area. Outline is of the Travertine District, Chickasaw National Recreation Area. Origin of the coordinate system is the intersection of Oklahoma State Highway 7 and Oklahoma State Highway 177. Contour interval, 100 ntesla.

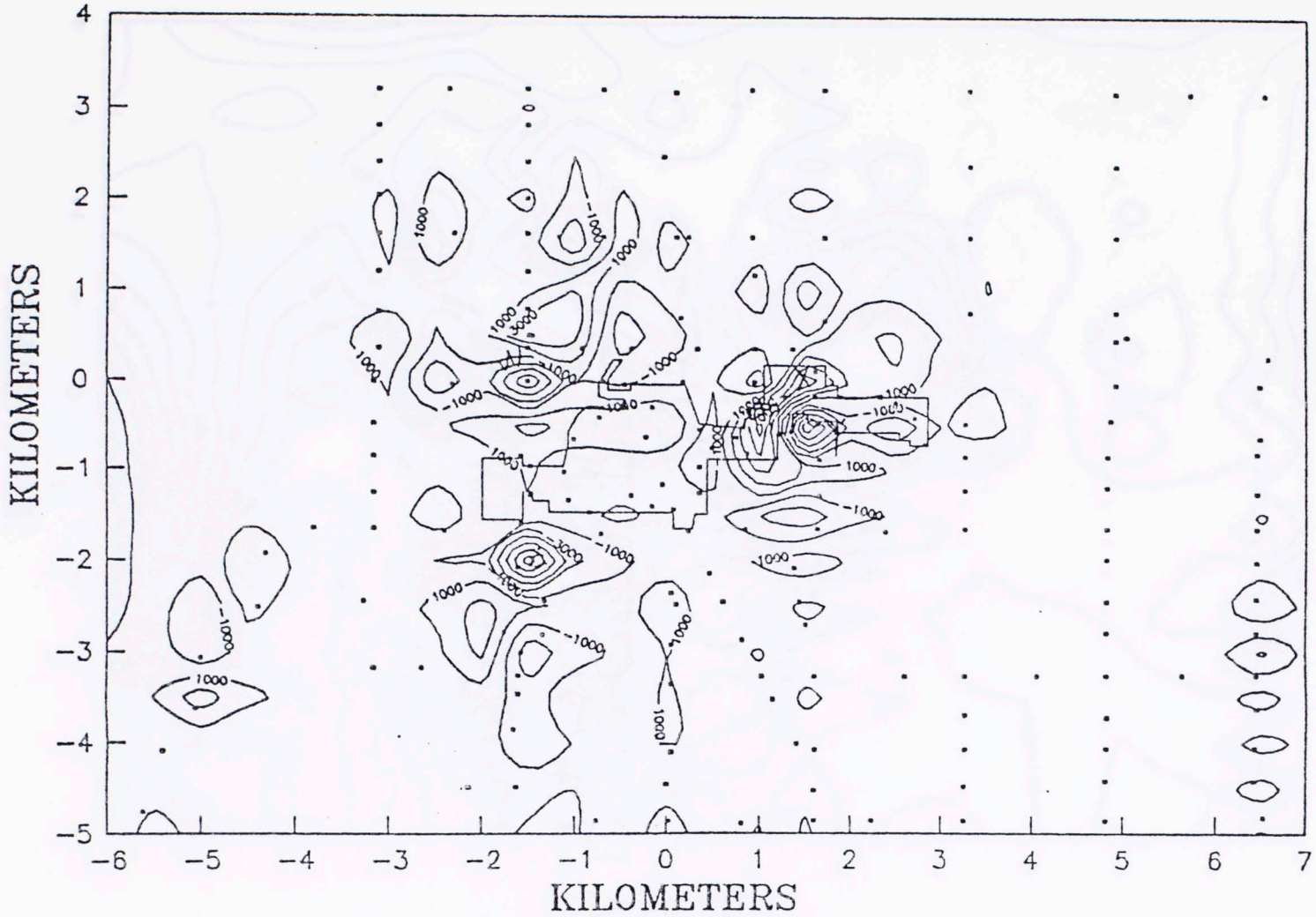

Figure 22. Map showing Second vertical derivative of the pole reduced magnetic anomalies for the area of Chickasaw National Recreation Area. Outline is of the Travertine District, Chickasaw National Recreation Area. Origin of the coordinate system is the intersection of Oklahoma State Highway 7 and Oklahoma State Highway 177. Contour interval, 2000 ntesla/kilometer squared.

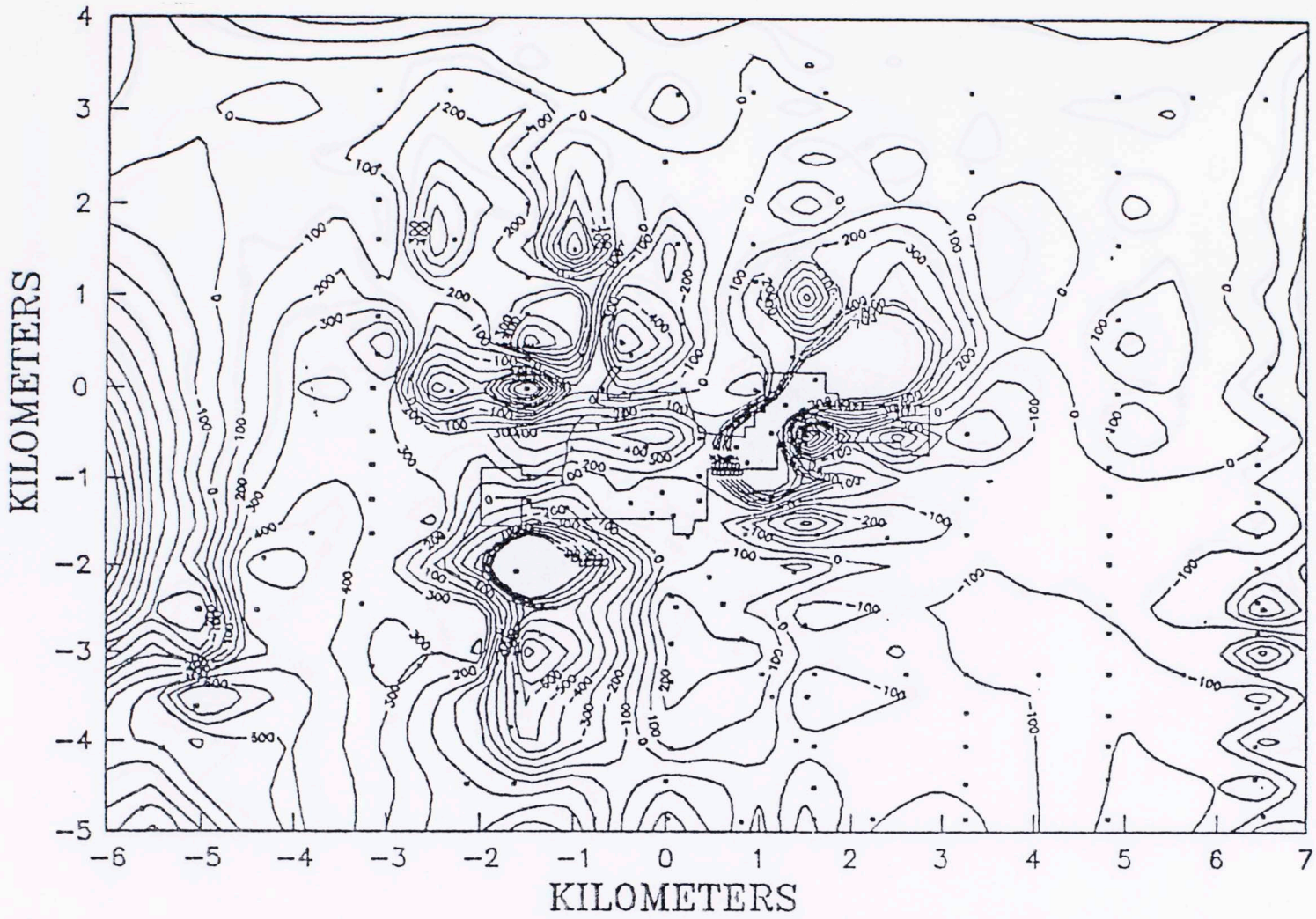

Figure 23. Map showing 0.25 KM downward continuation of pole reduced magnetic anomalies for the area of Chickasaw National Recreation Area. Outline is of the Travertine District, Chickasaw National Recreation Area. Origin of the coordinate system is the intersection of Oklahoma State Highway 7 and Oklahoma State Highway 177. Contour interval, 100 ntesla.

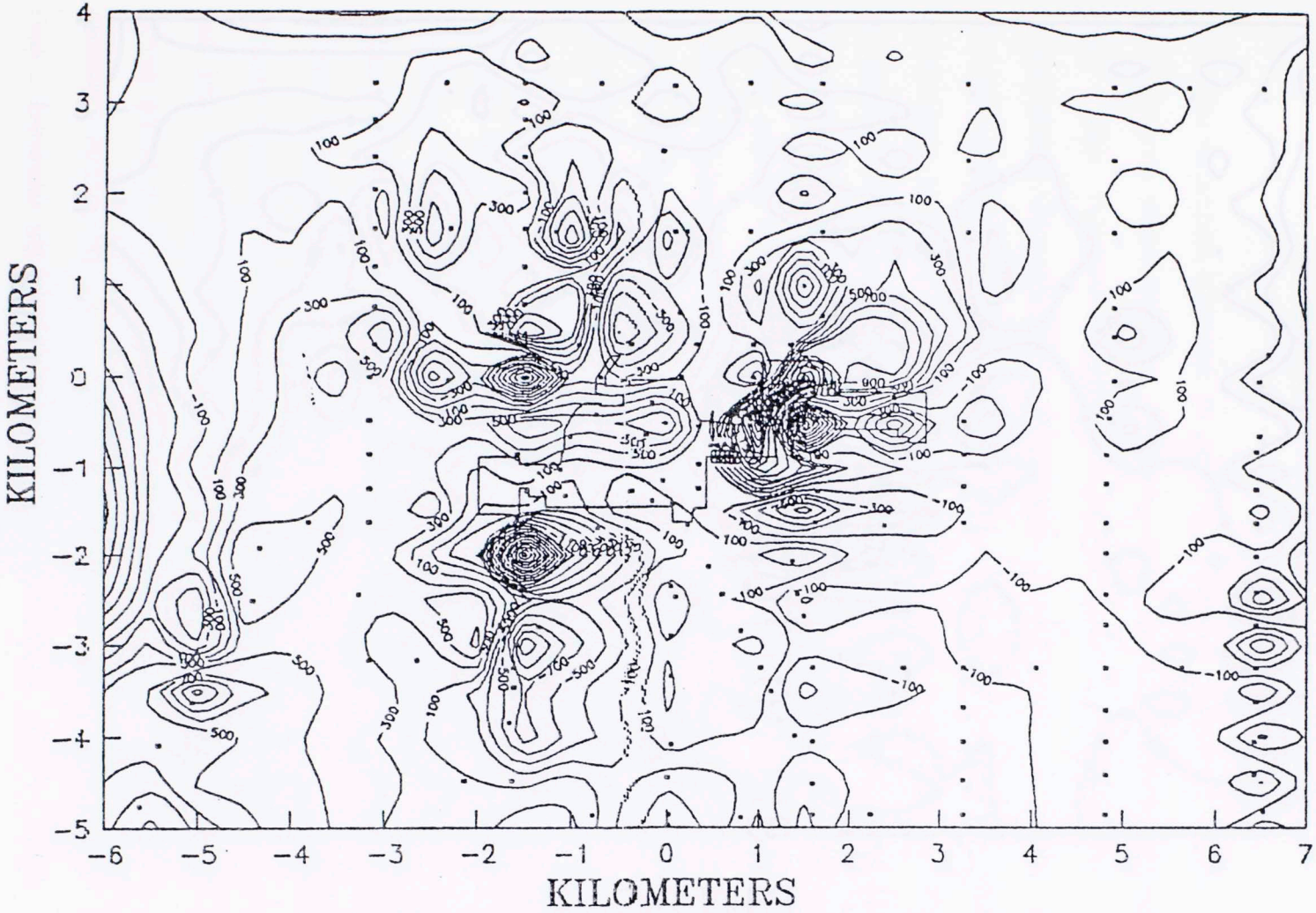

Figure 24. Map showing 0.35 KM downward continuation of pole reduced magnetic anomalies for the area of Chickasaw National Recreation Area. Outline is of the Travertine District, Chickasaw National Recreation Area. Origin of the coordinate system is the intersection of Oklahoma State Highway 7 and Oklahoma State Highway 177. Contour interval, 100 ntesla.

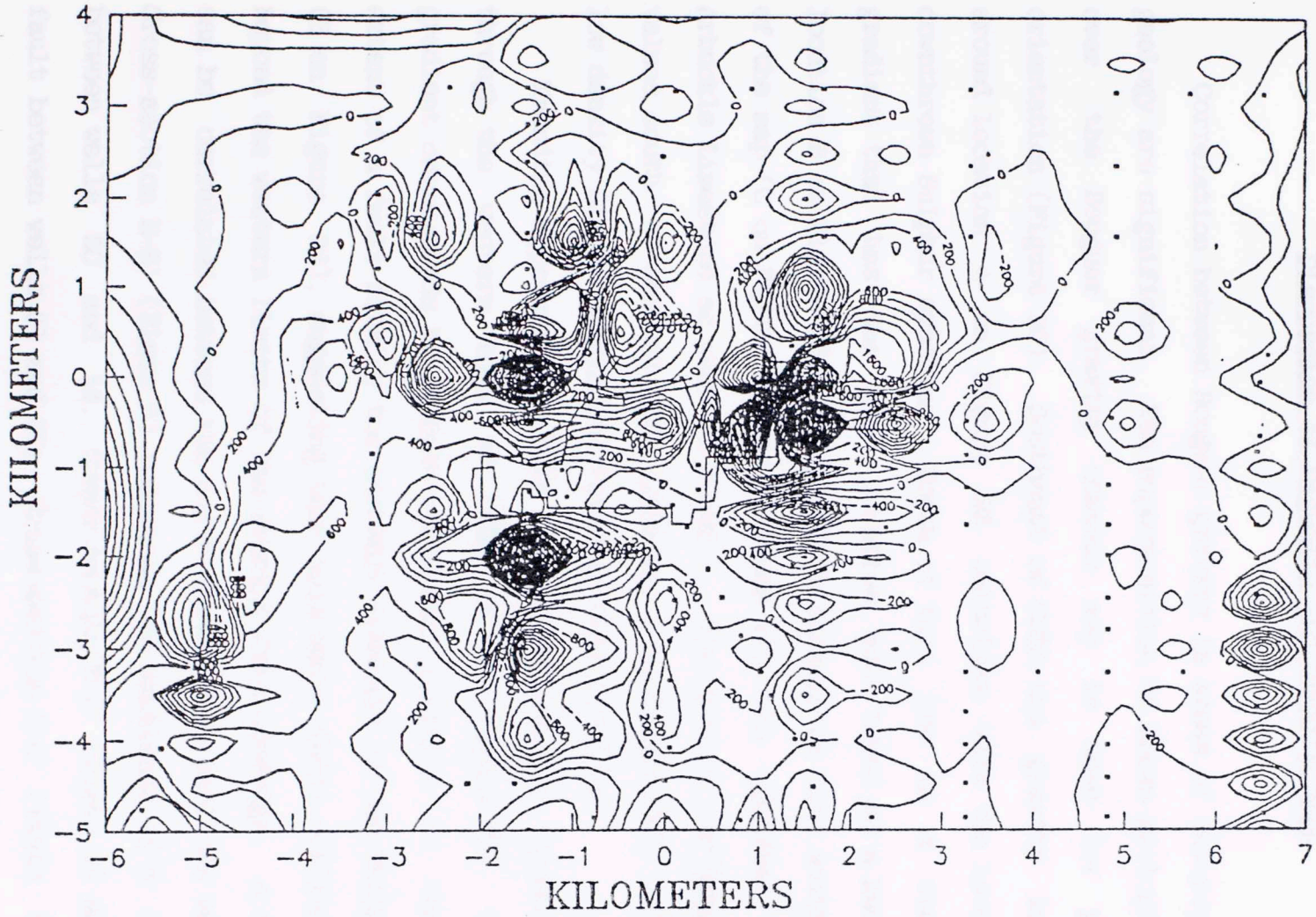

Figure 25. Map showing 0.45 KM downward continuation of pole reduced magnetic anomalies for the area of Chickasaw National Recreation Area. Outline is of the Travertine District, Chickasaw National Recreation Area. Origin of the coordinate system is the intersection of Oklahoma State Highway 7 and Oklahoma State Highway 177. Contour interval, 100 ntesla.

Discussion of Magnetic and Gravity Maps

Correlation between Bouguer gravity in areas of outcrop with known geology are significant. The superposition of known geologic features over the Bouguer gravity contour map is done for purposes of orientation (Figure 26). Southeast of CNRA the gravity low centered around location A on Figure 26 coincides with the location of the downthrown Sulphur syncline. South of this low is a steep gravity gradient that has the same location and trend as a known fault at location B on Figure 26. The positive anomaly in this southeast corner of the map (C on Figure 26) corresponds with the uplifted outcrop of Arbuckle Limestone as seen on Plate 1. The area of low Bouguer gravity values south of central CNRA (location D on Figure 26), coincides with low density Simpson sediments found at this location.

Trending approximately N52W is a strong gravity gradient cutting through the western edge of CNRA (E on Figure 26). This gravity gradient corresponds to in both trend and position to the northwest extent of a fault forming the southern boundary of the Sulphur Syncline (B on Figure 26), suggesting that this major fault continues westward beyond the western limits of the gravity data coverage. A major fault can be correlated between the north-south cross-sections west of CNRA. Cross-section E-E' (Plate 6) indicates the existence of a major fault between wells 20 and 18. Cross-section D-D' (Plate 5) shows a major fault between wells 81 and 39. Cross-section C-C' (Plate 4) shows a major fault between wells 92 and 38. On each of these cross-sections the fault with the greatest vertical offset also has the same sense of

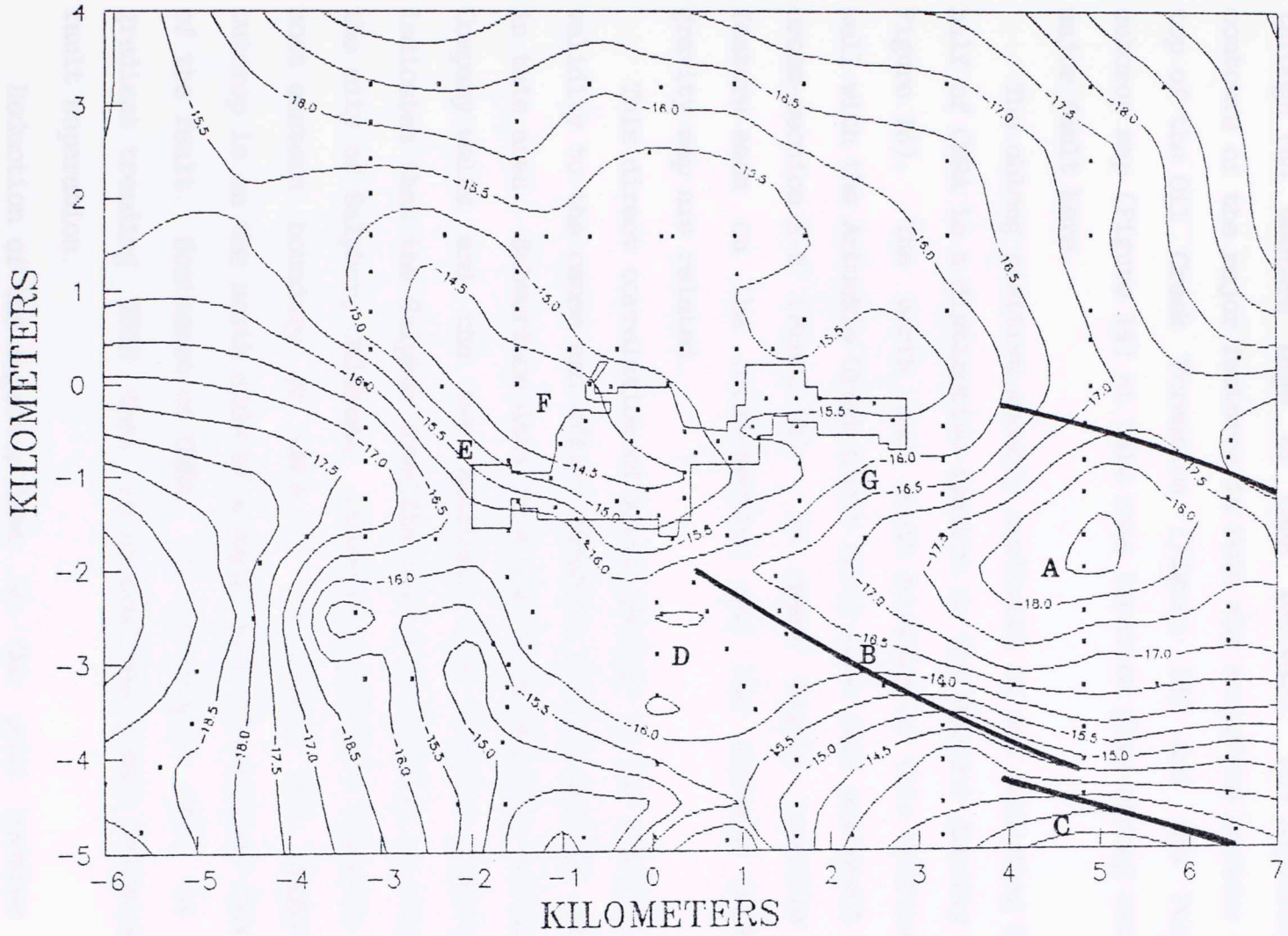

Figure 26. Figure showing the superposition of known faults over map of the Bouguer Gravity anomalies. Outline is of the Travertine District, Chickasaw National Recreation Area. Origin of the coordinate system is the intersection of Oklahoma State Highway 7 and Oklahoma State Highway 177. Contour interval, 0.5 mgal.

motion (upthrown to the north) as the others. Correlation of these cross-sections results in a continuation of the this major fault through the western edge of CNRA westward. The northwest trending contours of the major features in both the structure contour map of the top of the Oil Creek Formation (Figure 13) and the Pennsylvanian subcrop map (Figure 14) at this same location give strong evidence of a major fault here.

The oblong positive anomaly northwest of and including the western half of CNRA is a distinctive feature on the Bouguer gravity map (F. on Figure 16). The north and south boundary of this feature correlate well with the Arbuckle Group horst block seen just northwest of CNRA on cross-section E-E' (Plate 6). It seems highly possible that the feature seen on the cross-section and the anomaly on the Bouguer gravity map are related.

This direct correlation of known geology to the gravity data lends validity to the cause and effect relation between geology and gravity in this area. Subsurface data from the three Oklahoma Gas and Electric Company wells and the two National Park Service observation wells indicates that the Sulphur Syncline does not continue to plunge beneath the city of Sulphur, Oklahoma. Outcrop of Arbuckle Dolomite near the most eastern boundary of CNRA (F on Figure 26), suggest that the outcrop is on the north side of a fault with the Sulphur Syncline south of the fault. Southeast of CNRA, (G on Figure 26), is a gravity gradient trending N65E that is located were other evidence indicates fault separation.

Reduction of the magnetic data to the pole results in a map (Figure 27) with anomalies more correctly located above the bodies causing those anomalies. The map view geometry of the pole-reduced

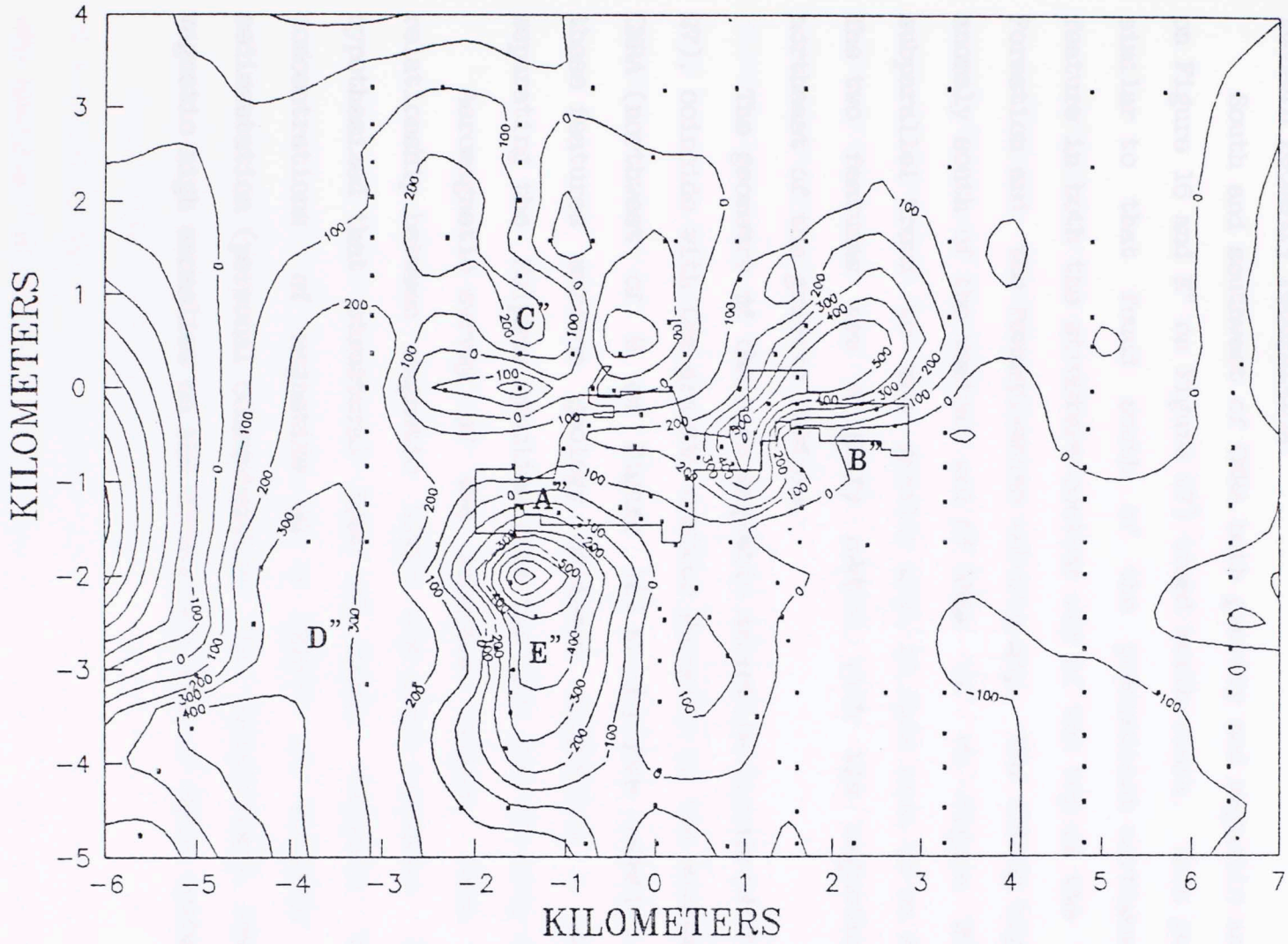

Figure 27. Map showing pole reduced magnetic anomalies for the area of Chickasaw National Recreation Area. Outline is of the Travertine District, Chickasaw National Recreation Area. Origin of the coordinate system is the intersection of Oklahoma State Highway 7 and Oklahoma State Highway 177. Contour interval, 100 ntesla.

magnetic anomalies is similar to those of the Bouguer gravity (Figure 16). Comparison of these maps is done here primarily in terms of pattern geometry recognition.

South and southwest of CNRA both gravity and magnetic anomalies (E on Figure 16 and E" on Figure 27) trend north-south. This geometry is similar to that found south of the predominant northwest trending feature in both the structure contour map of the top of the Oil Creek Formation and the Pennsylvanian subcrop map. The oblong high magnetic anomaly south of the western end of CNRA (E" on Figure 27), has a subparallel trend to the gravity high in this area (E on Figure 16). The two features are slightly offset with the magnetic feature northeast of the gravity feature.

The geometry of the high magnetic anomalies (north of B" on Figure 27), coincide with the gravity contour geometry on the eastern half of CNRA (northwest of B on Figure 16) at the same location. South of these features surface geology evidence suggesting a major fault separating the Sulphur Syncline from the CNRA and the city of Sulphur.

Aeromagnetic survey of the Arbuckle Region have shown a relationship between magnetic highs and fault contacts. It has been hypothesized that structural lows at these contacts have high concentrations of magnetite as a result of tectonic controlled sedimentation (personal communication: Dr. Robert Fay), resulting in magnetic high anomalies on the downthrown side of fault contacts.

GRAVITY MODELLING

Interpretation of potential field data such as gravity by itself is difficult. This is due to the fact that a given potential field can result from any number of variations in geology because there is no unique relationship between gravity data values and causative geology. A two-dimensional (2-D) gravity and magnetic inversion program called SAKI (Webring, 1985) was used to develop density models based on gravity data over an area of known geology. This model is subsequently used to interpret geologic relationships in areas of limited surface or subsurface control.

Model Inversion Program

SAKI is a 2-D computer modelling program that uses a least-squares algorithm to fit a theoretical gravity response of a density model to an observed gravity profile. Fitting is achieved through least-squares matrix inversion of modelled gravity profiles.

In the SAKI program the geologic model consists of an assemblage of n-sided polygons. Polygons represent cross-sections of 2-D form and are assigned a density. The program user's understanding of the geology being modelled limits nonuniqueness of a solution to a given set of gravity data.

In order to model gravity, a starting density model is required. The density model is comprised of polygon vertex locations and body densities.

Application of Geologic Data

Estimation of densities and body geometry are made using oil well logs from the oil field just west of Sulphur. Most of the logs had spontaneous potential and resistivity curves only. These logs were used to define formation thickness. Only a few more recent wells had bulk density information. The formation densities used in this modelling were obtained from the Caffin-Greer well (1N-2E-34), the Cops No. 1 well (1N-2E-33), the Lethridge "A" well (1N-3E-8), and the Flemming No. 1 well (1N-3E-32).

From these density logs a weighted average density was computed for each formation. Table 3 shows the formations, the formation thicknesses and the weighted average density for those formations.

For modelling purposes, the rock below the Simpson Group (below the Joins Formation) down to the basement was considered a single density unit. This unit is composed primarily of Arbuckle Limestone/Dolomite and includes the Honey Creek and Reagan Formations. The weighted average density for this "Arbuckle" unit was computed to be 2.73 grams per cubic centimeter.

Above the Arbuckle density unit are considerably less dense sedimentary rocks of the Simpson Group. For the purposes of modelling, these rocks were considered a single unit whose density varies from location to location. Unlike the Arbuckle unit which is below land

Table 3.--Formation Names, Thicknesses and Densities

Formation Name	Thickness (meters)	Density (grams/ cubic centimeter)
Hunton Limeston	61	2.63
Sylvan Shale	69	2.44
Viola Limestone	168	2.57
Bromide	107	2.45
Upper McLish	113	2.6
Lower McLish	40	2.3
Oil Creek Shale	98	2.5
Oil Creek Limey Sand	55	2.4
Oil Creek Sandstone	22	2.3
Joins	67	2.4
Arbuckle	1344	2.73

Densities are computed weighted average densities taken from bulk density logs of the Caffin-Greer well, 1N-2E-34; the Cops No. 1 well, 1N-2E-33; the Lethridge "A" well, 1N-3E-8; and the Flemming No. 1 well, 1N-3E-32.

surface in most of the study area, the thickness of these sediments is variable due to both erosion and geometry. The densities used for modelling of these sediments were recomputed in accordance with formation thickness indicated by various surface and subsurface data controls. At any given location a representative density was computed for the Simpson Group. This representative density depends on the thickness of the individual units comprising the Simpson Group (Table 3) at this location. The unit divisions making up the Simpson Group for this purpose include: the Bromide Formation; upper and lower McLish Formation; Oil Creek Formation shale, limey sand and sandstone; and the Joins Formation.

Using Ham's Map of the Arbuckle Mountains (1954), surface evidence from this study, and both oil and water well subsurface data, geologically plausible cross-sections were constructed. From these cross-sections, density models consisting of polygons and their relative densities were developed.

Six Bouguer gravity profiles were used in the modelling portion of this study (Figure 28). The six profiles are along the north-south section lines and are 1.609 km (1 mile) apart. The section lines also represent the baseline for relative Bouguer gravity values. The shaded area between the curve and section line indicates that section of the curve with values above -16 miligals. To the right of the section line Bouguer values are below -16 miligals. The gravity profiles are labeled from left to right 6, 5, 4, 3, 2, and 1.

The dominant feature in these profiles is an east-west trending "gravity trough" that coincides very closely with the location of the Sulphur Syncline seen on Plate 1 southeast of CNRA. A region of relative low gravity is seen south of the western half of CNRA with a

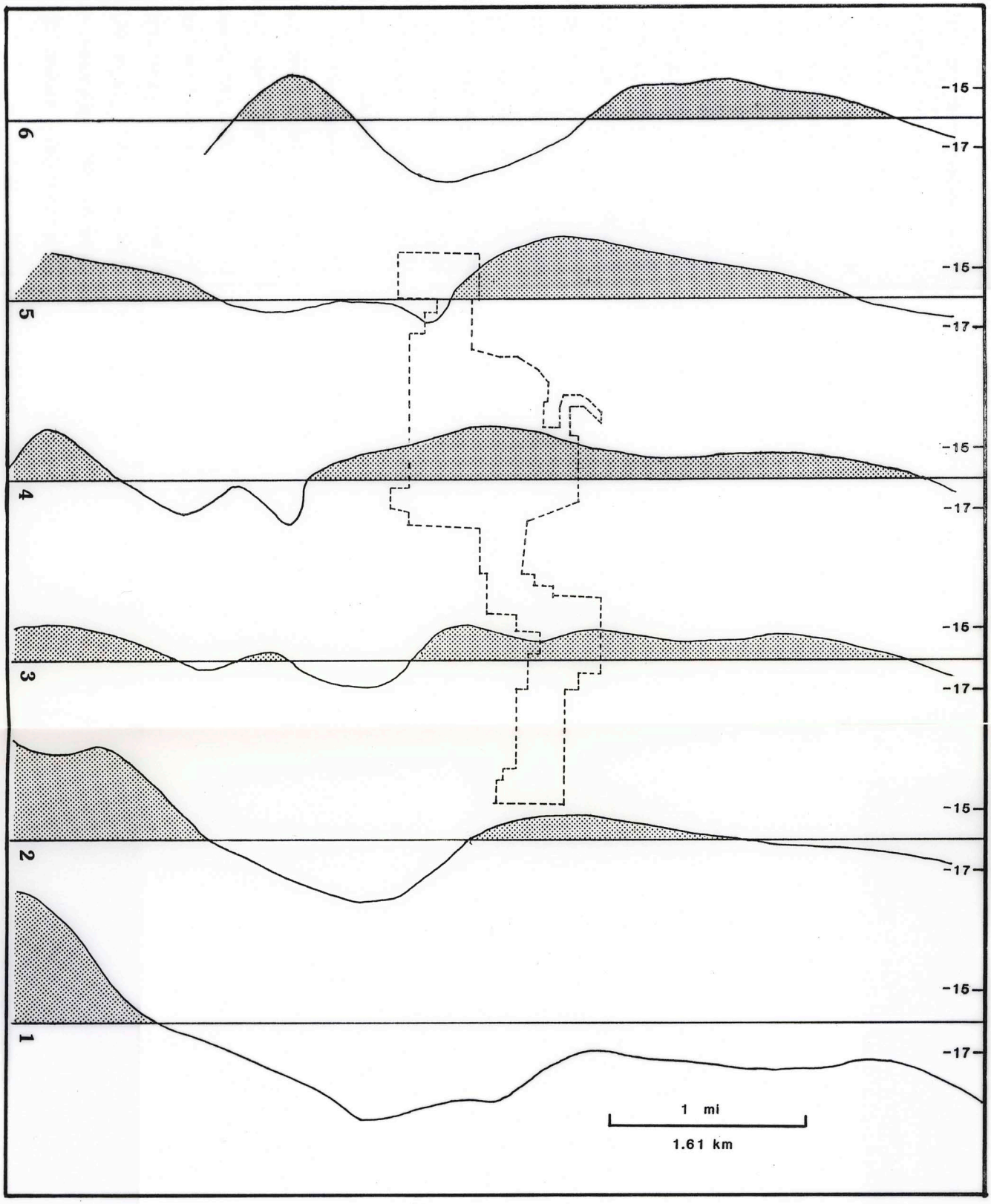

Figure 28. Figure showing locations of Bouguer Gravity profiles and curves showing values relative to -16 miligals. Values higher than -16 miligals are represented by the shaded area between the curves and left of the lines

"gravity trough" trending northwest. This area has limited subsurface control and no outcrop other than Vanoss conglomerate. The undulating nature of profiles 3, 4, and 5, suggested a more complex fault geometry than found below profiles 6, 2, and 1.

Graphic representations for the SAKI modelling are shown in the upper half of Figures 29-34. The numbered polygons represent the density units and are considered to be infinite in extent into and out of the plane of cross-section shown. The solid line on the graph represents the computed theoretical gravity value given the density model. The plusses on this graph represent the observed gravity values. The plusses that appear just above the numbered polygons along the 0.0 axis indicate locations of data stations relative to the cross-section.

Construction of the density model for Bouguer gravity profile 1 (Figure 29) was aided by the fact that line of profile traversed Pre-Pennsylvanian outcrop. This profile was considered to have the most geologic control and therefore could be used to refine density relationships used in subsequent modelling of profiles.

Given the constrained density model, the computed Bouguer gravity was fit to the observed data (Figure 29). The geologic cross-section was a well constrained starting point for modelling this profile, and the density was adjusted to obtain a fit.

Allowing the SAKI program to vary the density of polygon 3 in this model resulted in a very good fit with a density of 2.663 grams per cubic centimeter. As the upper Arbuckle Group is known to be karsted, (Fairchild et al., 1989), the lower density of this upthrown northern block is reasonable. The density logs indicated that in oil wells, the upper 170 meters (560 feet) of the Arbuckle Group has a density below

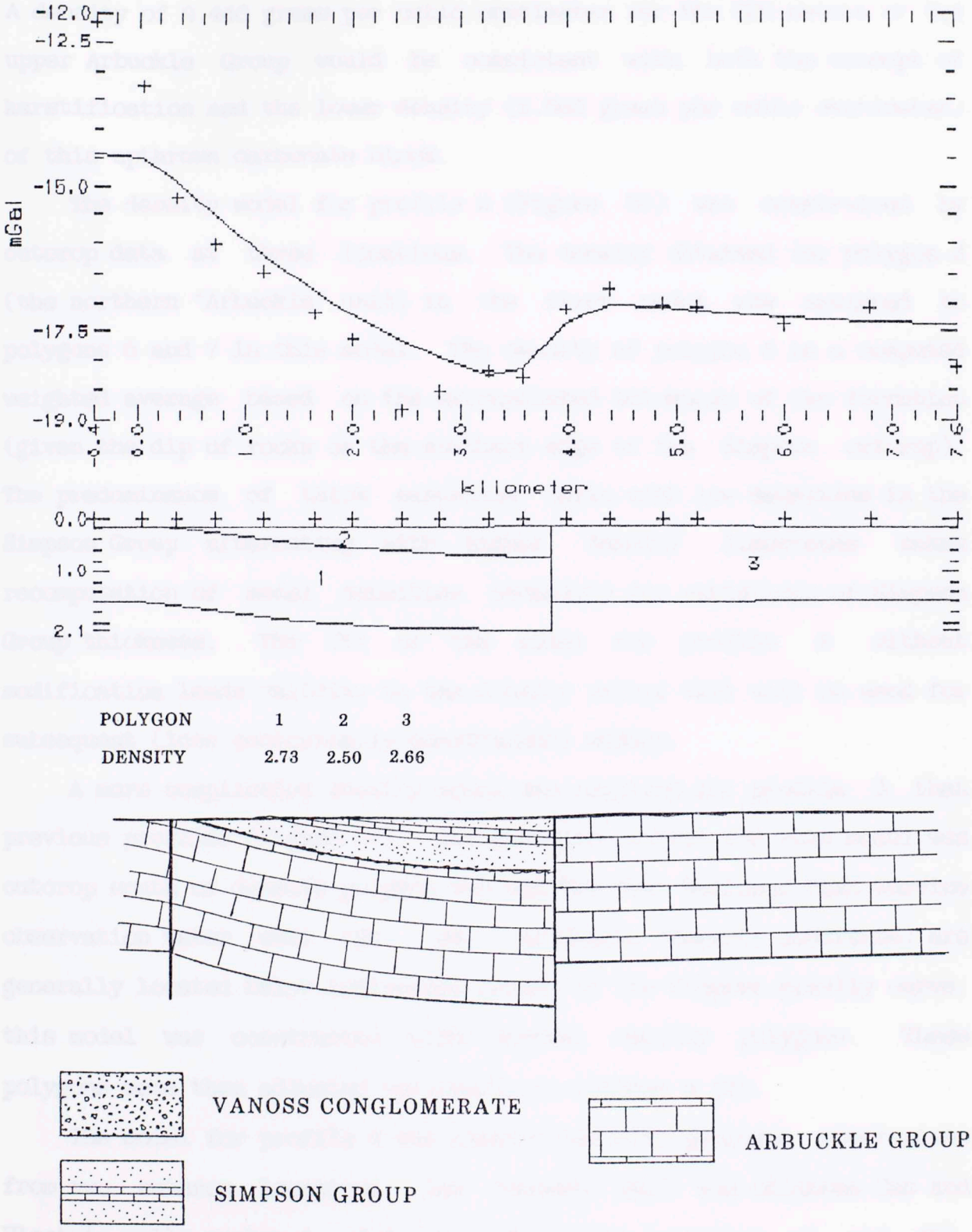

Figure 29. Figure showing observed and computed Bouguer gravity profiles, the polygon density model (vertical exaggeration 0.5), and the interpreted geologic cross-section for profile number 1.

the overall weighted average computed for the "Arbuckle" density unit. A density of 2.446 grams per cubic centimeter for the 300 meters of the upper Arbuckle Group would be consistent with both the concept of karstification and the lower density (2.663 grams per cubic centimeter) of this upthrown carbonate block.

The density model for profile 2 (Figure 30) was constrained by outcrop data at three locations. The density obtained for polygon 3 (the northern "Arbuckle" unit) in the first model was assigned to polygons 6 and 7 in this model. The density of polygon 5 is a computed weighted average based on the extrapolated thickness of the formation (given the dip of rocks on the southern edge of the Simpson outcrop). The predominance of thick sandstone units with low densities in the Simpson Group alternating with higher density limestones makes recomputation of model densities necessary for variations of Simpson Group thickness. The fit of the model for profile 2 without modification lends validity to the density values that will be used for subsequent (less geologically-constrained) models.

A more complicated density model was required for profile 3 than previous profiles (Figure 31). The geologic control for this model was outcrop south of density polygon two and the West National Park Service observation water well (No. 98). As faults (density contrasts) are generally located below inflection points of the Bouguer gravity curve, this model was constructed with several density polygons. These polygons were then adjusted vertically to achieve a fit.

The model for profile 4 was constructed with geologic constraints from two outcrop locations, the Vendome well, and Oklahoma Gas and Electric wells number 1 and 2 (subsurface data locations 41 and 42). Faults were inferred below the inflection points of the Bouguer gravity

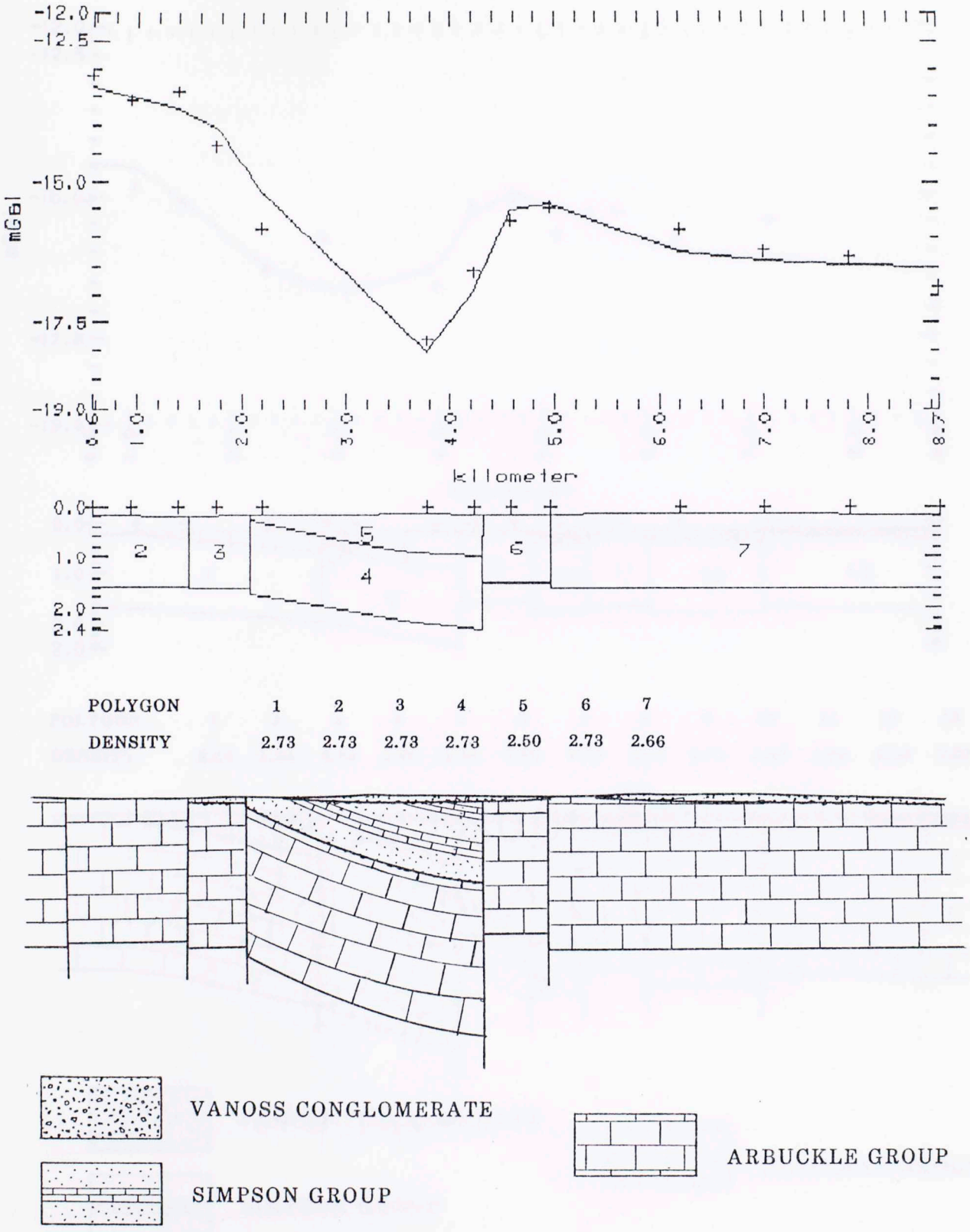

Figure 30. Figure showing observed and computed Bouguer gravity profiles, the polygon density model (vertical exaggeration 0.5), and the interpreted geologic cross-section for profile number 2.

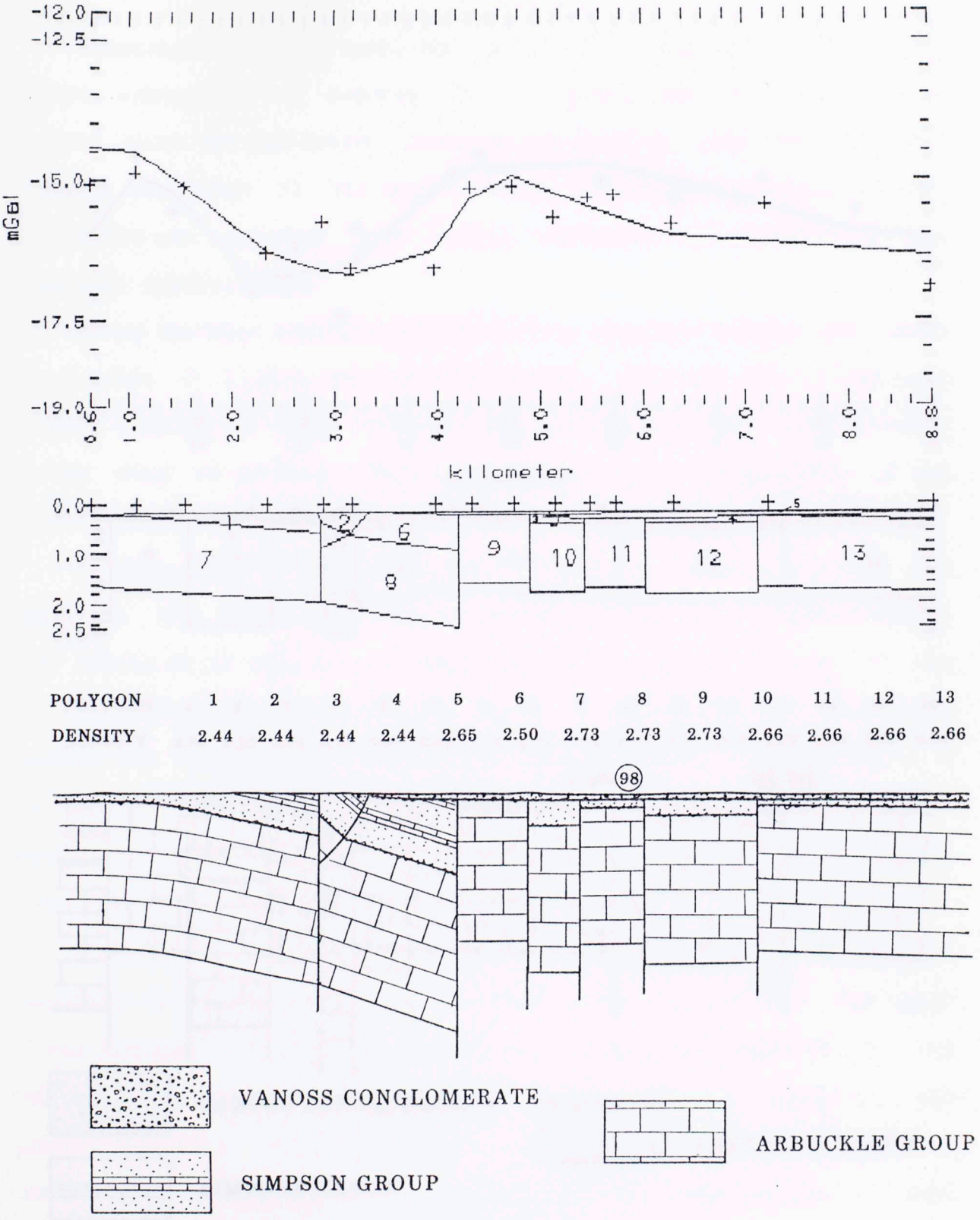

Figure 31. Figure showing observed and computed Bouguer gravity profiles, the polygon density model (vertical exaggeration 0.5), and the interpreted geologic cross-section for profile number 3.

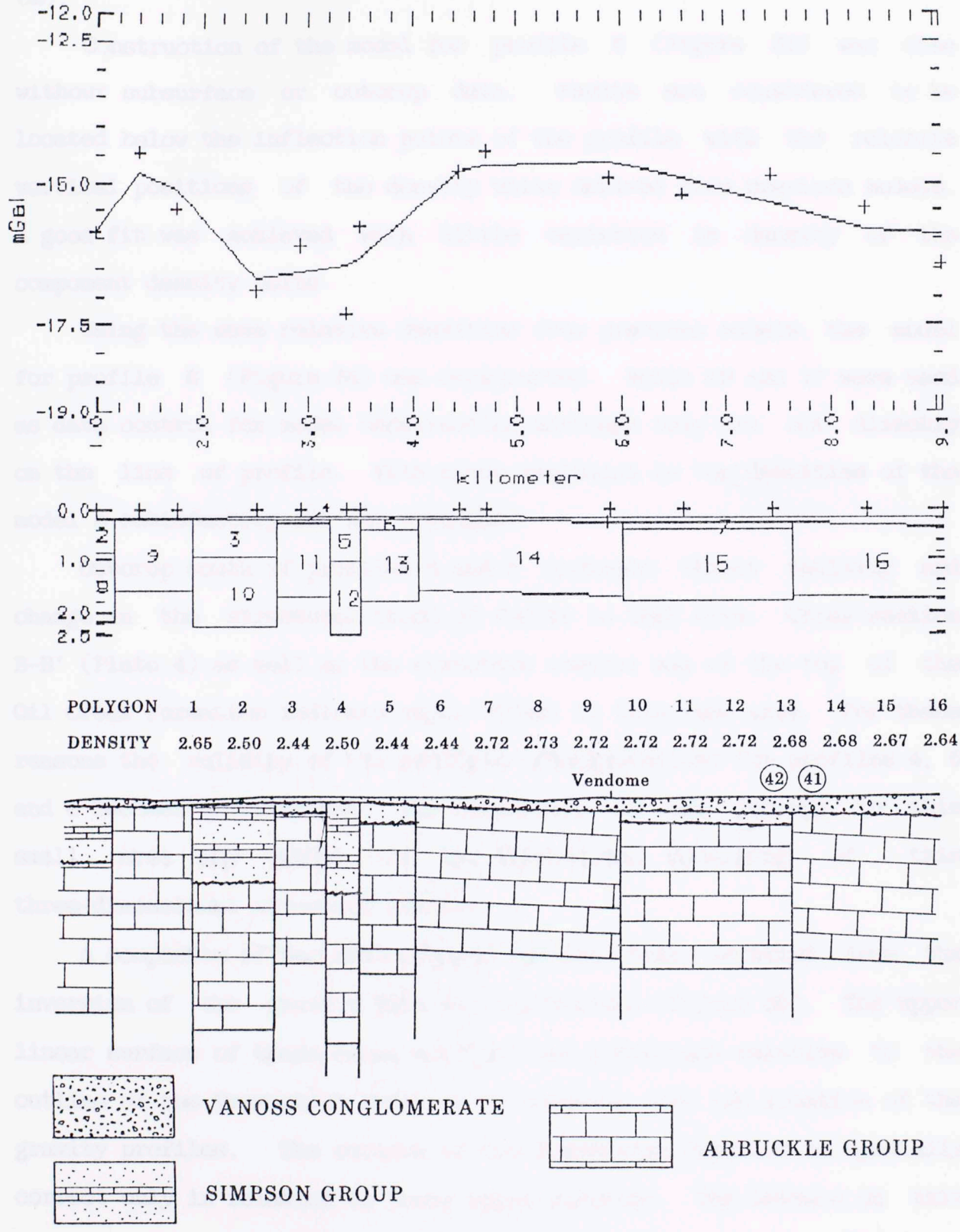

Figure 32. Figure showing observed and computed Bouguer gravity profiles, the polygon density model (vertical exaggeration 0.5), and the interpreted geologic cross-section for profile number 4.

curve and density units were moved vertically to achieve a fit (Figure 32).

Construction of the model for profile 5 (Figure 33) was done without subsurface or outcrop data. Faults are considered to be located below the inflection points of the profile with the relative vertical positions of the density units derived from previous models. A good fit was achieved with little variation in density of the component density units.

Using the same relative densities from previous models, the model for profile 6 (Figure 34) was constructed. Wells 29 and 17 were used as data control for model construction although they are not directly on the line of profile. With minor variation in the densities of the model a satisfactory fit was obtained.

Outcrop south of profiles 4 and 5 indicate thrust faulting and change in the structural trend of faults in that area. Cross-section B-B' (Plate 4) as well as the structure contour map of the top of the Oil Creek Formation indicate major offset in this same area. For these reasons the validity of the geologic interpretations for profiles 4, 5 and 6 becomes questionable. The complexity of the geology in this small area may render the two-dimensional modelling of this three-dimensional situation suspect.

A composite of the SAKI density models that resulted from the inversion of the gravity data was constructed (Figure 35). The upper linear surface of these cross-sections are positioned relative to the outline of the Travertine District to coincide with the location of the gravity profiles. The outline of the Travertine District is spacially correct only in relation to these upper surfaces. The letters on this figure are at locations of known or suspected faults. The North

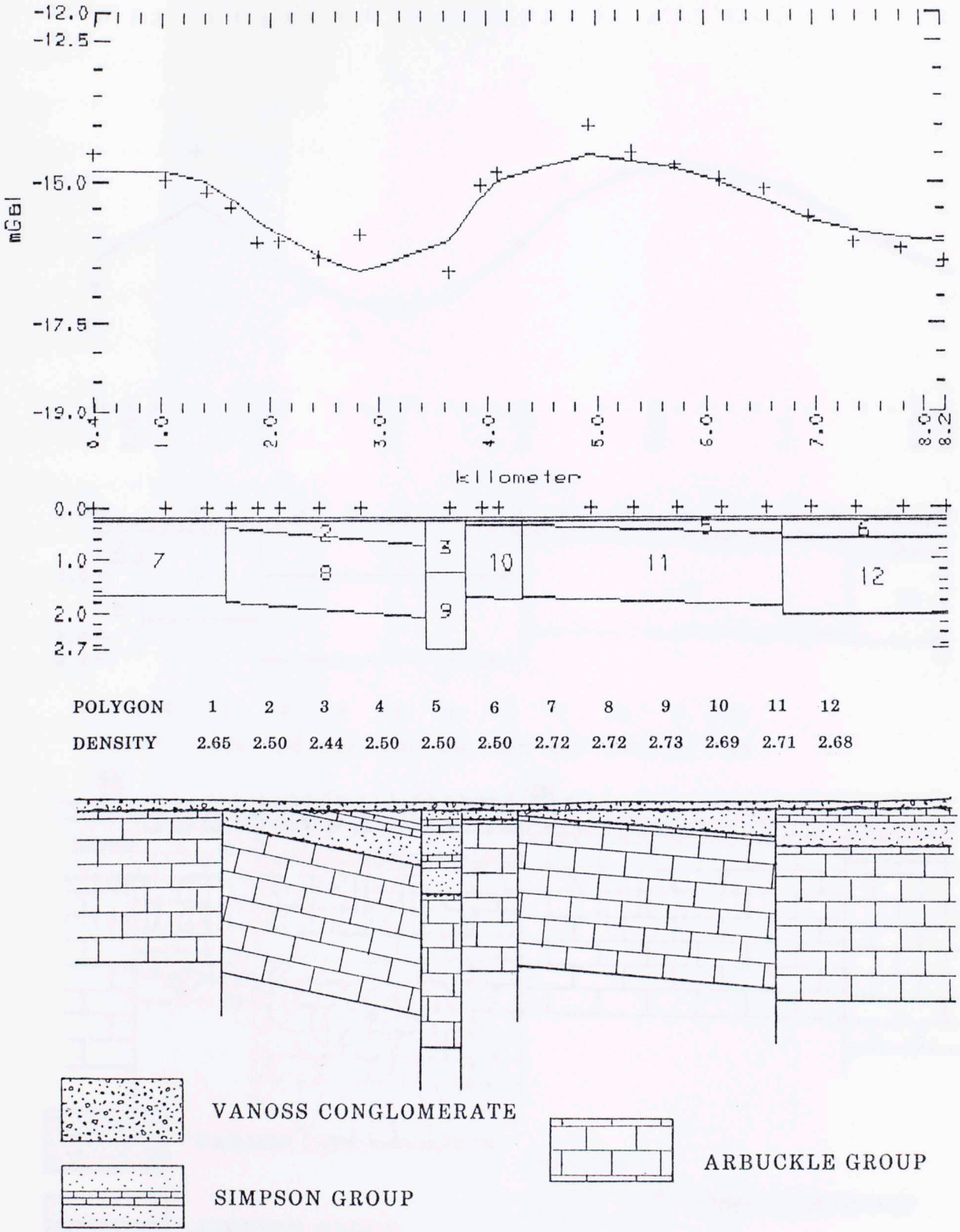

Figure 33. Figure showing observed and computed Bouguer gravity profiles, the polygon density model (vertical exaggeration 0.5), and the interpreted geologic cross-section for profile number 5.

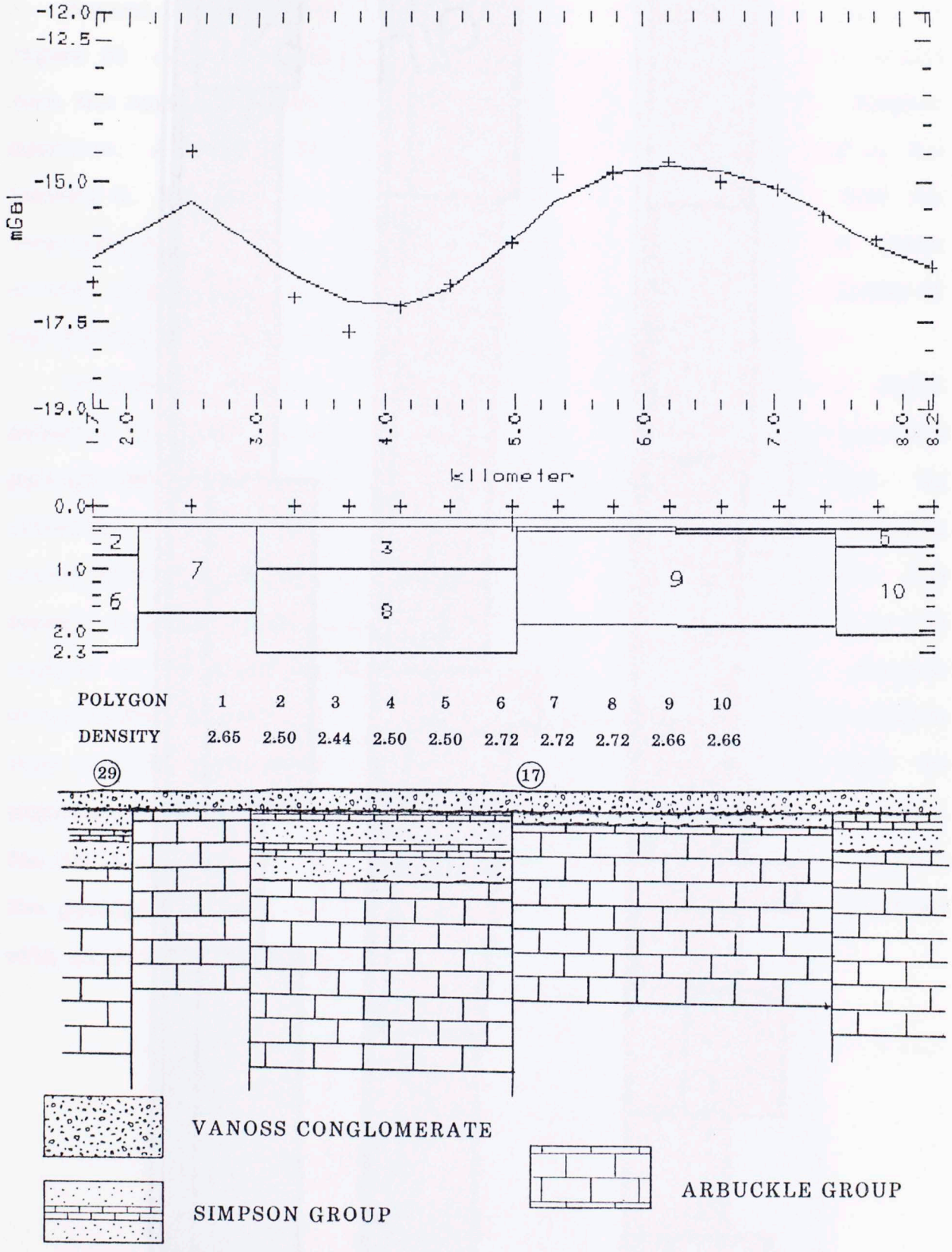

Figure 34. Figure showing observed and computed Bouguer gravity profiles, the polygon density model (vertical exaggeration 0.5), and the interpreted geologic cross-section for profile number 6.

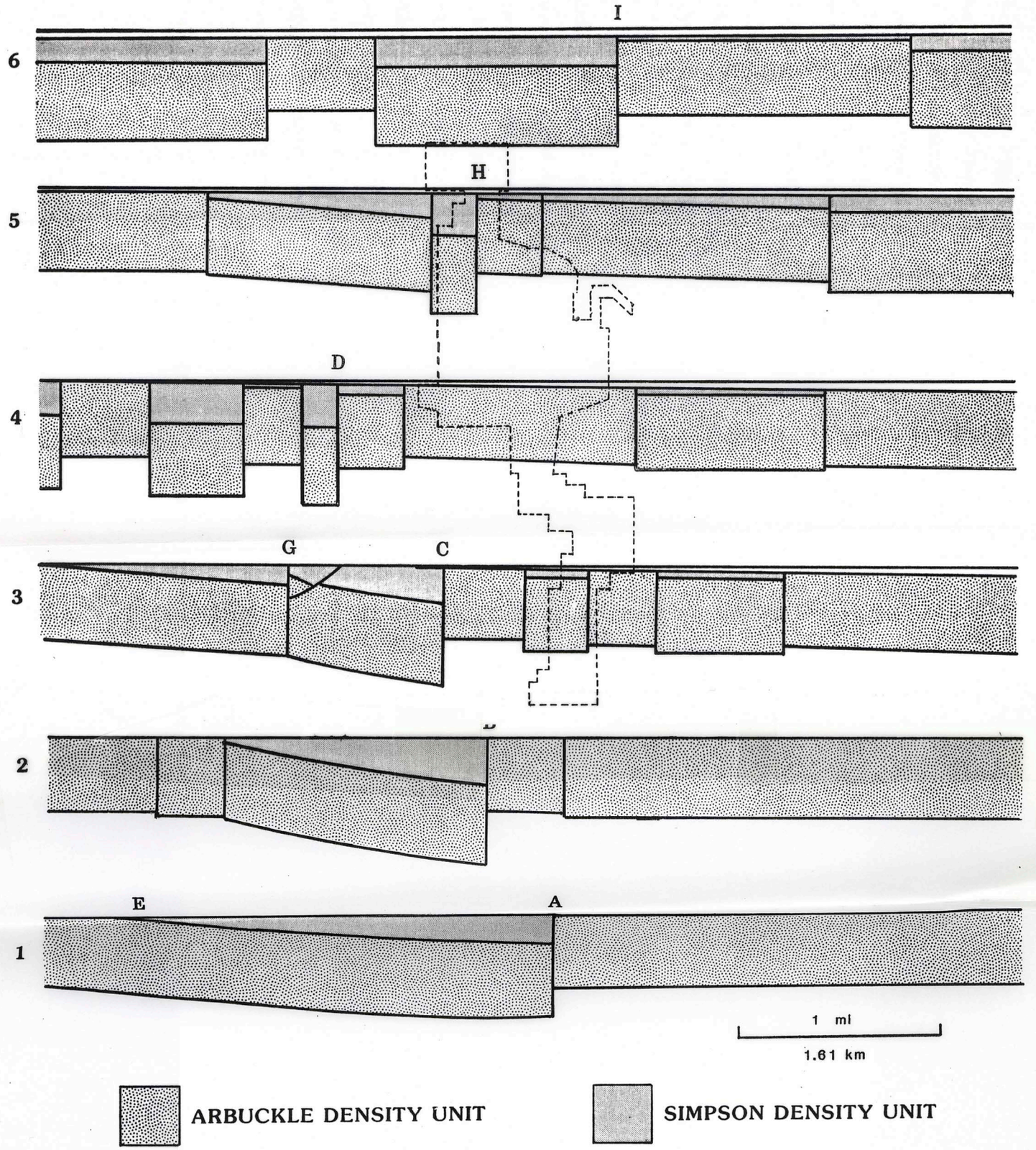

Figure 35. Figure showing composite arrangement of SAKI density models. Upper-most linear surface of each model coincides with location of section lines relative to the outline of CNRA. Vertical exageration is 0.5.

Sulphur Fault has been mapped at the location indicated by the letter A. Several lines of evidence suggests that locations A, B, C, and D on Figure 35 can be connected to infer a single fault. This fault would form the northern boundary of what has been known as the Sulphur Syncline. A fault is known to exist at the locations designated by the letters E, F, and G on this figure. Several facts indicate that the locations E, F, G, D, H, and I can be connected to delineate the trace of the major fault that continues westward from the western limits of the gravity data (top of the page on this illustration).

No data is currently available to indicate cross-sectional fault geometry for this area. It is doubtful that the faults in this geologically disturbed area are in fact strictly vertical in orientation as shown in the density models and geologic interpretations. Filtering of the gravity data indicates that the anomaly causing relationships are near surface and dominated by the contact of the dense Arbuckle Group rock against the less dense Simpson Group rocks. Because this density contrast is shallow, fault deviation from vertical would have to be unrealistically extreme to result in significant changes in the gravity values at a given location. While the fault geometry of the interpretations may not accurately reflect the geologic situation, relative offsets are thought to be consistent with existing subsurface configurations.

INTERPRETATION OF GEOLOGICAL AND GEOPHYSICAL DATA

Several different forms of evidence have been presented in this study to delineate approximate fault locations. In order to define these faults, criteria were formulated to index the type of data and the degree of confidence in the fault location interpretations (listed below in the order of relative importance beginning with the most important).

1. Offset: Juxtaposition of rocks of different ages either in outcrop or adjacent wells (definition of a fault).

2. Outcrop: Rock deformation and rotation adjacent to fault zones typified by high dip angle or highly fractured rock.

3. Trend: Fault proposed on trend of a known major fault or fault zone.

4. Gravity: Locations of high gravity gradients. Gradients indicate density contrasts, which may be due to faulting.

5. Magnetics: Locations where magnetic anomalies correlate or corroborate other fault indications.

Rock offset (criterion 1) is the only criterion from this list that can be used by itself for fault definition. The other criteria are best used in combination with each other, and then must be considered to suggest rather than define fault location.

Though gravity and magnetic data (criteria 4 and 5) are not definitive as fault location criteria, modelling shows a strong correlation between gravity values and known geologic relationships at several locations. Because of this agreement, in areas of little or no corroborative criteria gravity data can be used to extrapolate fault trends.

The locations of the interpreted faults in the study area shown on Plate 7. Those faults with a high degree of interpretive confidence (offset indicated by subsurface or outcrop data) or known location are shown as a solid line. Dashed lines indicate several criteria other than offset giving strong indication of fault location.

Fault 1 northwest of CNRA is indicated by the strong gravity gradient and subsurface data (see cross-sections C-C', Plate 4; cross-section D-D', Plate 5; and cross-section E-E', Plate 6). Relative vertical position of the rock along this fault, as illustrated by the cross-sections, is in agreement with the gravity data. Insufficient subsurface data is available to define the manner or exact location of the western termination of this fault.

Fault 2 is indicated by offset between several wells (see cross-sections A-A', Plate 2, and cross-section D-D', Plate 5). Offset is also documented on both the structure contour map of top of the Oil

Creek Formation (Figure 13), and the Pennsylvanian subcrop map (Figure 14). Relation to other faults at the southern end of this fault is not well known due to lack of data.

Fault 3 is indicated on both the structure contour map of top of the Oil Creek Formation (Figure 13), and the Pennsylvanian subcrop map (Figure 14). Offset between several wells constrains to both location and trend of this fault.

Fault 4 is indicated at several subsurface locations (see cross-section C-C', Plate 4 and cross-section D-D', Plate 5). Approximately 229 meters (750 feet) of offset is found on this fault. Location of the eastern termination of this fault is not known due to lack of data.

Fault 5 is the major structural feature in the area and is the logical continuation of the fault forming the southern boundary of the Sulphur Syncline. (See cross-section C-C', Plate 4; cross-section D-D', Plate 5; and cross-section E-E', Plate 6; the structure contour map of the top of the Oil Creek Formation, and the Pennsylvanian subcrop map). The existence of this fault is indicated by the Bouguer gravity anomaly map (Figure 16), and the gravity profile illustration (Figure 28).

Fault 6 is indicated by an offset with a displacement of approximately 345 meters (1132 feet) (see cross-section B-B', Plate 3). The northern end of this fault is an extrapolation based on gravity data.

Fault 7 is indicated by offset (see cross-section B-B', Plate 3) and the subparallel, but offset geometry of the gravity and magnetic anomalies shown in Figure 16 and Figure 21.

Faults 8 and 9 are faults shown by Ham (1954). Subsurface data

indicates offset of the Oil Creek Formation of approximately 762 meters (2500 feet) between wells 32 and 34 (cross-section B-B', Plate 3.

Faults 10, and 11 are shown by Ham (1954). Fault 10 is generally referred to as the North Sulphur Fault and extends southeastward from the location shown (Plate 1).

Fault 12 is indicated by outcrop southeast of CNRA. The elevation of the Arbuckle Group in the East Observation and West Observation wells and the Oklahoma Gas and Electric Company water wells is evidence for structural separation of the Sulphur Syncline from these wells. The strong gravity gradient trending northeast just south of the eastern end of CNRA with the parallel orientation of the magnetic anomalies supports location of a major fault at this location.

Faults 13 and 14 are those found by surface geology reconnaisance (Figure 9) and discussed in the surface geology section of this thesis.

Fault 15 is indicated by high dipping Viola outcrop and highly fractured Viola (Figure 8). These outcrop locations are on the same trend as the fault zone that forms the northern boundary of the Mill Creek syncline.

The structural fabric shown on Plate 7 is compatible with a left-lateral wrench fault model (Wilcox, et. al. 1973). Deformation resulting from left-lateral transpression results in preferred, predictable orientations of features (Sylvester, 1984) to the major strike-slip wrench zone (Figure 36). With continued wrenching the faults interconnect in an anastomosing manner that is characteristic of wrench systems. Formation of a braided geometry (Figure 37), results when faults interconnect (Wilcox, 1974). Wrench zones found in the Arbuckle region consist of long and straight major faults with branching and braided subsidiary structures. Where the main faults

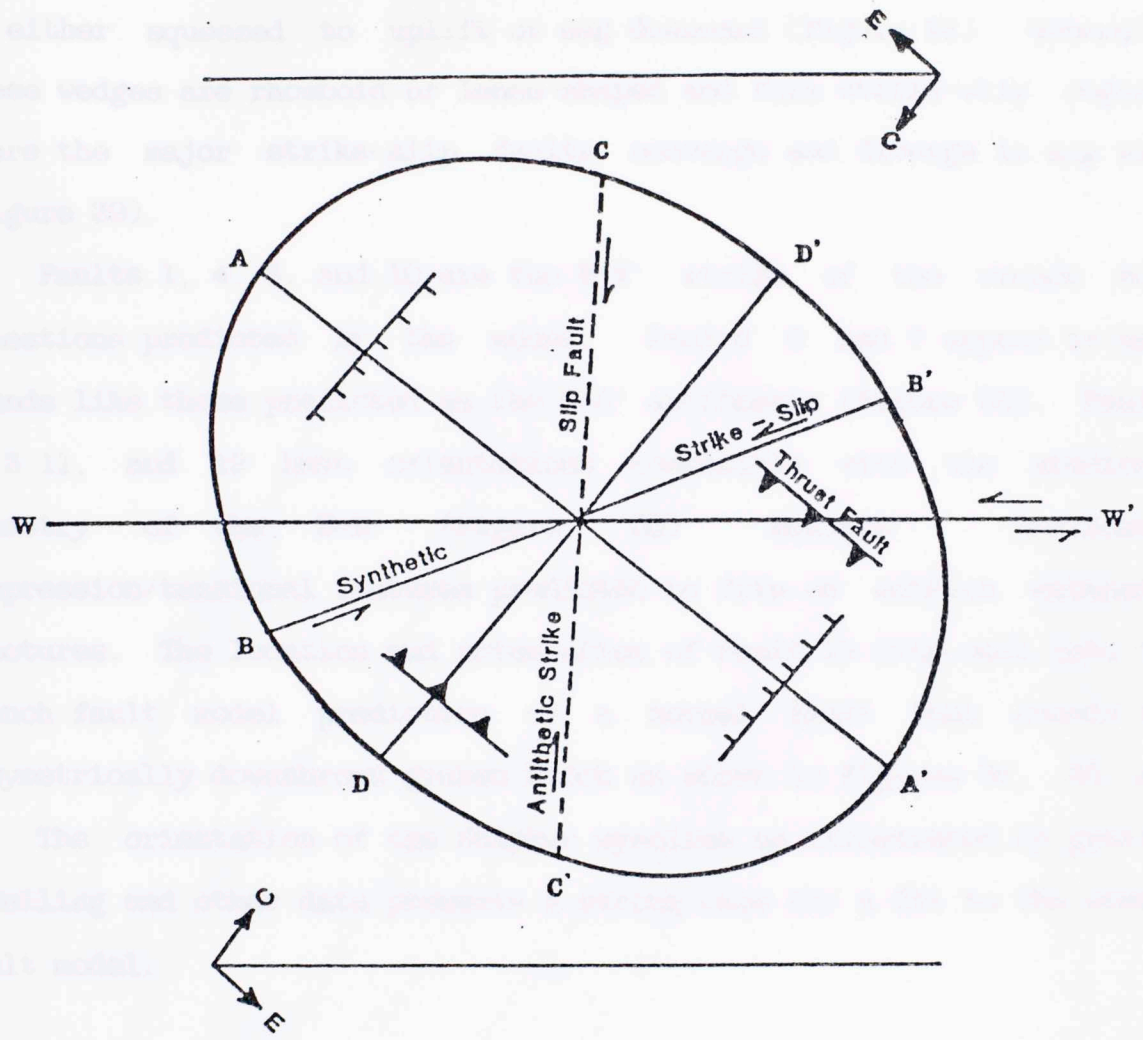

Figure 36. Geometric relation of folds and faults in a left-lateral wrench system combined schematically with strain ellipse and principle strain directions to show:

A-A' axis of maximum extension as well as axis of folds
B-B' synthetic faults at low angle to the wrench strike
C-C' antithetic faults at high angle to the wrench strike
D-D' axis of maximum compressive stress
W-W' strike of the wrench zone

Modified from Sylvester, 1984.

change strike, splays branch away with some rejoining the major fault. Wedge shaped blocks can result (Wilcox, 1974), from this rejoining and be either squeezed to uplift or sag downward (Figure 38). Generally these wedges are rhomboid or lense-shaped and form strike-slip regimes where the major strike-slip faults converge and diverge in map view (Figure 39).

Faults 1, 4, 5, and 10 are the W-W' strike of the wrench zone lineations predicted by the model. Faults 6 and 7 appear to have trends like those predicted as the C-C' antithetic (Figure 36). Faults 2, 3 11, and 12 have orientations compatible with the predicted geometry of the D-D' (Figure 36) maximum horizontal compression/tensional features predicted to form en echelon extension fractures. The location and orientation of Fault 12 fits well into the wrench fault model prediction of a normal fault that bounds the assymetrically downthrown graben block as shown in Figures 37, 38 and 39. The orientation of the Sulphur syncline as illustrated by gravity modelling and other data presents a strong case for a fit to the wrench fault model.

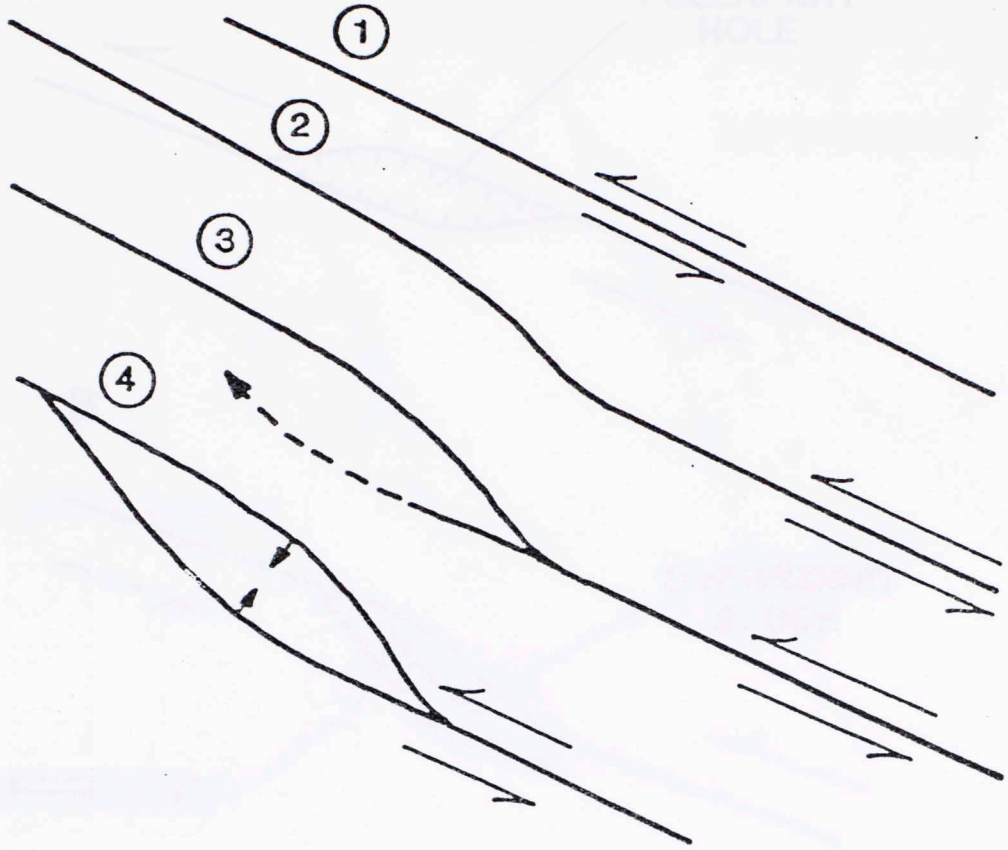

Figure 37. Map view showing progressive developement of fault splays and wedges resulting from left-lateral strike-slip faulting. Straight fault (1) gradually developes a bend through time (2 and 3) and eventually forms a fault wedge (4).
Modified from Crowell, 1974.

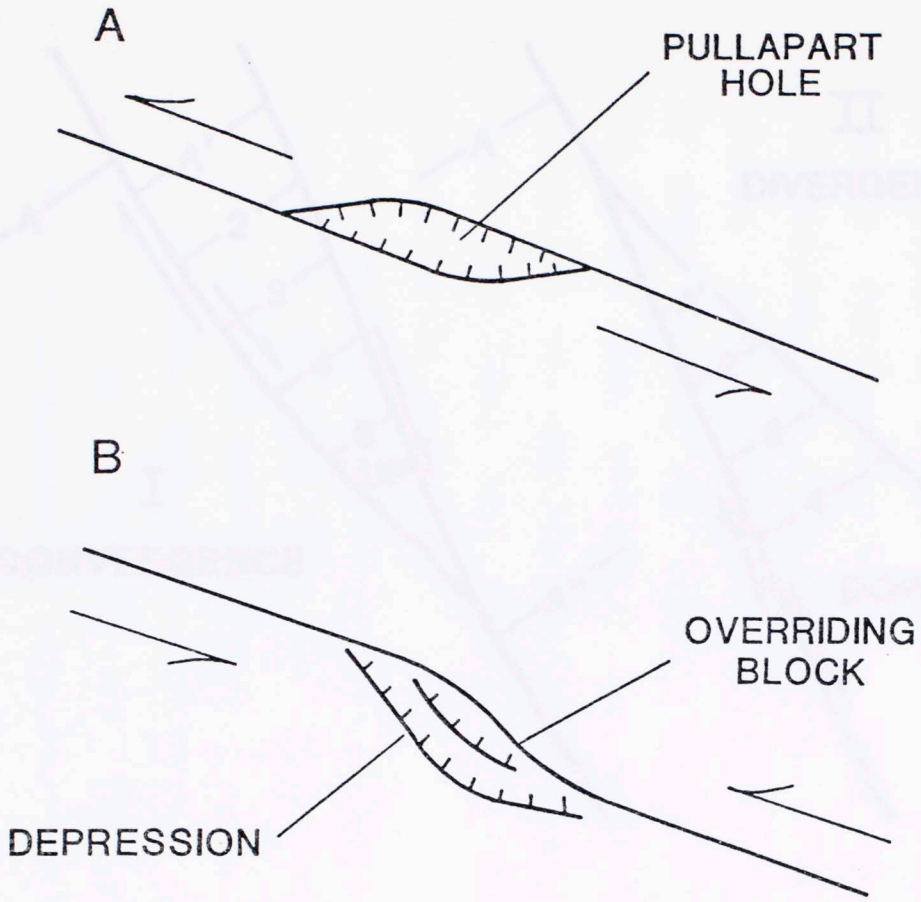

Figure 38. Map view showing formation of down-thrown wedge blocks along a left-lateral strike-slip fault with double bend. A, Pullapart hole; B, depression formed when overriding block depresses overriden block. Modified from Crowell, 1974.

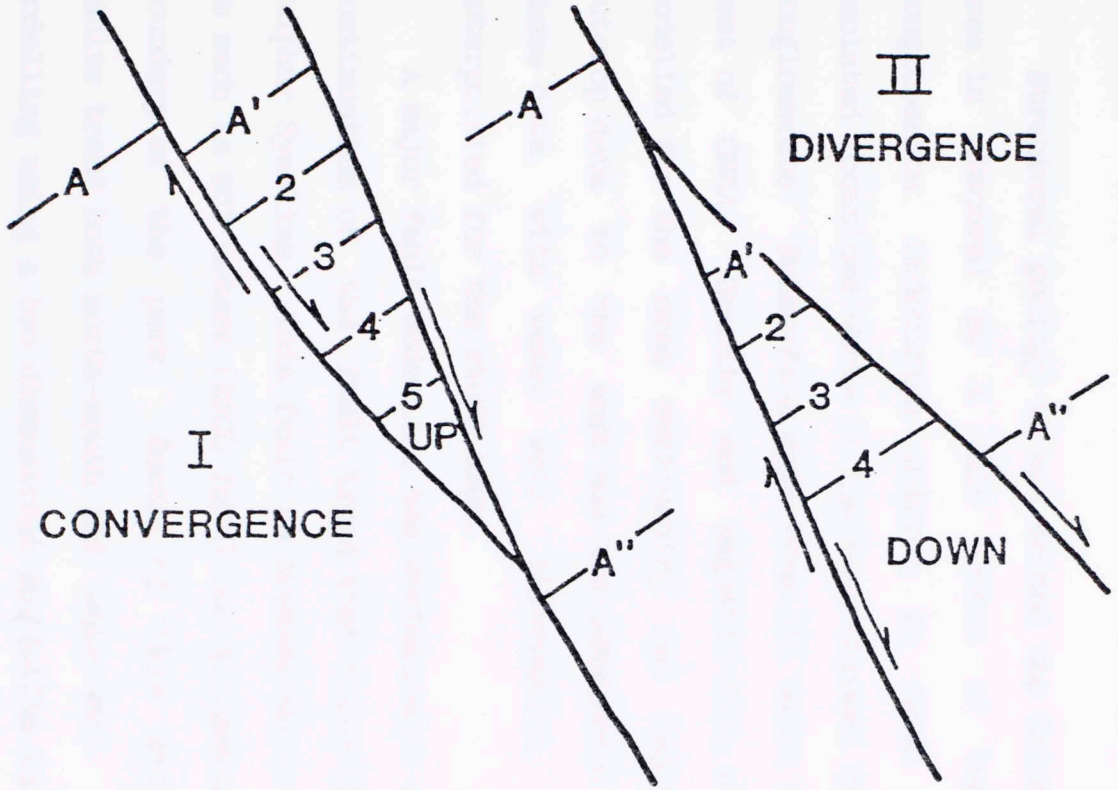

Figure 39. Map view showing uplift of tip of fault wedge with convergence of right-slip faults, and subsidence of tip with divergence. Taken from Crowell, 1974.

SUMMARY AND CONCLUSIONS

Structural geology in and around the Chickasaw National Recreation Area is obscured by a thin veneer of Pennsylvanian-aged Vanoss Conglomerate. Ordovician outcrop is found east of CNRA at a few isolated locations where it has been exposed by erosion of the Vanoss Conglomerate. Subsurface data from oil wells is available for the area west of CNRA. Gravity and magnetic data were acquired, reduced and modelled for the area surrounding and including CNRA between the outcrop data to the east and the subsurface data to the west. Using these data, with water well information, fault locations are interpolated for the study area.

A major fault underlies the western-most end of CNRA and is a continuation of the fault trend that forms the southern border of the Sulphur Syncline. This fault is downthrown to the south with offset of as much as 853 meters (2800 feet) one kilometer west of the western boundary of the park. South of this major fault is an area where faults trend both north-south and east-west. Difficulty in gravity modelling using a two dimensional algorithm indicates multiple faulting and significant trend variation in this area. North of this fault (north of and including the western half of CNRA), a structural high is indicated by the gravity data and the subsurface data. This structural high is coincident with the location of the artesian wells in that area.

The North Sulphur Fault on the northern boundary of the Sulphur Syncline does not continue northwestward in a linear fashion below the Vanoss Conglomerate. Southeast of the eastern half of CNRA, a major fault with at least 488 meters (1600 feet) of offset and trending N45E, forms the northwestern boundary of the Sulphur Syncline. This fault is a normal fault as predicted by the wrench fault model and is a transtensive feature of the left-lateral wrench system. The Sulphur Syncline is not a syncline but a rhomboidal, assymetrically downthrown block.

The convergence of faults, and the indication (from gravity inversion analysis) of lower rock densities for the area contiguous to Antelope and Buffalo Springs (eastern end of CNRA), helps to verify the possibility of fracture and karstification at this location.

Interpretation of several different forms of data leads to the conclusion that the structural geometry of the study area is consistent with that of the left-lateral wrench fault model. The structural fabric seen in the study area exhibits a main through-going wrench system with attendant features. Faults with geometries best explained as en echelon extension features, transtensional normal faults, and antithetic faults are found in the study area. The Travertine District of the Chickasaw National Recreation area is evidently one of convergence and termination of several different faults.

REFERENCES SITED

Barthel, C.J. Jr., 1985, Hydrolgeologic Investigation of Artesian Spring flow, Sulphur, Oklahoma, Area: Univ. of Okla. M.S. Thesis.

Bartlett, W.L., 1980, Experimental wrench faulting at confining pressure: Thesis, Dep. of Geology, Texas A and M Univ. August, 98 pp.

Booth, S.L., 1981, Structural analysis of portions of the Washita Valley fault zone, Arbuckle Mountains, Oklahoma: Shale Shaker, v. 31, p. 107-120.

Carter, D.W., 1979, A study of strike-slip movement along the Washita Valley Fault, Arbuckle Mountains, Oklahima: Shale Shaker, v. 30, p. 80-108.

Crowell, J.C., 1974, Origin of late Cenozoic basins in southern California, in tectonics and sdimentation: Soc. Econ. Paleontologists and Mineralogists Special Pub. 22, p. 190-204.

Crowell, J.C., 1974, Sedimentation along the San Andreas fault, California, in Dott,R.H., and Shaver, R.H. (eds.), Modern and Ancient geosynclinal sedimentation: Soc. Econ. Paleontologists and Mineralogists Special Pub. 19, p. 292-303.

Dunham, R.J., 1955, Pennsylvanian conglomerates, structure, and orogenic history of Lake Classen area, Arbuckle Mountains, Oklahoma: Am. Assoc. Pet. Geol. Bull., v. 39, p. 1-30.

Emmons, R.C., 1969, Strike-slip rupture patterns in sand models: Tectonophysics, v. 7, p. 71-87.

Fairchild, R.W., Hanson, R.L., and Davis, R.E., 1982, Hydrology of the Arbuckle Mountain area, south-central Oklahoma: U.S. Geological Survey Open-File Report 82-775, 156 p.

Fay, R.O., 1988, I-35 Roadcuts; Geology of Paleozoic strata in the Arbuckle Mountains of southern Oklahoma: Geological Society of America Centennial Field Guide--South-Central Section, 1988.

Feinstein, S., 1981, Subsidence and thermal history of the Southern Oklahoma Aulacogen; Implications for petroleum exploration: Am. Assoc. Pet. Geol. Bull., v. 65, p. 2521-2533.

Ham, W.E., 1945, Geology and Glass Sand Resources, Central Arbukle Mountains, Oklahoma Geological Survey Bulletin No. 65, 103 pp.

Ham, W.E., 1954, Collings Ranch Conglomerate Late Pennsylvanian, in Arbuckle Mountains, Okla: Am. Assoc. Pet. Geol. Bull., v. 38, p. 2035-2045.

Ham, W.E., 1954, McKinley, M.E., and others, 1954, Geologic map and section of the Arbuckle Mountains, Oklahoma: Oklahoma Geological Survey, Norman, Okla.

Ham, W.E., 1956, Structural geology of the Arbuckle Mountain regiona (abs.): Am. Assoc. Pet. Geol. Bull., v. 40, p. 425-426. Ham, W.E., and R.E. Denison, and C.A. Merrit, 1964, Basement rocks and structural evolution southern Oklahoma: Oklahoma Geological Survey Bulletin No. 95, 302 pp.

Harding, T.P., 1985, Seismic characteristics and identification of negative flower structures, positive flower structures, and positive structural inversion: Am. Assoc. Pet. Geol. Bull., v. 69, p. 582-600.

Hass, T., 1978, Structural Analysis of a Portion of the Reagan Fault Zone, Okla: Univ. of Okla. M.S. Thesis, 56 pp.

Hildenbrand, T.G., FFTFIL, a filtering program based on two-dimensional Fourier analysis, U.S. Geological Survey Open-File Report 83-237, 1983.

Islam, Q., and Nelsen, K.C., 1984, Detailed fault history in the east and central portions of the Arbuckle Mountains, Oklahim: Geological Society of America Programs with Abstracts, v. 16, no.3,

p. 87.

Luke, R.F., 1975, Structure of the Eastern Part of the Mill Creek Syncline: Univ. of Okla., M.S. Thesis, 59 p.

Moody, J.D., and Hill, M.J., 1956, Wrench-fault Tectonics: Am. Assoc. Pet. Geol. Bull., v. 67, p. 1207-1246.

Phillips, E.H., 1983, Gravity slide thrusting and folded faults in western Arbuckle Mountains and vicinity, Southern Oklahima: Am. Assoc. Pet. Geol. Bull.,v. 67, p. 1363-1390.

Pruatt, M.A., 1975, The Southern Oklahoma Aulacogen: A Geophysical Geological Investigation: Univ. of Okla. M.S. Thesis. 59 p.

Schramn, M.W. Jr., 1965 [1966], Resume of Simpson (Ordovician) Stratigraphy: Tulsa Geol. Soc. Digest,v. 33, p. 26-34.

Sylvester, A.G., and Smith, R.R., 1976, Tectonic transpression and basement controlled deformation on San Andreas Fault zone, Salton Trough, California: Am. Assoc. Pet. Geol. Bull., v. 60, p. 2081-2102.

Tenney, C., 1984, Facies analysis of the Kindblade formation, Upper Arbuckle Group, Southern Oklahoma: Univ. of Okla. M.S. Thesis.

Tanner, J.H., 1967, Wrench Fault Movements along Washita Valley Fault, Arbuckle Mountain Area, Okla: Am. Assoc. Pet. Geol. Bull., v. 51, p. 126-141

Tapp, J.B., 1978, Breccias and megabreccias of the Arbuckle Mountains, Southern Oklahoma Aulacogen, Oklahoma: Univ. of Okla. M.S. Thesis.

Tapp, J.B., 1988, Structural styles in the Arbuckle Mountains, southern Oklahoma: Geological Society of America Field Guide--South-Centra Section, p. 177-182.

Tomlinson, C.W., and McBee, W., 1962, Pennsylvanian Sediments and Oroginies of Ardmore District, Oklahoma: in Pennsylvanian System in the United

States, C.C. Branson, ed.: Am. Assoc. Petrol. Geol., Tulsa, Oklahoma, p. 461-500.

Tomlinson, C.W., McBee, William Jr., 1959, Pennsylvanian Sediments and Orogenies of Ardmore district, Okla., in Petroleum geology of Southern Okla. - a symposium, vol. 2,: Am. Assoc. Petroleum Geol., p. 2-52.

Webring,M., SAKI: A Fortran Program for Generalized Linear Inversion of Gravity and Magnetic Profiles, U.S. Geological Survey, Open File Report 85-112, 1985.

Wickham, J.S., and Dennison, R., 1978, Structural style of the Arbuckle region: Geological Society of America South Central Section Field Trip no. 3 Guidebook, 111 pp.

Wilcox, R.E., T.P. Harding, and D.R. Seely, 1973, Basic wrench tectonics: Am. Assoc. Pet. Geol. Bull., v. 57, p. 74-96.

Wiltse, E.W., 1978, Surface and subsurface study of the Southwest Davis Oil Field, Sec. 11 and 14,T1W,R1E, Murray County, Oklahoma: Univ. of Okla., M.S. Thesis.

APPENDIX

Gravity and Magnetic Data Reduction Programs

APPENDIX

```
C       PROGRAM GRAVCOR
C
C THIS PROGRAM IS DESIGNED TO CORRECT GRAVITY DATA FOR
C BOUGUER ANOMALIES, FREE AIR ANOMOLIES, AND DRIFT DUE
C TO TIDAL EFFECTS
C
C CATES & SCOTT, SEPTEMBER 11, 1987
C
C THIS PROGRAM WAS CHANGED ON SEPT. 27, 1988 TO INCORPORATE THE DIFFERENCE
C BETWEEN THE GRAVITY READING AT THE VENDOME WELL AND THE KNOWN GRAVITY
C VALUE IN THE BASEMENT OF GOULD HALL IN NORMAN OKLAHOMA.
C
C THE PROGRAM WAS CHANGED TO ALSO RESULT IN A OUTPUT FORMAT THAT WAS MORE
C COMPATIBLE WITH THE IMPLEMENTATION OF THE FFT FILTERING PORTION OF THE
C CNRA H2O STUDY
C
      IMPLICIT REAL*8 (A-H,O-Z)
      CHARACTER SITE*13(1000),FNAME*128
      DIMENSION TIME(1000), RDG(1000),LAT(1000),EL(1000),DAY(1000)
     *,XLON(1000),GLAT(1000)
      REAL IGF, LAT,XLON,GLAT
C
      WRITE (*,'(A)') 'ENTER NAME OF INPUT DATA FILE:'
      READ (*,'(A)') FNAME
      OPEN (FILE=FNAME,UNIT=5,STATUS='OLD')
      WRITE (*,'(A)') 'ENTER NAME OF OUTPUT DATA FILE:'
      READ (*,'(A)') FNAME
      OPEN (FILE=FNAME,UNIT=6,STATUS='UNKNOWN')
      NRDG = 1
      PI=3.14159
C
C READ DATA FOR A NEW LOCATION.....
 10    READ (5,'(A,18X,F3.0,4X,2F2.0,2X,F4.0,2X,F5.1)',END=100)
     *                SITE(NRDG),DAY(NRDG),HOUR,RMIN,EL(NRDG),RDG(NRDG)
      write (*,'(2x,a,2x,f4.0,2x,2f3.0,2x,f5.0,2x,f6.1)') site(nrdg),
     *      day(NRDG),hour,rmin,el(nrdg),rdg(nrdg)
C
C CONVERT ELEVATIONS FROM FEET TO METERS
      EL(NRDG)=EL(NRDG)/3.281
C
C CONVERT LATITUDE FROM DEGREES,MINUTES,SECONDS TO DECIMAL DEGREES
      READ(SITE(NRDG),'(3F2.0)')DEG,DMIN,SEC
      DLAT=DEG+(DMIN/60.)+(SEC/3600.)
      GLAT(NRDG)=DLAT
      READ(SITE(NRDG),'(6X,F3.0,2F2.0)')XDEG,XMIN,XSEC
      DLON= -(XDEG+(XMIN/60.)+(XSEC/3600.))
      XLON(NRDG)=DLON
C
C     CONVERT DECIMAL DEGREES TO RADIANS
      LAT(NRDG)=((DLAT)*PI)/180.
C
C     DELINEATE TIME IN DECIMAL DAYS AND READ INTO ARRAY
      TIME(NRDG) = DAY(NRDG) + (HOUR + RMIN / 60.) / 24.
C
C READ TWO OTHER SAMPLES FROM SAME LOCATION....
      DO 20 I=1,2
           READ (5,'(50X,F5.1)') VALUE
           RDG(NRDG) = RDG(NRDG) + VALUE
20    CONTINUE
      RDG (NRDG) = (RDG (NRDG) / 3.)*.0965
      NRDG = NRDG + 1
      GOTO 10
C
```

APPENDIX

```
C ALL THE DATA HAVE BEEN READ...NOW APPLY TIDAL CORRECTION....
100   CONTINUE
      NRDG = NRDG - 1
C
C CORRECT FOR VARIATION OVER THE DAY THE READINGS WERE COLLECTED,
C AS WELL AS VARIATION FROM DAY TO DAY...ALL READINGS WILL BE CORRECTED
C TO THE TIME WHEN THE FIRST CONTROL READING WAS TAKEN
      ICTL = 1
      IPNT = 1
C     WRITE (6,'(A,1X,F8.2)') SITE(1), RDG(1)
150   CONTINUE
      IPNT = IPNT + 1
      IF (SITE (IPNT) .NE. SITE(1)) GOTO 150
C
C RETURN TO THE CONTROL POINT
C FIRST COMPUTE CORRECTION BACK TO LAST CONTROL POINT READING
      SLOPE = ( RDG(IPNT) - RDG(ICTL) ) / ( TIME(IPNT) - TIME(ICTL) )
C
C NOW COMPUTE CORRECTION FROM LAST CONTROL POINT READING TO TIME ZERO
      RINT =  RDG(ICTL) - RDG(1)
C
C APPLY TO CORRECTION TO THE LAST GROUP OF READINGS
      DO 160 I=ICTL+1,IPNT
         VALUE = RDG(I) - (SLOPE * (TIME(I) - TIME(ICTL))) - RINT
C
C COMPUTE GRAVITY OBSERVED
      GOB=VALUE+(979657.4-(70.9))
C
C DEFINE SQUARES OF SIN(LAT) AND SIN(2LAT) TO REDUCE ROUND-OFF ERROR
      XLAT=SIN(LAT(I))
      XLAT=XLAT*XLAT
      XLAT2=SIN(2*LAT(I))
      XLAT2=XLAT2*XLAT2
C
C DEFINE INTERNATIONAL GRAVITY FORMULA
      IGF=978031.8*(1.0+(0.0053024)*XLAT-0.0000059*XLAT2)
C
C APPLY FREE AIR CORRECTION
      GFA=GOB-IGF+(0.3085)*EL(I)
C
C COMPUTE BOUGUER ANOMOLY
C
      GBU = GFA - 0.112 * EL(I)
C
C WRITE THE RESULTS
C       WRITE (6,'(A,F17.2)') SITE(I), GBU
C       WRITE (6,'(A,3F9.2,F7.2,F12.2,F9.2,F9.2)')SITE(I),EL(I),DAY(I),
C     *  RDG(I),VALUE,GOB,GFA,GBU
C        WRITE (6,'(F8.4,2X,F7.4,3F9.2)')XLON(I),GLAT(I),EL(I),GFA,GBU
        WRITE(6,'(F12.5,2X,F12.5,2X,F9.2)')XLON(I),GLAT(I),GBU
160   CONTINUE
C
C FINISHED WITH THIS GROUP, RESET POINTER TO LAST CONTROL POINT VISIT (ICTL)
      ICTL = IPNT
      IF (IPNT .NE. NRDG) GOTO 150
C
C WE'RE ALL DONE!
      ENDFILE (6)
      CLOSE (5)
      CLOSE (6)
      STOP ' METAMORPHISM! ****'
      END
```

APPENDIX

```
C PROGRAM MAGCOR.FOR
C
C CORRECT MAGNETIC DATA FOR DRIFT OVER TIME
C CATES & SCOTT, SEPTEMBER 11, 1987
C
      CHARACTER SITE*13(1000),FNAME*128
      DIMENSION TIME(1000),RMAG(1000),DAY(1000),GLON(1000),GLAT(1000)
      REAL DLAT,DLON
C
      WRITE (*,'(A)') 'ENTER NAME OF INPUT DATA FILE:'
      READ (*,'(A)') FNAME
      OPEN (FILE=FNAME,UNIT=5,STATUS='OLD')
      WRITE (*,'(A)') 'ENTER NAME OF OUTPUT DATA FILE:'
      READ (*,'(A)') FNAME
      OPEN (FILE=FNAME,UNIT=6,STATUS='UNKNOWN')
      NRDG = 1
C READ DATA FOR A NEW LOCATION.....
10    READ (5,'(A,18X,F3.0,4X,2F2.0,15X,F5.0)',END=100)
     *                SITE(NRDG),DAY(NRDG),HOUR,RMIN,RMAG(NRDG)
      WRITE (*,'(2X,A,F4.0,2X,F3.0,2X,F3.0,2X,F6.0)')SITE(NRDG),
     *DAY(NRDG),HOUR,RMIN,RMAG(NRDG)
C   CONVERT LATITUDE FROM DEGREES,MINUTES,SECONDS TO DECIMAL DEGREES
       READ(SITE(NRDG),'(3F2.0)')DEG,DMIN,SEC
       GLAT(NRDG)=DEG+(DMIN/60.)+(SEC/3600.)
C       GLAT(NRDG)=DLAT
       READ(SITE(NRDG),'(6X,F3.0,2F2.0)')XDEG,XMIN,XSEC
       GLON(NRDG)=-(XDEG+(XMIN/60.)+(XSEC/3600.))
C       GLON(NRDG)=DLON
C       WRITE (*,'(F8.4,F2.4)')GLON,GLAT
      TIME(NRDG) = DAY(NRDG) + (HOUR + RMIN / 60.) / 24.
C
C READ TWO OTHER SAMPLES FROM SAME LOCATION....
      DO 20 I=1,2
           READ (5,'(57X,F5.0)') VALUE
           RMAG(NRDG) = RMAG(NRDG) + VALUE
20    CONTINUE
      RMAG(NRDG) = RMAG(NRDG) / 3.
      NRDG = NRDG + 1
      GOTO 10
C
C ALL THE DATA HAVE BEEN READ...NOW APPLY DRIFT CORRECTION
100   CONTINUE
      NRDG = NRDG - 1
C
C CORRECT FOR VARIATION OVER THE DAY THE READINGS WERE COLLECTED,
C AS WELL AS VARIATION FROM DAY TO DAY...ALL READINGS WILL BE CORRECTED
C TO THE TIME WHEN THE FIRST CONTROL READING WAS TAKEN
      ICTL = 1
      IPNT = 1
150   CONTINUE
      IPNT = IPNT + 1
      IF (SITE (IPNT) .NE. SITE(1)) GOTO 150
```

APPENDIX

```
C WE'VE RETURNED TO THE CONTROL POINT
C FIRST COMPUTE CORRECTION BACK TO LAST CONTROL POINT READING
      SLOPE = ( RMAG(IPNT) - RMAG(ICTL) ) / ( TIME(IPNT) - TIME(ICTL) )
C
C NOW COMPUTE CORRECTION FROM LAST CONTROL POINT READING TO TIME ZERO
      RINT =  RMAG(ICTL) - RMAG(1)
C
C APPLY TO CORRECTION TO THE LAST GROUP OF READINGS
      DO 160 I=ICTL+1,IPNT
         VALUE = RMAG(I) - (SLOPE * (TIME(I) - TIME(ICTL))) - RINT
C     WRITE (6,'(A,10X,F8.2)') SITE (IPNT),VALUE
C      WRITE (6,'(A,3F12.3)')SITE(IPNT),RMAG(I),TIME(I),VALUE
      WRITE (6,'(2F8.4,F10.3)') GLON(I),GLAT(I),VALUE
160   CONTINUE
      VALUE = RMAG(IPNT) - (SLOPE * (TIME(IPNT) - TIME(ICTL))) - RINT
      ICTL = IPNT
      IF (IPNT .NE. NRDG) GOTO 150
C
C ALL DONE!
      ENDFILE (6)
      CLOSE (5)
      CLOSE (6)
      STOP ' PALEO WANDER'
      END
```